CHAPTER 6 CONCLUSIONS

As a result of the geological survey and the geochemical survey of the soil in the 30 km^2 area of 8 km long in the east-west direction and 4 km long in the south-north direction from the Pagar Gunung deposit to the Patahajang (Barute) mineralization zone, the relationship between the deposit and geology, geological structure and igneous activities has been clarified. The survey results of this area are summarized in the following.

(1) Geologically, this area consists of the Muara Botung Formation and Patahajang Formation formed of andesite, dacite, sandstone, mudstone and limestone, and these Formation are correlative with Silungkang Formation of Peusangan Group, Permian-Carboniferous System in Sumatra Island. These Formations are further divided into 7 Members.

(2) The muscovite granodiorite that is widely distributed in the northern part of the survey area has undergone mylonitization, and shows banded texture and has become mylonite. Also, it has been intrued by Juraic tonalitic porphyry and quartz diorite porphyry.

(3) There is a synclinal structure, having an synclinal axis of N 60° W in the central part of survey area, that is, from the Summit of T. Pagar Gunung to the ridge of T. Mandagang, and the arrangement of tonalite and quartz diorite stocks are also regulated to this direction.

(4) There are the following ore deposits or mineralized zones in the survey area.

(a) Silver-bearing lead-zinc deposit (Skarn deposit)

Pagar Gunung West deposit
Pagar Gunung East deposit (Outcrop B)

(b) Disseminated sphalerite mineralized zone

Barute mineralized zone

(c) Pyrite mineralized zone

Pagar Gunung East deposit (Outcrop A)
A. Sambak pyrite disseminated zone

(d) Others

Quartz vein containing molybdenite

(5) The Pagar Gunung West deposit is embedded in the alternated Member of Clastic rock and volcanic rock of the Patahajang Formation. It's strike and dip are about N 90° E and 30° S and has a maximum vein width of 2.50 m, and it's strike length is about 200 m while it's width changes from thick to thin along the extension. Furthermore, together with Pagar Gunung West deposit (Outcrop A) situating 650 m east of it, it is classified into silver-bearing lead-zinc skarn deposit, replacing muddy limestone and accompanied by calcic skarn minerals like clinopyroxene, epidote and calcite. Further in the east by 6 km, there is the Barute mineralized area accompanied by sphalerite emplaced in the same stratigraphical horizon of Pagar Gunung ore deposit.

(6) In the muscovite granodiorite and dacitic tuffaceous rock that are distributed in the northern marginal part of the survey area, there is a silicification zone accompanied by pyrite dissemination. Especially on Outcrop A of the Pagar Gunung East deposit there is a pyrite dissemination zone of about 20 m width in the dacitic tuffaceous sandstone, and bedded or banded pyrite deposit is distributed.

(7) Through the geochemical survey of the soil, it is found that anomalous areas overlapping with path-finder elements of Au, Ag, Cu, Pb, Zn coincides with outcrop lines of Pagar Gunung ore deposits and the Barute-Patahajang mineralized area. Also, an anomalous area of gold, silver, copper, lead and zinc overlapping each other was discovered 3 km long and 1 km wide from the A. Mandagan upstream to the Barute mineralized area. This anomalous area is situated in the same horizon and Alternated Member of Clastic rock and Volcanic rock of Patahajang Formation as the Pagar Gunung ore deposit and Barute mineralized zone.

In addition, an anomalous area of silver (and gold) is recognized in the neighborhood of stocks of tonalite and quartz diorite, which have intruded into limestone, in the A. Sabul upstream in the west of Simpang Pining. While there are other anomalous areas of silver (and gold) in places such as the north ridge of the A. Salidi in the limestone area and the ridge of T. Pagar Gunung in the south of Pagar Gunung mineralized area, but in these places no quartz diorite or tonalite are exposed. When it is considered that silver (gold) shows the aureale margin of quartz diorite and the like, there is a possibility of quartz diorite latently existing in these areas. Also, distribution of skarn deposits could be conceivable.

Fig. II-3-33 Microscopic Photograph of Thin Section and Ore Sample, Muara Sipongi Area B

Abbreviation

q	:	Quartz
pl	:	Plagioclase
bi	:	Biotite
mu	:	Muscovite
hy	:	Hypersthene
au	:	Augite
fe	:	Ferric mineral
ca	:	Calcite
chl	:	Chlorite
se	:	Sericite
ep	:	Epidote
cp	:	Chalcopyrite
sp	:	Sphalerite
ga	:	Galena
po	:	Pyrrhotite
py	:	Pyrite
r.f.and	:	Rock fragment (andesite)

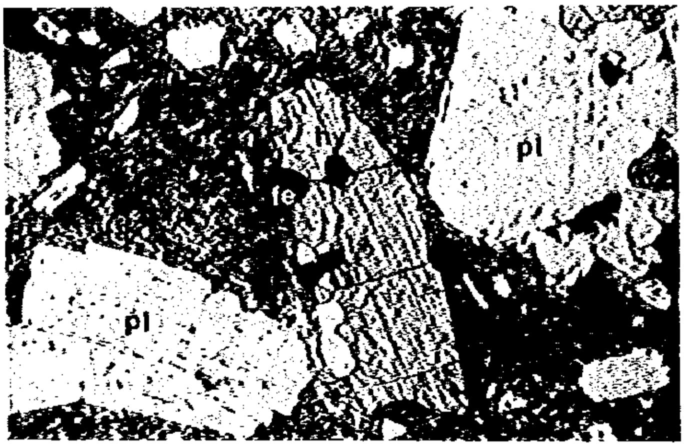

Sample No.: L-29
Location : T. Pagar Gunung
Rock name : Pyroxene andesite
Formation : Tertiary volcanic rock

only lower polar
0 0.5mm

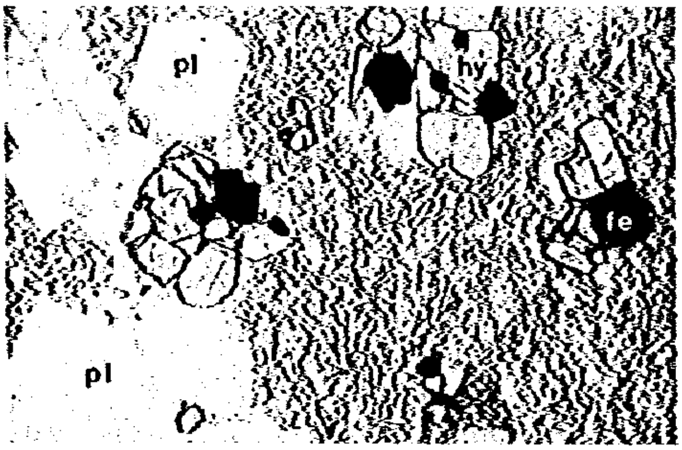

Sample No.: L-100
Location : T. Simpang Opat
Rock name : Pyroxene andesite
Formation : Tertiary volcanic rock

only lower polar
0 0.5mm

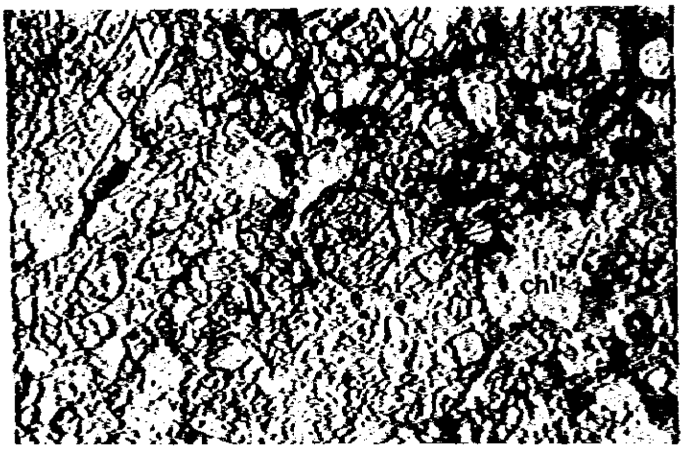

Sample No.: L-2
Location : West of T. Mandagang
Rock name : Pyroxenite
Formation : Basic volcanic rock Member Patahajang Formation

only lower polar

0 0.5mm

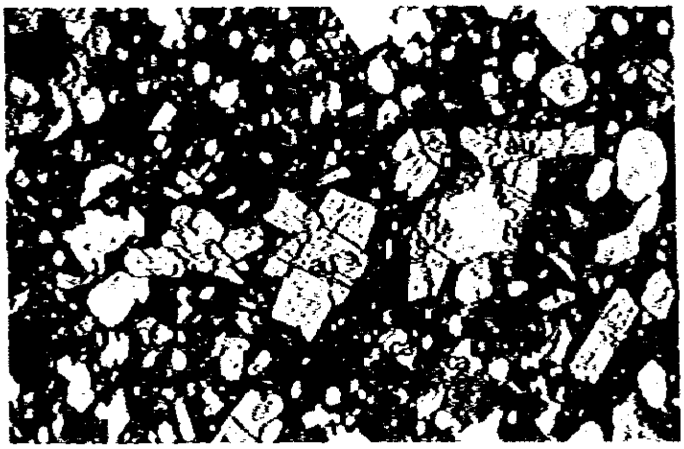

Sample No.: L-3
Location : West of T. Mandagang
Rock name : Pyroxenite
Formation : Basic volcanic rock Member Patahajang Formation

only lower polar

0 0.5mm

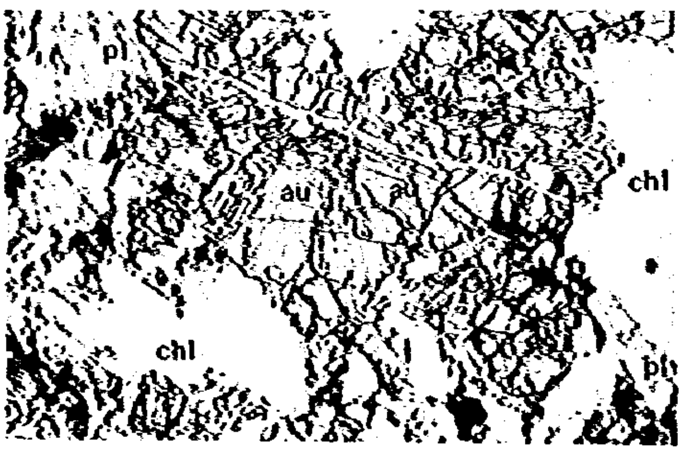

Sample No.: L-113
Location : T. Pagar Gunung
Rock name : Basaltic tuff
Formation : Basic volcanic rock Member Patahajang Formation

only lower polar

0 0.5mm

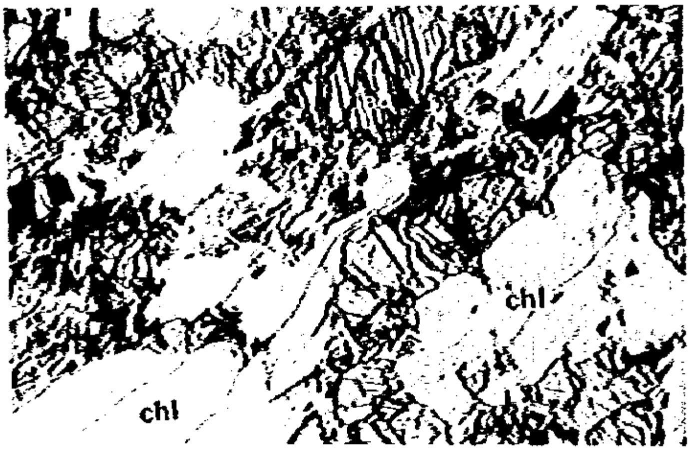

Sample No.: L-125
Location : T. Pagar Gunung
Rock name : Basaltic tuff
Formation : Basic volcanic rock Member Patahajang Formation

only lower polar
0 0.5mm

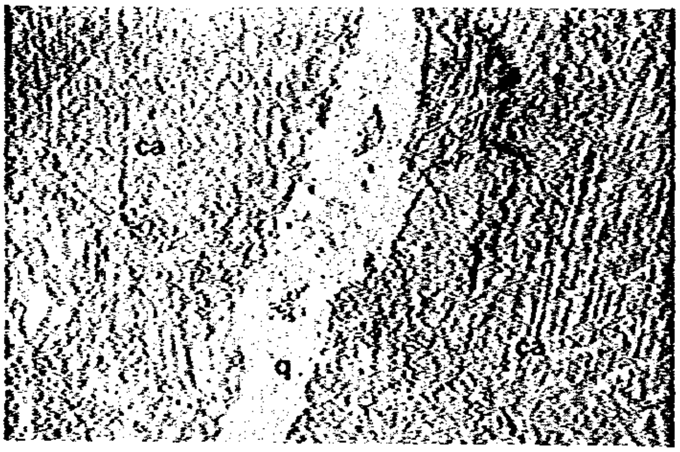

Sample No.: L-1
Location : West of T. Mandagang
Rock name : Limestone
Formation : Lower limestone Member Patahajang Formation

only lower polar
0 0.5mm

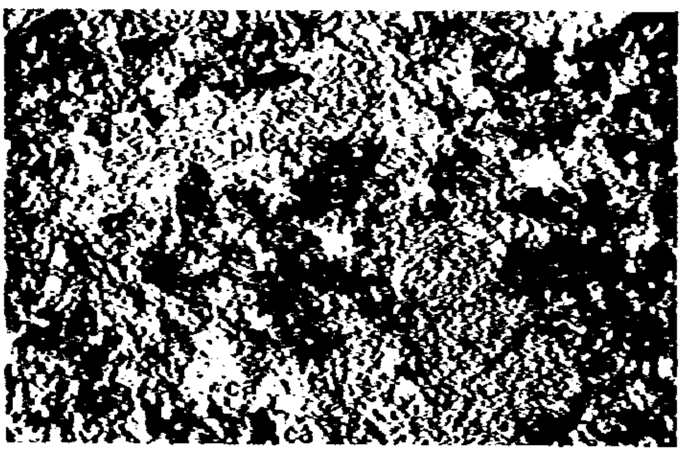

Sample No.: L-19
Location : Tributary of A. Sabul
Rock name : Meta andesite
Formation : Andesite Member Patahajang Formation

cross polars
0 0.5mm

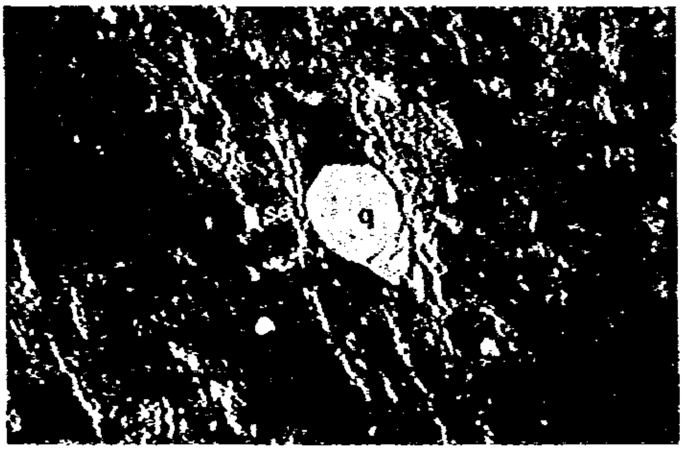

Sample No.: M-2
Location : A. Mandagang
Rock name : Phyllitic mudstone
Formation : Alternated Member of clastic rock and volcanic rock Patahajang Formation

cross polars

0 0.5mm

Sample No.: KR-21
Location : A. Sambak
Rock name : Sandstone
Formation : Alternated Member of clastic rock and volcanic rock Patahajang Formation

cross polars

0 0.5mm

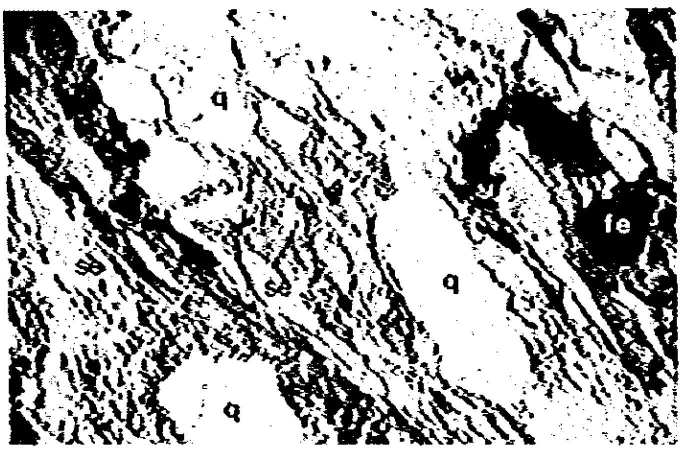

Sample No.: L-138
Location : A. Palelo
Rock name : Dasitic sandy tuff
Formation : Alternated Member of clastic rock and volcanic rock Patahajang Formation

only lower polar

0 0.5mm

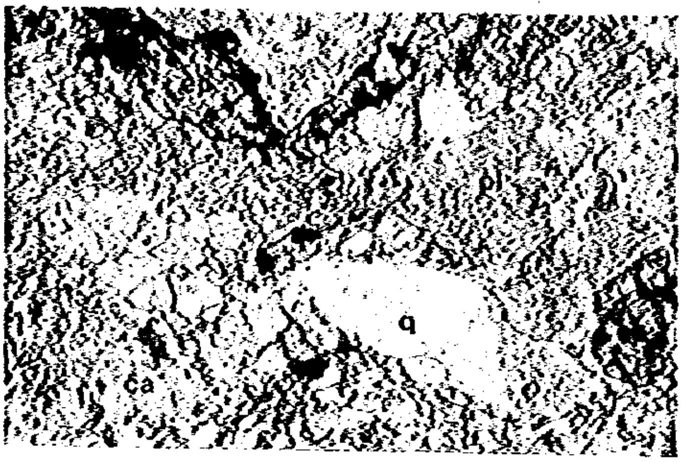

Sample No.: L-147
Location : Tributary of A. Sambak
Rock name : Andesitic tuff
Formation : Alternated Member of clastic rock and volcanic rock Patahajang Formation

only lower polar
0 0.5mm

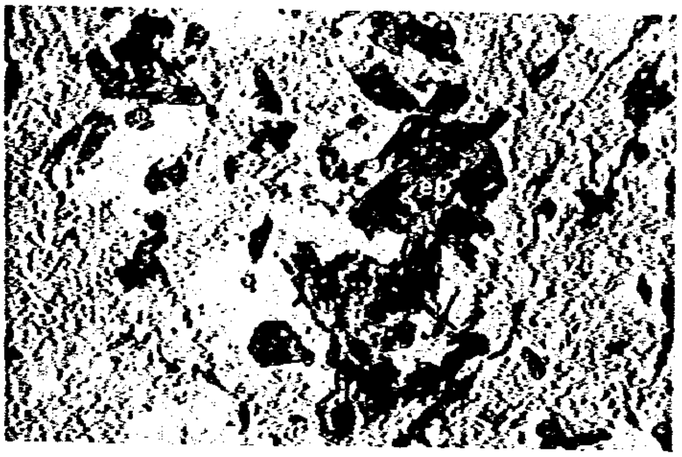

Sample No.: L-156
Location : A. Palelo
Rock name : Dacitic tuff
Formation : Alternated Member of clastic rock and volcanic rock Patahajang Formation

only lower polar
0 0.5mm

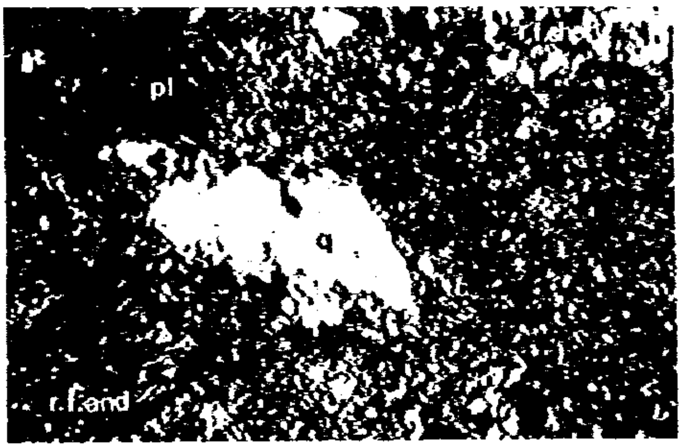

Sample No.: K-10
Location : B. Pungkut
Rock name : Dacitic tuff
Formation : Alternated Member of clastic rock and volcanic rock Patahajang Formation

cross polars
0 0.5mm

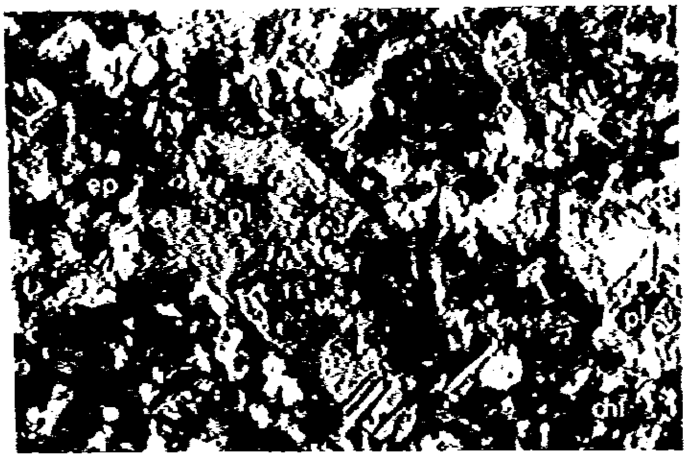

Sample No.: L-132
Location : A. Palelo
Rock name : Andesite
Formation : Alternated Member of clastic rock and volcanic rock Patahajang Formation

cross polars

0 0.5mm

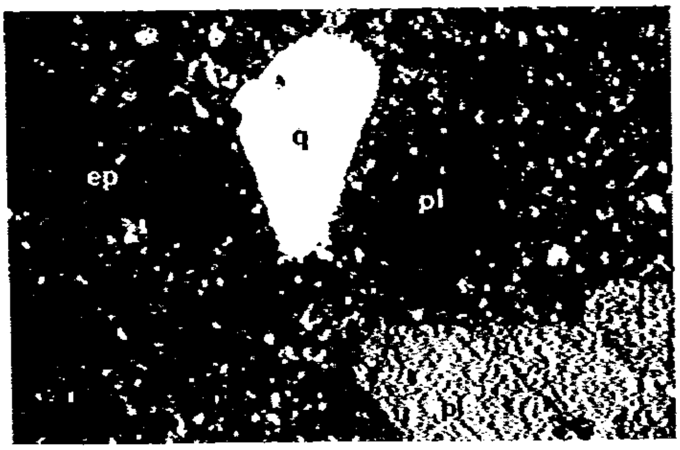

Sample No.: M-18
Location : A. Mabobar
Rock name : Dacite
Formation : Dacite Member Patahajang Formation

cross polars

0 0.5mm

Sample No.: M-21
Location : A. Mabobar
Rock name : Dacitic tuff
Formation : Dacite Member Patahajang Formation

only lower polar

0 0.5mm

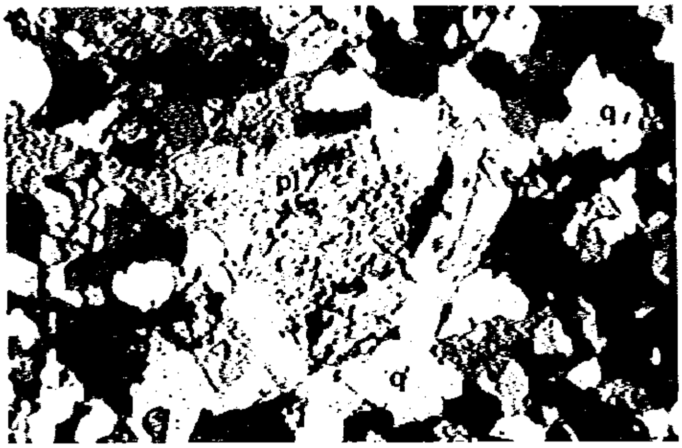

Sample No.: K-15
Location : A. Matimba
Rock name : Tonalite porphyry

cross polar
0 0.5mm

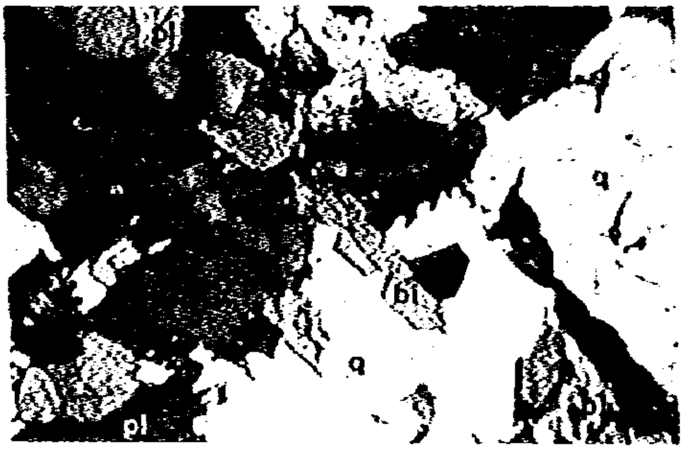

Sample No.: K-28
Location : B. Pungkut
Rock name : Tonalite

cross polar
0 0.5mm

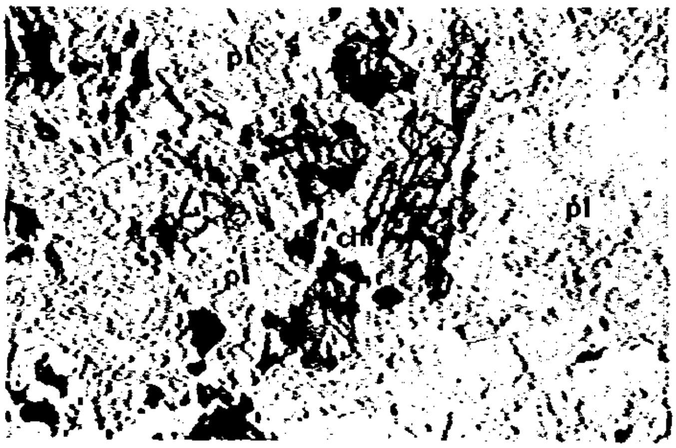

Sample No.: L-41
Location : A. Sabul
Rock name : Diorite porphyry

only lower polar
0 0.5mm

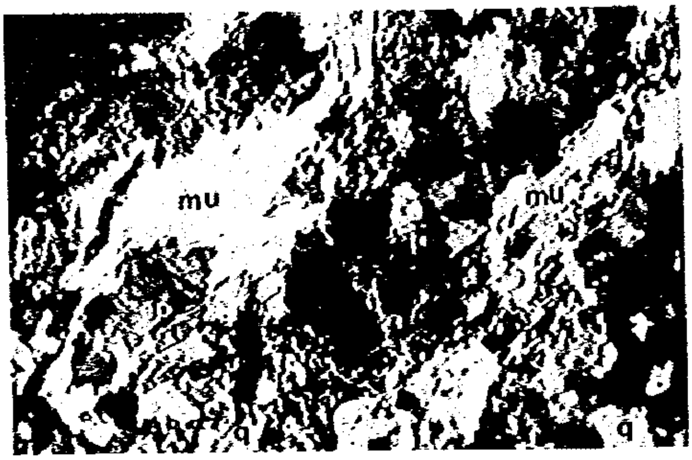

Sample No.: L-131
Location : A. Palelo
Rock name : Muscovite granodiorite (mylonite)

cross polars
0 0.5mm

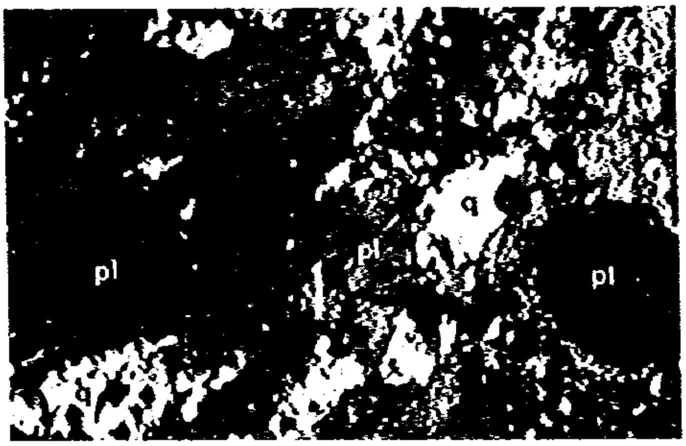

Sample No.: M-40
Location : A. Karlan
Rock name : Muscovite granodiorite (mylonite)

cross polars
0 0.5mm

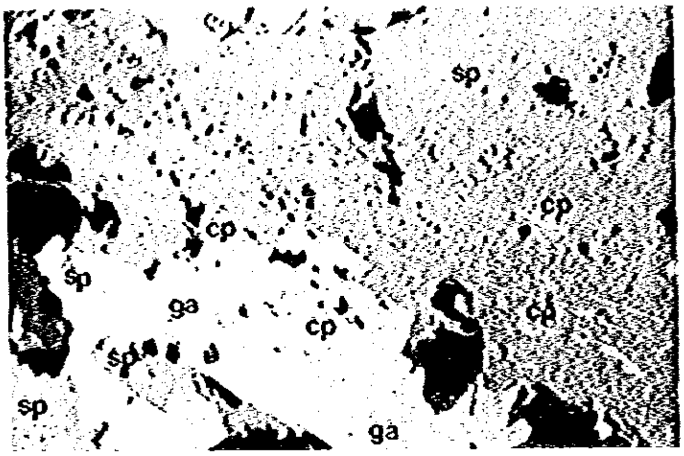

Sample No.: KR-37
Location : Pagar Gunung West ore deposit Adit No. 2
Ore name : Massive chalcopyrite-galena-sphalerite ore

0 0.2mm

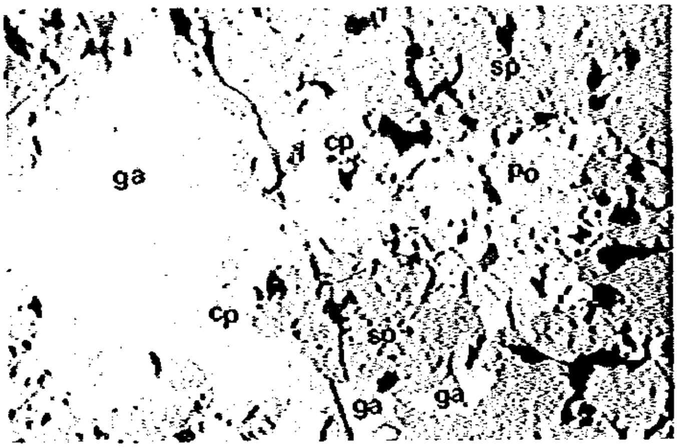

Sample No.: KR-52
Location : Pagar Gunung West ore deposit Adit No. 6
Ore name : Massive pyrrhotite-chalcopyrite-galena-sphalerite ore

0 0.2mm

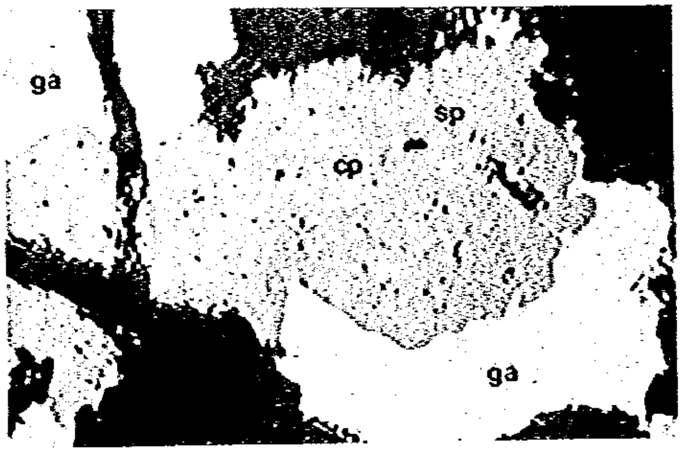

Sample No.: ZH-3.5
Location : A. Palelo Pagar Gunung East ore deposit Outcrop B
Ore name : Massive chalcopyrite-galena-sphalerite ore

0 0.2mm

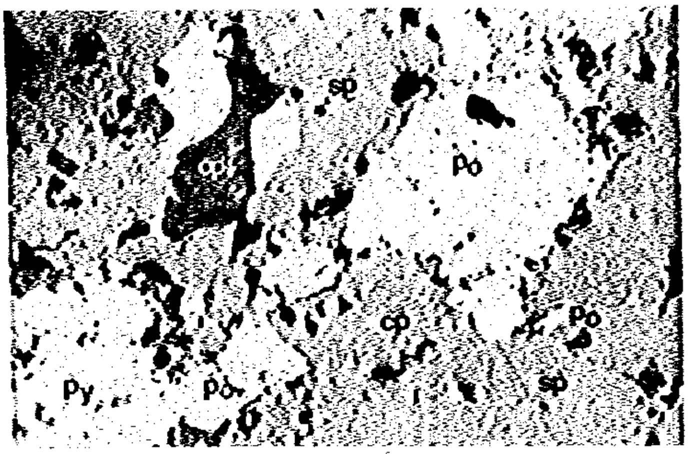

Sample No.: ZH-3.5
Location : A. Palelo Pagar Gunung East ore deposit Outcrop B
Ore name : Massive pyrrhotite chalcopyrite-galena-sphalerite-ore

0 0.2mm

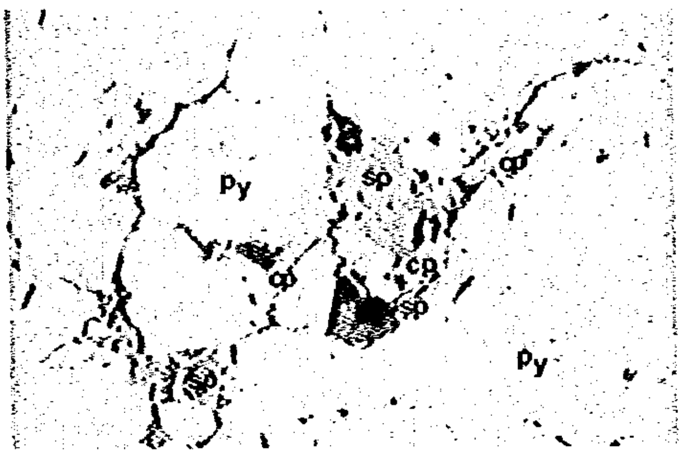

Sample No.: L-139
Location : A. Palelo Pagar Gunung East ore deposit Outcrop A
Ore name : Massive pyrite ore

0 0.2mm

Table II-3-9 Assay Result of Geochemical Survey, Muara Sipongi Area B

Sample No.	Coordinates X	Coordinates Y	Au ppb	Ag ppm	Cu ppm	Pb ppm	Zn ppm
KS1	6505	-1010	4	0.4	70	240	545
KS2	6530	-1365	1	0.4	59	39	130
KS3	6680	-1530	4	0.1	38	14	46
KS4	7020	-1910	20	0.1	48	17	68
KS5	7585	-2050	75	0.1	82	14	112
KS6	6150	-535	11	0.4	108	280	900
KS7	6960	-1275	4	0.2	51	46	131
KS8	7335	-1770	2	0.1	45	17	95
KS9	7620	-1700	5	0.1	37	24	81
KS10	6190	-1175	4	0.1	55	25	535
KS11	5080	-210	30	0.6	134	51	350
KS12	4720	-570	24	0.9	74	25	93
KS13	4435	-815	65	1.0	94	22	145
KS14	5165	-770	21	0.5	71	23	96
KS15	5340	-540	21	0.6	112	33	440
KS16	5710	-280	24	1.1	72	550	1000
KS17	4775	-2010	2	0.1	63	16	124
KS18	4820	-1410	5	0.1	35	12	82
KS19	5150	-1520	45	0.4	65	42	148
KS20	5035	-1140	65	0.4	95	33	151
KS21	4260	-1815	6	0.1	70	11	73
KS22	3900	-1800	12	0.1	75	8	102
KS23	4140	-1310	30	0.3	128	21	139
KS24	4120	-1090	72	1.5	130	30	205
KS25	4475	-1235	52	0.6	75	19	105
KS26	6375	-1740	9	0.3	48	35	171
KS27	6675	-1970	16	0.2	54	22	103
KS28	5875	-2020	4	0.1	58	9	88
KS29	5120	210	21	0.9	660	70	270
KS30	370	1135	12	1.7	38	93	2500
KS31	340	1705	33	1.1	89	38	220
KS32	225	2130	19	0.1	76	44	171
KS33	-20	1865	95	2.0	34	44	250
KS34	490	1930	8	0.7	41	16	109
KS35	745	1600	11	0.4	124	31	139
KS36	640	1390	8	0.1	35	47	210
KS37	615	890	2	0.1	49	9	130
LS1	560	35	39	0.1	123	7	93
LS2	770	-80	46	0.1	125	4	105
LS3	1220	210	1	0.1	81	1	56
LS4	1260	-115	4	0.1	54	3	59
LS5	1535	-730	57	0.9	104	10	84
LS6	1270	-975	49	0.1	74	22	94
LS7	345	-295	37	0.2	68	19	100
LS8	790	250	4	0.1	155	4	113
LS9	1045	440	4	0.1	25	7	40
LS10	800	650	5	0.1	23	7	28
LS11	385	390	29	0.4	78	46	121
LS12	280	790	11	0.1	21	10	28
LS13	95	700	7	0.1	74	12	40

Sample No.	Coordinates X	Y	Au ppb	Ag ppm	Cu ppm	Pb ppm	Zn ppm
LS14	700	-655	15	1.3	85	26	137
LS15	920	-320	105	0.1	72	21	66
LS16	1380	-440	5	0.1	27	6	51
LS17	1030	-640	29	0.1	89	16	95
LS18	970	-945	24	0.6	67	30	112
LS19	100	-170	230	3.9	115	14	102
LS20	110	60	1	0.1	99	2	83
LS21	-80	425	5	0.1	23	8	40
LS22	165	110	15	0.1	88	5	93
LS23	-155	-100	46	2.4	73	19	142
LS24	-625	20	82	1.3	59	11	99
LS25	-35	-390	53	0.4	58	35	109
LS26	550	-400	38	1.2	72	15	110
LS27	390	-755	3	0.2	24	13	54
LS28	2460	-2070	2	0.1	22	14	61
LS29	2710	-1780	14	0.1	43	6	80
LS30	2540	-1380	21	0.1	88	21	136
LS31	2850	-1285	7	0.1	64	25	105
LS32	2900	-895	35	0.1	33	8	39
LS33	2320	-1640	100	0.4	120	26	113
LS34	2200	-1910	1	0.1	62	10	96
LS35	1340	-1290	8	0.1	32	9	56
LS36	1840	-1740	3	0.1	20	8	41
LS37	2060	-1500	11	0.1	36	8	77
LS38	2230	-1250	27	0.1	64	37	176
LS39	2145	-920	43	0.4	110	22	125
LS40	1340	-620	43	0.6	97	31	109
LS41	2450	-855	61	0.1	84	21	116
LS42	1680	-1330	7	0.1	48	13	78
LS43	1650	-1040	37	0.1	70	14	123
LS44	3465	-1880	8	0.3	63	10	103
LS45	3105	-1570	24	0.2	70	11	72
LS46	2830	-2020	4	0.1	73	8	97
LS47	-640	465	12	0.5	44	8	50
LS48	-1020	530	30	1.3	54	32	73
LS49	-2430	1645	2	0.1	64	3	192
LS50	-2315	2060	1	0.1	22	20	94
LS51	-1980	2130	1	0.1	22	27	48
LS52	-1850	1850	1	0.1	21	17	72
LS53	-2020	1580	2	0.1	38	11	67
LS54	-2310	1350	2	0.1	30	11	66
LS55	-1520	965	56	0.1	63	26	72
LS56	-1180	860	12	0.5	32	7	55
LS57	-1205	1945	1	0.1	19	15	35
LS58	-1290	1205	5	0.1	80	5	86
LS59	-1630	1550	11	0.1	66	8	99
LS60	-1155	1550	1	0.1	30	9	74
LS61	-1500	1315	1	0.1	19	20	59
LS62	-1800	1355	1	0.3	19	14	47
LS63	-1500	2140	8	0.1	86	23	120

Sample No.	Coordinates X	Coordinates Y	Au ppb	Ag ppm	Cu ppm	Pb ppm	Zn ppm
LS64	-1420	2440	1	0.1	50	46	122
LS65	-1740	2445	2	0.1	15	16	43
LS66	-700	2625	2	0.3	15	27	46
LS67	-1150	2545	1	0.1	19	15	57
LS68	-1110	2305	6	0.1	29	10	111
KRS1	5740	-520	31	2.7	250	3000	4700
KRS2	5620	-675	9	0.5	60	240	1600
KRS3	5720	-1005	28	2.0	88	700	2000
KRS4	5810	-1220	13	0.2	74	350	800
KRS5	5540	-1305	19	0.1	95	23	124
KRS6	5900	-1570	24	0.1	62	13	96
KRS7	5795	-1800	3	0.1	74	11	120
KRS8	5575	-2030	5	0.1	81	10	103
KRS9	5425	-1770	16	0.1	107	38	152
KRS10	4600	-1725	3	0.1	72	15	109
KRS11	4205	-1600	11	0.1	64	18	88
KRS12	3895	-1530	44	0.3	48	59	154
KRS13	3510	-1400	2	0.1	78	26	33
KRS14	3155	-1140	8	0.8	41	15	54
KRS15	3575	-1050	13	0.1	78	18	110
KRS16	-840	2105	15	0.7	32	20	73
KRS17	-550	2300	15	0.8	50	91	275
KRS18	-190	2040	8	0.3	57	23	125
KRS19	-270	2280	1	0.1	17	14	72
HS1	3570	-90	16	0.5	31	35	66
HS2	3210	35	53	0.8	42	15	74
HS3	2760	180	5	0.1	24	11	38
HS4	3660	180	43	1.0	103	1000	270
HS5	4395	405	29	0.6	600	38	164
HS6	2440	90	1	0.1	53	16	51
HS7	2270	580	4	0.1	32	13	57
HS8	1730	-175	1	0.1	57	9	69
HS9	2160	-10	30	0.1	100	12	101
HS10	2520	-260	88	1.0	60	69	147
HS11	2770	-125	34	1.0	75	51	250
HS12	2445	-515	171	0.8	90	32	75
HS13	2105	-365	74	0.7	65	62	146
HS14	2785	-710	140	0.3	55	37	220
HS15	2960	-325	86	0.2	78	73	176
HS16	3310	-380	45	1.6	44	25	84
HS17	3600	-300	64	0.5	103	38	184
HS18	4480	155	74	2.7	190	1200	560
HS19	4685	-170	23	0.3	84	205	585
HS20	4205	-90	39	0.4	96	41	178
HS21	4030	-300	54	0.6	117	39	215
HS22	3840	-400	58	0.3	100	28	153
HS23	3045	-760	73	0.5	45	26	40
HS24	1200	680	31	0.2	203	64	295
HS25	3870	680	19	1.3	63	87	295
HS26	3300	460	64	1.9	108	580	1150

Sample No.	Coordinates X	Coordinates Y	Au ppb	Ag ppm	Cu ppm	Pb ppm	Zn ppm
HS27	3430	800	66	1.2	81	1700	1200
HS28	3220	1130	13	1.3	40	86	147
HS29	2820	600	132	2.0	44	425	176
HS30	3060	800	38	1.1	41	265	225
HS31	2980	1170	14	0.5	31	39	180
HS32	2630	910	20	0.3	52	23	67
HS33	4270	-470	41	0.4	90	25	98
HS34	3850	-830	51	2.9	38	29	59
HS35	3380	-750	270	0.8	60	123	210
HS36	4480	760	26	0.2	43	57	68
HS37	3630	1040	52	0.3	44	161	129
HS38	3360	1385	19	1.4	39	44	50
HS39	3055	1575	28	0.7	92	176	205
HS40	3200	1750	23	0.2	39	70	123
HS41	3590	1640	113	0.3	30	46	110
HS42	4775	500	10	0.5	350	330	445
HS43	1430	1550	10	0.3	68	55	150
HS44	1100	1630	1	0.2	45	13	83
HS45	860	1045	2	0.1	82	3	80
HS46	1215	1345	1	0.1	42	16	119
HS47	2045	1630	16	0.3	60	270	285
HS48	2150	1355	5	0.2	24	89	132
HS49	1385	1105	5	0.2	72	78	235
HS50	1200	800	3	0.1	62	6	73
HS51	1455	640	4	0.1	78	6	87
HS52	1635	470	7	0.3	86	11	98
HS53	1365	265	3	0.1	106	5	78
HS54	1630	90	3	0.1	73	8	77
HS55	1300	190	6	0.1	81	8	52
HS56	2040	470	4	0.1	111	13	78
HS57	1890	815	9	0.1	80	94	181
HS58	1730	1100	25	0.5	100	91	570
HS59	1800	1420	4	0.3	54	44	390
HS60	2260	1000	2	0.7	35	5	38
HS61	2475	1225	5	0.2	31	10	35
HS62	2160	1590	15	0.2	85	69	171
HS63	2375	2010	10	0.3	53	39	168
HS64	1720	1895	12	0.5	64	83	235
HS65	1425	1950	3	0.2	23	12	104
HS66	2810	1395	2	0.7	22	8	30
HS67	2685	1830	9	0.6	50	31	134
HS68	3030	1930	15	0.1	51	15	55
HS69	2810	2170	9	0.1	46	49	189
HS70	2525	2440	1	0.1	37	23	119
HS71	2220	2500	3	0.1	31	110	68
HS72	1830	2515	7	0.3	27	60	75
HS73	1530	2205	12	0.7	21	14	71
HS74	2060	2160	4	0.1	28	20	193
700.0	-720	2065	19	0.2	89	48	375
700.5	-750	2020	26	0.9	47	14	330

Sample No.	Coordinates X	Y	Au ppb	Ag ppm	Cu ppm	Pb ppm	Zn ppm
ZA1.0	-770	1970	1	0.4	22	15	81
ZA1.5	-790	1930	1	0.1	30	10	45
ZA2.0	-810	1885	1	0.1	16	10	35
ZA2.5	-830	1840	1	0.5	15	10	40
ZA3.0	-850	1800	1	0.4	16	26	56
ZA3.5	-875	1750	1	0.3	13	23	47
ZA4.0	-900	1700	2	1.1	12	17	41
ZA4.5	-920	1660	1	0.1	17	20	46
ZA5.0	-935	1615	1	0.3	18	12	63
ZA5.5	-960	1565	1	0.2	19	7	49
ZA6.0	-980	1520	1	0.1	39	7	56
ZA6.5	-1010	1490	3	0.1	41	6	81
ZA7.0	-1030	1435	1	0.1	33	7	51
ZA7.5	-1055	1390	3	0.1	15	7	17
ZA8.0	-1080	1340	3	0.1	31	5	61
ZA8.5	-1100	1290	3	0.1	46	10	63
ZA9.0	-1120	1250	5	0.1	86	3	115
ZA9.5	-1140	1200	5	0.1	87	5	90
ZA10.0	-1160	1160	3	0.1	86	4	114
ZA10.5	-1180	1115	9	1.7	19	7	36
ZA11.0	-1205	1070	142	0.5	39	18	57
ZA11.5	-1220	1020	22	1.4	25	9	50
ZA12.0	-1245	970	6	0.2	84	4	83
ZB0.0	-595	2000	20	0.2	39	33	410
ZB0.5	-615	1955	7	2.4	19	10	74
ZB1.0	-640	1905	6	0.4	20	24	109
ZB1.5	-660	1865	4	1.1	19	30	119
ZB2.0	-675	1820	8	0.3	29	64	158
ZB2.5	-700	1775	10	1.0	40	365	480
ZB3.0	-720	1730	2	0.2	22	19	103
ZB3.5	-740	1685	4	0.1	70	41	174
ZB4.0	-760	1640	13	0.1	39	18	106
ZB4.5	-780	1590	5	0.6	63	143	295
ZB5.0	-800	1545	2	0.1	136	9	138
ZB5.5	-825	1500	3	0.1	34	10	46
ZB6.0	-845	1460	4	0.2	24	9	65
ZB6.5	-865	1410	7	0.2	15	9	36
ZB7.0	-890	1370	1	0.1	32	8	73
ZB7.5	-910	1320	2	0.2	27	7	57
ZB8.0	-930	1275	3	0.1	24	5	46
ZB8.5	-950	1230	1	0.1	37	2	57
ZB9.0	-970	1190	4	0.1	31	5	69
ZB9.5	-1000	1140	8	0.1	40	4	56
ZB10.0	-1025	1095	23	0.1	80	4	81
ZB10.5	-1045	1050	68	0.8	64	61	177
ZB11.0	-1070	1000	21	1.2	26	30	72
ZB11.5	-1090	950	23	0.8	28	10	52
ZB12.0	-1110	910	31	0.6	46	31	245
ZC-2.0	-370	2110	2	2.5	38	38	162
ZC-1.5	-390	2070	5	0.6	58	24	100

Sample No.	Coordinates X	Coordinates Y	Au ppb	Ag ppm	Cu ppm	Pb ppm	Zn ppm
ZC-1.0	-410	2025	2	0.5	29	14	89
ZC-0.5	-430	1980	31	1.0	63	42	260
ZC0.0	-455	1935	74	1.0	63	143	350
ZC0.5	-475	1890	8	0.7	18	23	162
ZC1.0	-500	1845	42	0.2	30	89	159
ZC1.5	-520	1800	39	0.8	32	157	250
ZC2.0	-540	1760	24	2.2	30	389	1600
ZC2.5	-560	1710	10	1.3	39	150	370
ZC3.0	-580	1665	7	0.7	32	73	163
ZC3.5	-600	1620	4	0.6	40	97	182
ZC4.0	-625	1575	5	0.5	60	289	350
ZC4.5	-645	1530	7	0.4	116	48	325
ZC5.0	-670	1480	27	10.5	310	9500	3900
ZC5.5	-690	1440	1	0.1	49	13	91
ZC6.0	-710	1390	2	0.1	41	7	101
ZC6.5	-725	1350	2	0.1	54	5	103
ZC7.0	-750	1300	15	0.1	104	6	171
ZC7.5	-770	1260	2	0.1	51	4	79
ZC8.0	-790	1210	1	0.1	66	4	78
ZC8.5	-815	1165	3	0.1	50	6	330
ZC9.0	-835	1120	6	0.1	37	21	78
ZC9.5	-860	1075	12	0.1	60	7	62
ZC10.0	-880	1030	23	0.3	37	7	70
ZC10.5	-900	975	32	0.1	32	10	46
ZC11.0	-920	930	43	0.4	27	24	75
ZC11.5	-940	890	18	0.1	26	29	99
ZC12.0	-960	840	77	0.5	65	43	162
ZD0.0	-320	1870	33	0.1	38	38	210
ZD0.5	-340	1825	163	2.1	61	170	980
ZD1.0	-360	1780	175	7.4	55	300	1350
ZD1.5	-380	1740	41	2.1	37	138	2050
ZD2.0	-405	1690	155	2.1	88	460	3100
ZD2.5	-425	1650	2	0.2	73	36	112
ZD3.0	-450	1600	1	0.1	36	19	121
ZD3.5	-470	1555	23	0.1	40	120	160
ZD4.0	-490	1510	9	1.0	90	330	1050
ZD4.5	-510	1465	34	4.4	300	1400	590
ZD5.0	-530	1420	25	0.1	64	7	115
ZD5.5	-555	1375	1	0.1	82	1	80
ZD6.0	-575	1330	2	0.1	78	2	150
ZD6.5	-590	1280	3	0.1	78	2	115
ZD7.0	-620	1235	1	0.1	64	5	200
ZD7.5	-635	1190	3	0.1	58	1	280
ZD8.0	-660	1150	3	0.2	51	1	158
ZD8.5	-680	1100	1	0.1	48	32	72
ZD9.0	-700	1060	16	0.1	77	14	84
ZD9.5	-725	1010	1	0.1	86	3	68
ZD10.0	-745	960	18	0.2	58	10	120
ZD10.5	-765	915	6	0.1	104	3	104
ZD11.0	-785	870	26	0.6	72	21	137

Sample No.	Coordinates X	Y	Au ppb	Ag ppm	Cu ppm	Pb ppm	Zn ppm
ZD11.5	-805	820	1	0.1	70	2	96
ZD12.0	-825	780	2	0.1	104	1	110
ZE0.0	-180	1810	85	4.0	32	230	270
ZE0.5	-205	1760	53	1.8	36	310	420
ZE1.0	-225	1720	37	1.6	33	190	1300
ZE1.5	-245	1670	90	1.1	39	300	1000
ZE2.0	-270	1630	21	0.8	23	134	150
ZE2.5	-290	1580	17	2.7	36	240	535
ZE3.0	-310	1540	6	0.9	45	180	265
ZE3.5	-330	1435	25	2.1	410	3050	1750
ZE4.0	-350	1445	40	2.8	415	4650	4900
ZE4.5	-375	1400	16	0.4	148	460	1450
ZE5.0	-400	1350	1	0.1	67	11	91
ZE5.5	-415	1310	1	0.1	90	13	107
ZE6.0	-440	1265	2	0.1	106	2	190
ZE6.5	-460	1215	2	0.1	37	6	54
ZE7.0	-480	1170	4	0.1	73	13	60
ZE7.5	-505	1130	3	0.1	39	12	47
ZE8.0	-525	1080	4	0.3	32	10	44
ZE8.5	-545	1040	2	0.1	162	2	73
ZE9.0	-565	390	2	0.1	94	1	112
ZE9.5	-590	940	80	0.8	91	18	136
ZE10.0	-610	895	70	2.2	32	10	57
ZE10.5	-630	345	3	0.1	94	2	127
ZE11.0	-650	305	2	0.4	44	4	51
ZE11.5	-670	760	7	0.1	65	4	78
ZE12.0	-695	715	4	0.2	36	76	131
ZF0.0	-45	1745	30	2.8	33	190	250
ZF0.5	-70	1700	29	2.9	27	146	170
ZF1.0	-90	1655	6	1.7	22	162	82
ZF1.5	-110	1610	27	1.3	24	28	45
ZF2.0	-135	1565	3	0.7	21	40	45
ZF2.5	-155	1520	1	0.9	22	27	37
ZF3.0	-170	1470	4	0.7	25	76	51
ZF3.5	-195	1430	3	2.0	33	33	41
ZF4.0	-215	1380	5	0.7	34	15	47
ZF4.5	-240	1335	1	0.6	49	12	60
ZF5.0	-260	1290	1	0.2	52	8	77
ZF5.5	-280	1245	3	0.1	74	14	95
ZF6.0	-305	1200	1	0.1	30	6	235
ZF6.5	-325	1155	2	0.1	67	7	139
ZF7.0	-345	1110	2	0.1	37	6	57
ZF7.5	-370	1060	2	0.1	40	8	47
ZF8.0	-390	1015	3	0.1	59	3	58
ZF8.5	-410	970	6	0.1	57	8	53
ZF9.0	-430	920	8	0.2	23	8	39
ZF9.5	-450	875	6	1.6	24	10	50
ZF10.0	-475	830	3	1.0	20	6	31
ZF10.5	-495	785	6	0.1	29	3	56
ZF11.0	-515	740	1	0.1	40	5	90

Sample No.	Coordinates X	Y	Au ppb	Ag ppm	Cu ppm	Pb ppm	Zn ppm
ZF11.5	-540	695	1	0.1	85	4	82
ZF12.0	-560	650	1	0.1	56	4	72
ZG0.0	90	1680	95	2.5	55	275	1150
ZG0.5	70	1630	55	0.3	47	255	590
ZG1.0	40	1590	24	1.2	50	300	500
ZG1.5	20	1540	6	1.9	34	370	1300
ZG2.0	5	1500	23	1.8	56	390	540
ZG2.5	-20	1455	16	0.9	215	2000	1250
ZG3.0	-40	1410	7	1.4	210	2800	1250
ZG3.5	-60	1365	6	0.2	38	123	280
ZG4.0	-85	1320	3	0.4	39	14	119
ZG4.5	-105	1265	3	0.1	44	9	83
ZG5.0	-125	1220	1	0.1	45	17	102
ZG5.5	-145	1180	2	0.1	55	41	106
ZG6.0	-165	1140	1	0.1	42	42	128
ZG6.5	-185	1090	1	0.1	90	8	119
ZG7.0	-205	1045	1	0.1	48	18	74
ZG7.5	-230	1000	18	0.1	30	3	83
ZG8.0	-250	945	4	0.1	146	8	114
ZG8.5	-270	900	6	0.5	119	10	109
ZG9.0	-295	860	8	0.4	24	7	50
ZG9.5	-315	810	130	2.0	36	5	43
ZG10.0	-340	770	13	1.1	36	27	64
ZG10.5	-360	720	1	0.1	30	23	61
ZG11.0	-380	675	1	0.1	75	1	83
ZG11.5	-400	630	3	0.1	26	11	47
ZG12.0	-420	585	4	0.1	28	9	43
ZH0.0	225	1620	31	0.3	70	152	530
ZH0.5	200	1570	30	0.3	38	36	183
ZH1.0	180	1520	9	0.4	39	365	500
ZH1.5	160	1480	54	2.2	230	570	1950
ZH2.0	140	1435	44	0.7	130	370	1200
ZH2.5	120	1385	19	1.2	55	310	1200
ZH3.0	100	1345	9	1.9	98	325	1250
ZH3.5	80	1295	6	1.4	164	450	565
ZH4.0	60	1255	1	0.1	50	14	96
ZH4.5	35	1200	1	0.1	64	12	64
ZH5.0	10	1160	1	0.3	56	10	81
ZH5.5	-10	1115	1	0.1	42	9	44
ZH6.0	-30	1070	1	0.5	46	10	49
ZH6.5	-50	1020	1	0.2	39	6	48
ZH7.0	-70	980	2	0.1	84	3	111
ZH7.5	-95	925	1	0.1	36	11	83
ZH8.0	-115	835	1	0.1	80	13	72
ZH8.5	-135	840	1	0.5	34	9	33
ZH9.0	-160	795	2	0.3	25	5	34
ZH9.5	-180	750	11	3.8	22	14	46
ZH10.0	-200	705	65	1.2	29	6	36
ZH10.5	-220	660	4	0.1	130	7	118
ZH11.0	-245	615	1	0.1	48	8	280

Sample No.	Coordinates X	Coordinates Y	Au ppb	Ag ppm	Cu ppm	Pb ppm	Zn ppm
ZH11.5	-265	570	1	0.1	38	5	58
ZH12.0	-285	520	2	0.1	30	22	103
Z10.0	360	1555	13	0.1	66	13	106
Z10.5	340	1505	11	1.0	60	28	182
Z11.0	320	1460	13	0.1	46	8	37
Z11.5	295	1415	6	0.8	26	52	300
Z12.0	275	1370	12	0.2	33	51	134
Z12.5	255	1325	6	0.5	30	52	86
Z13.0	230	1275	6	1.0	43	74	195
Z13.5	210	1230	13	8.6	360	3000	2000
Z14.0	190	1185	6	0.4	45	33	205
Z14.5	170	1140	1	0.1	102	9	205
Z15.0	150	1095	1	0.1	68	9	76
Z15.5	130	1050	3	0.1	112	7	92
Z16.0	105	1010	1	0.4	78	8	190
Z16.5	85	950	3	0.1	66	5	62
Z17.0	60	910	3	0.1	58	13	66
Z17.5	40	865	2	0.1	48	6	97
Z18.0	20	820	2	0.1	76	7	143
Z18.5	0	780	2	0.1	67	14	74
Z19.0	-20	735	5	0.1	39	5	48
Z19.5	-45	685	3	0.1	30	14	37
Z110.0	-65	640	3	0.1	128	5	87
Z110.5	-90	595	2	0.1	99	2	94
Z111.0	-110	550	4	0.1	23	-10	37
Z111.5	-130	500	4	0.1	28	14	51
Z112.0	-155	460	3	0.1	45	46	148

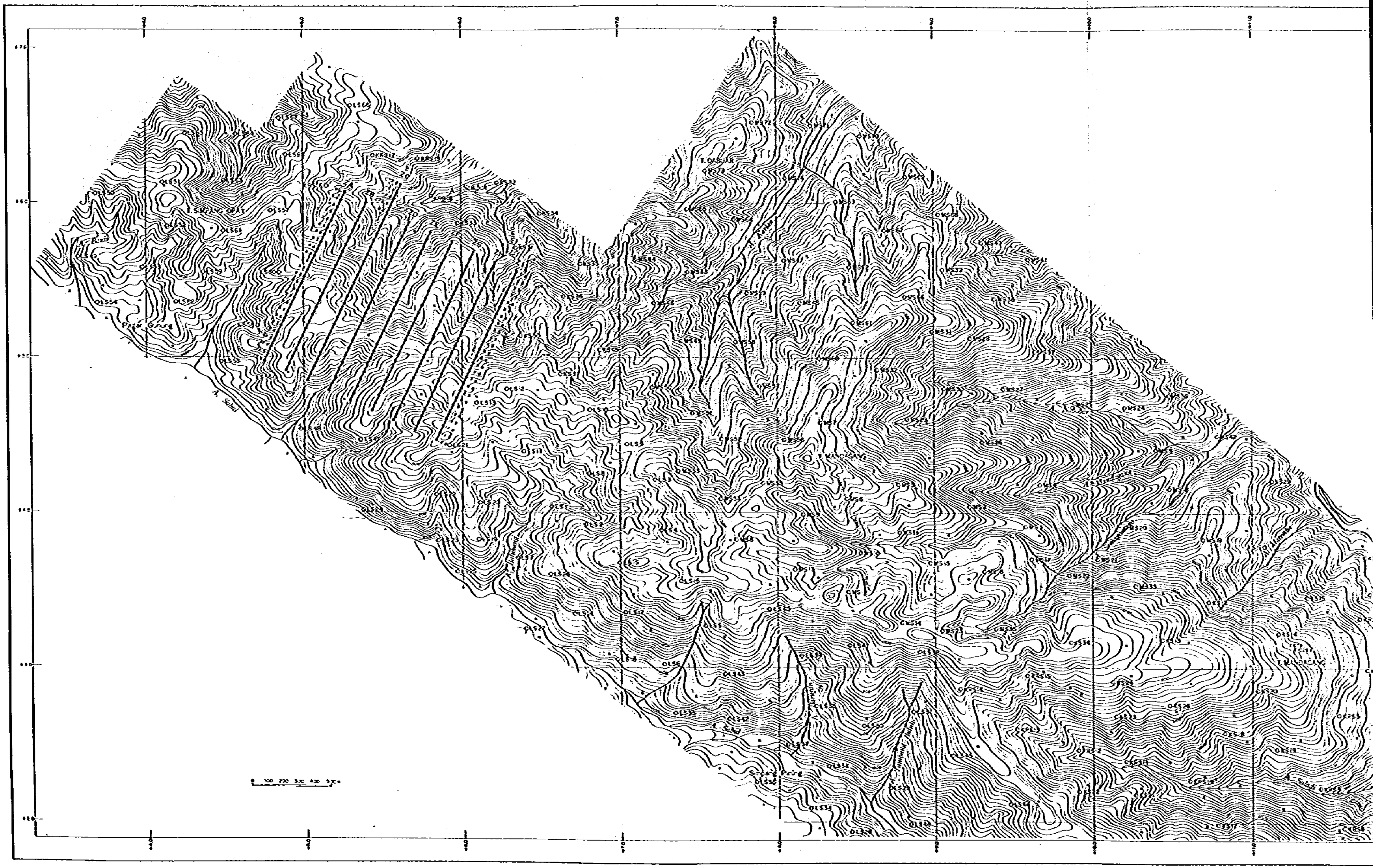

Fig. II-3-34 Location Map of Geochemical Samples in Mua

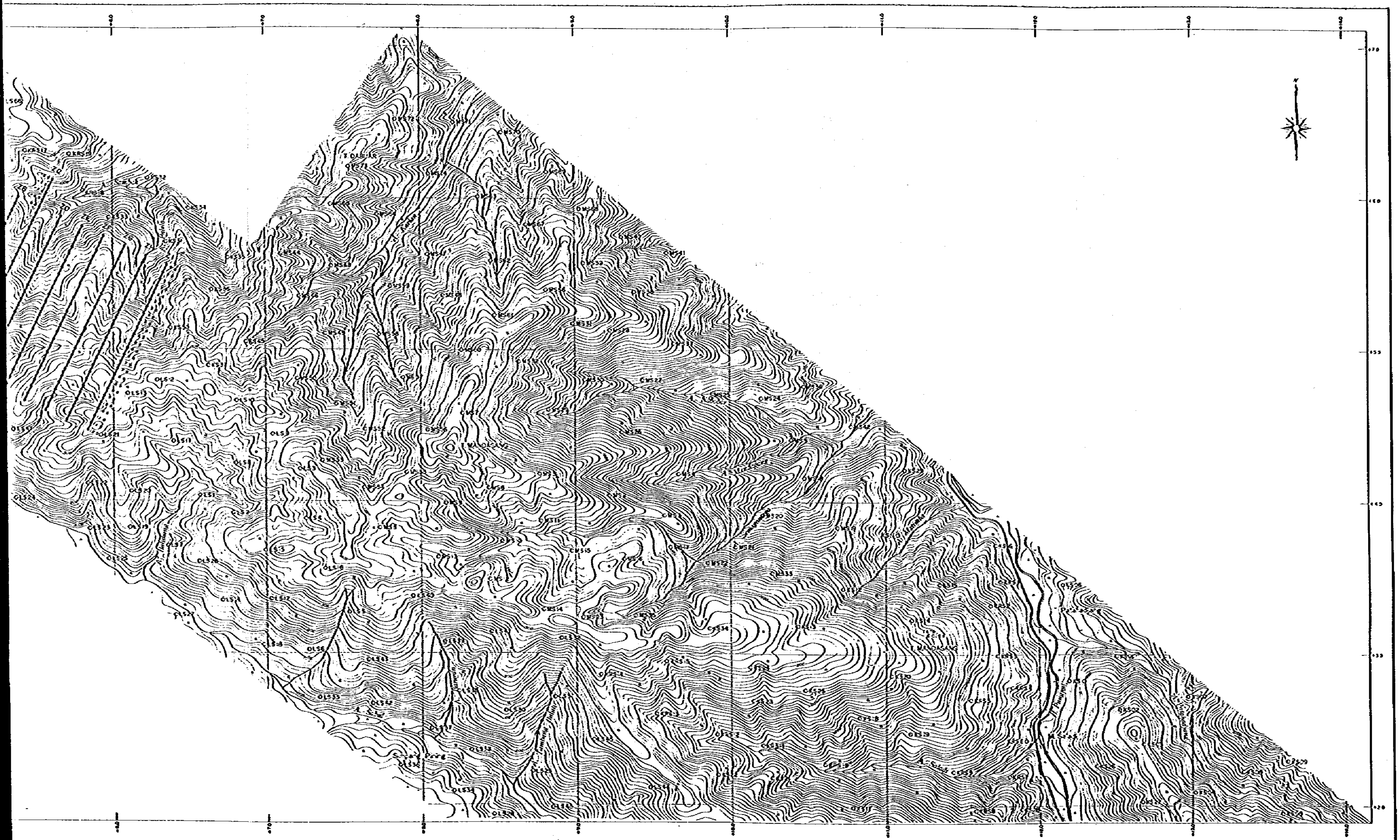

Fig. II-3-34 Location Map of Geochemical Samples in Muara Sipongi Area B

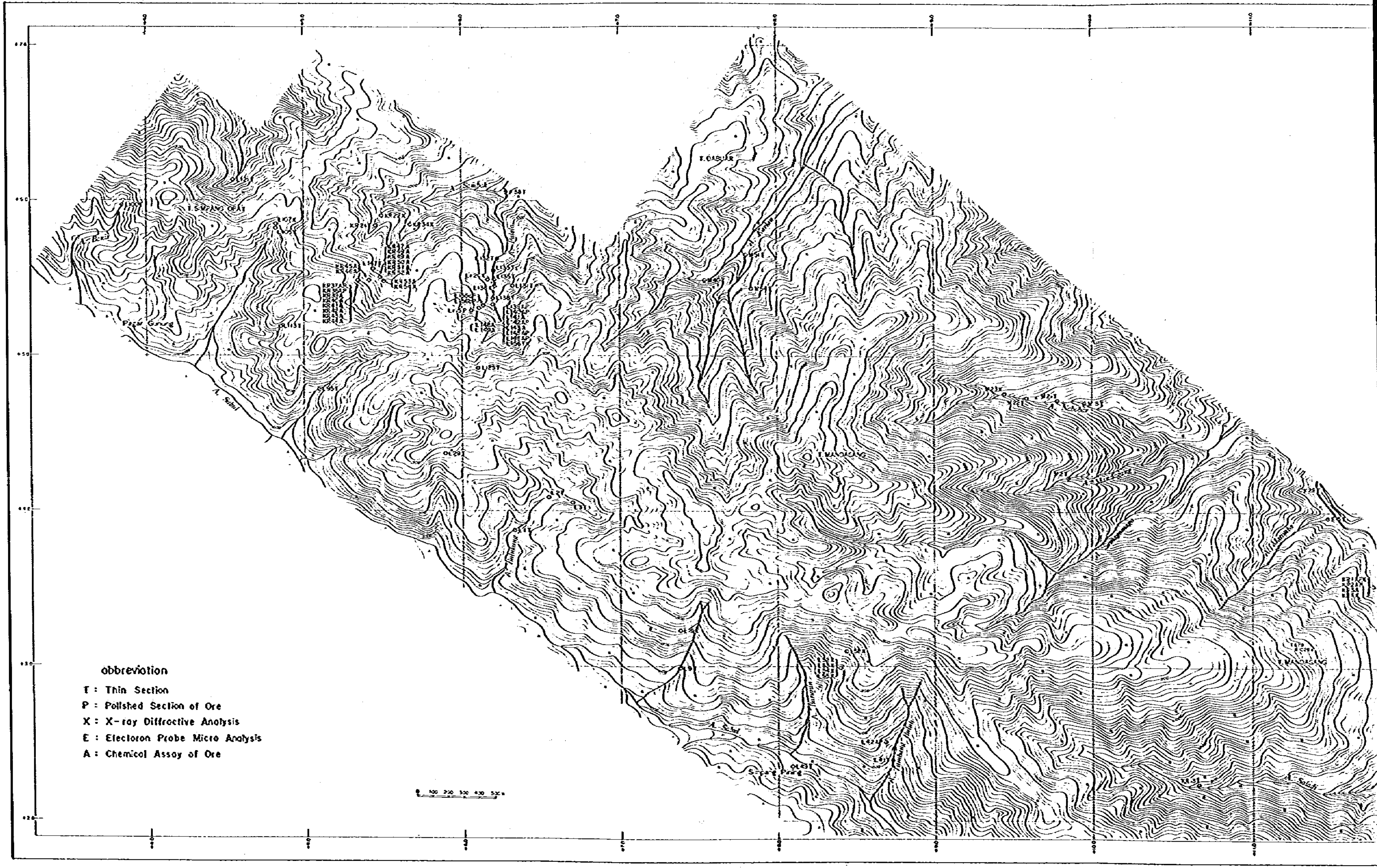

Fig. II-3-35 Location Map of Rock and Ore Samples Tested in

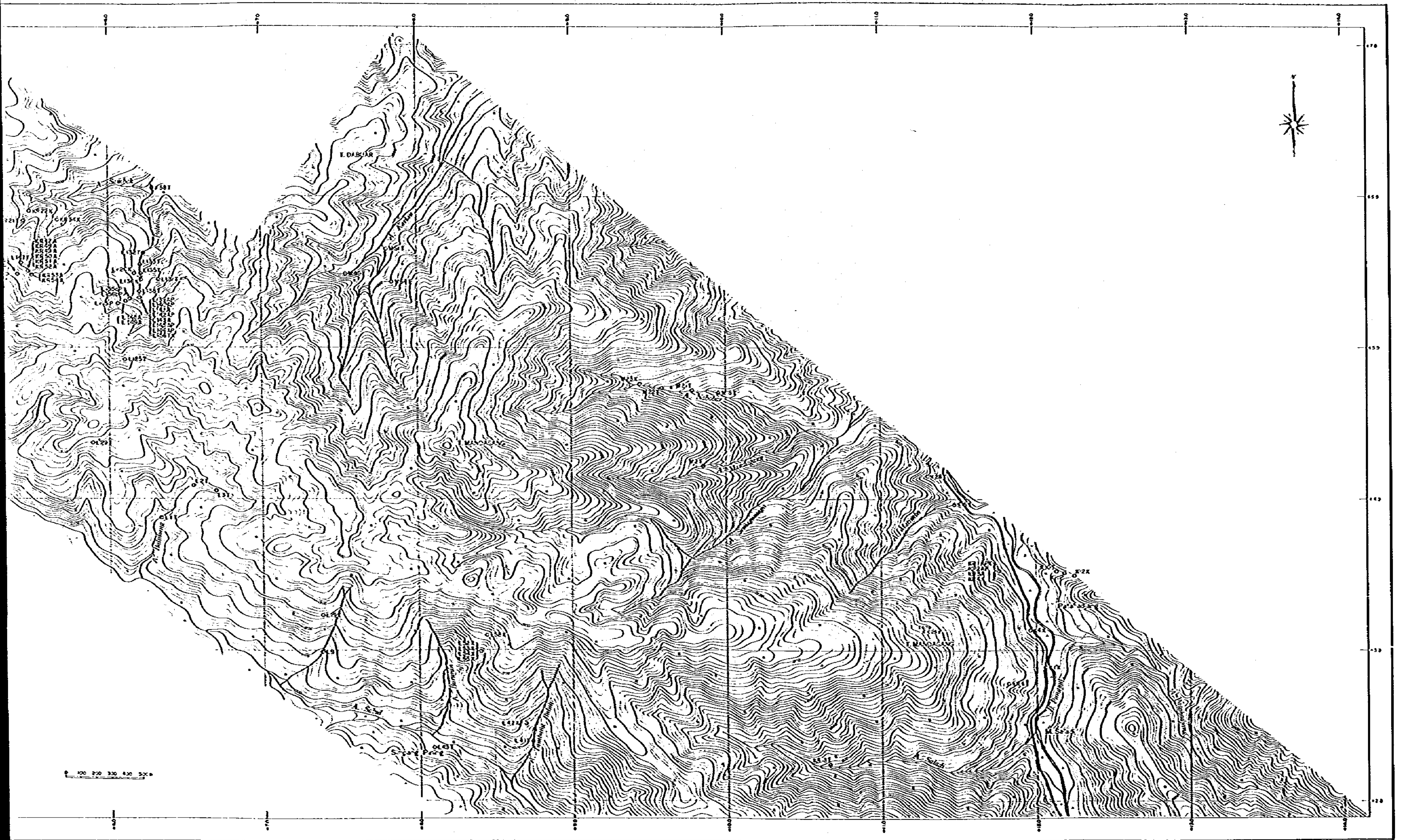

Fig. II-3-35 Location Map of Rock and Ore Samples Tested in Muara Sipongi Area B

PART III

GEOPHYSICAL SURVEY

(SPECTRAL INDUCED POLARIZATION METHOD)

CHAPTER 1 GENERAL DISCUSSION

1-1 THE PURPOSE OF THE SURVEY

In the first phase survey (1982), a reconnaissance survey consisting of geological and geochemical survey was conducted in the Muara Sipongi area, (extending over a 400 km^2 area). The distribution of several outcrops containing copper, lead and zinc sulphides were confirmed in Pagar Gunung. These deposits are of a contact metasomatic skarn type.

The outcrops can be sporadically found in a 200 meter elongated zone, extending in an East-West direction, however, the continuous extent of the deposits at the surface could not be traced due to the dense growth of the tropical rain forest.

In order to conduct a geophysical survey which would give clear results, the Spectral IP method was used. This method makes it possible to identify the kind of mineral, or type of deposit which exists, by means of the spectral responses to magnitude and phase. This method is the most modern method which is used for ore deposit surveys, as it allows for reliable acquisition of deep, low resistivity zones, by de-coupling the electro-magnetic phenomena, which was difficult to achieve by using the conventional IP method.

1-2 AREA OF THE SURVEY

The area of the survey is located to the south-east of Kotanopan, 9 kilometers away. The terrain has generally steep slopes, which are covered with dense tropical rain forest. However, the mountain tops are generally smoother and the vegetation is less dense than that of the sides (Fig. III-1-1).

1-3 THE QUANTITY OF WORK AND THE SURVEY PERIOD

There were a total of 9 survey lines, with a total length of 11,000 meters. The individual line lengths, and their results are shown below, in Table III-1-1:

Table III-1-1 List of Survey Lines

No.	Name of Line	Length of Line (m)	Measurement Value (point)
1	Line A	1,200	40
2	Line B	1,200	39
3	Line C	1,400	49
4	Line D	1,200	40
5	Line E	1,200	40
6	Line F	1,200	40
7	Line G	1,200	40
8	Line H	1,200	40
9	Line I	1,200	40
	Total	11,000 (m)	368 (point)

Survey Period

Mobilization and Preparation	From 30 May 1983 to 13 June 1983
Line Brushing and Survey	From 11 June 1983 to 9 July 1983
SIP Data Acquisition	From 14 June 1983 to 18 July 1983
Data Processing at Site	From 19 July 1983 to 12 August 1983
Demobilization	13 August 1983
Data Processing, Physical Property Measurement and Interpretation	From 15 August to 31 December 1983
Submittal of Report	10 February 1984

Specifications

(1)	Total Line Length	11,000 m
(2)	Number of Lines	9 lines
(3)	Number of Data Point	368 points
(4)	Line Interval	150 m
(5)	Station Interval	100 m
(6)	Electrode Separation Factor	n = 1 - 5
(7)	Electrode Configuration	Dipole-Dipole Array

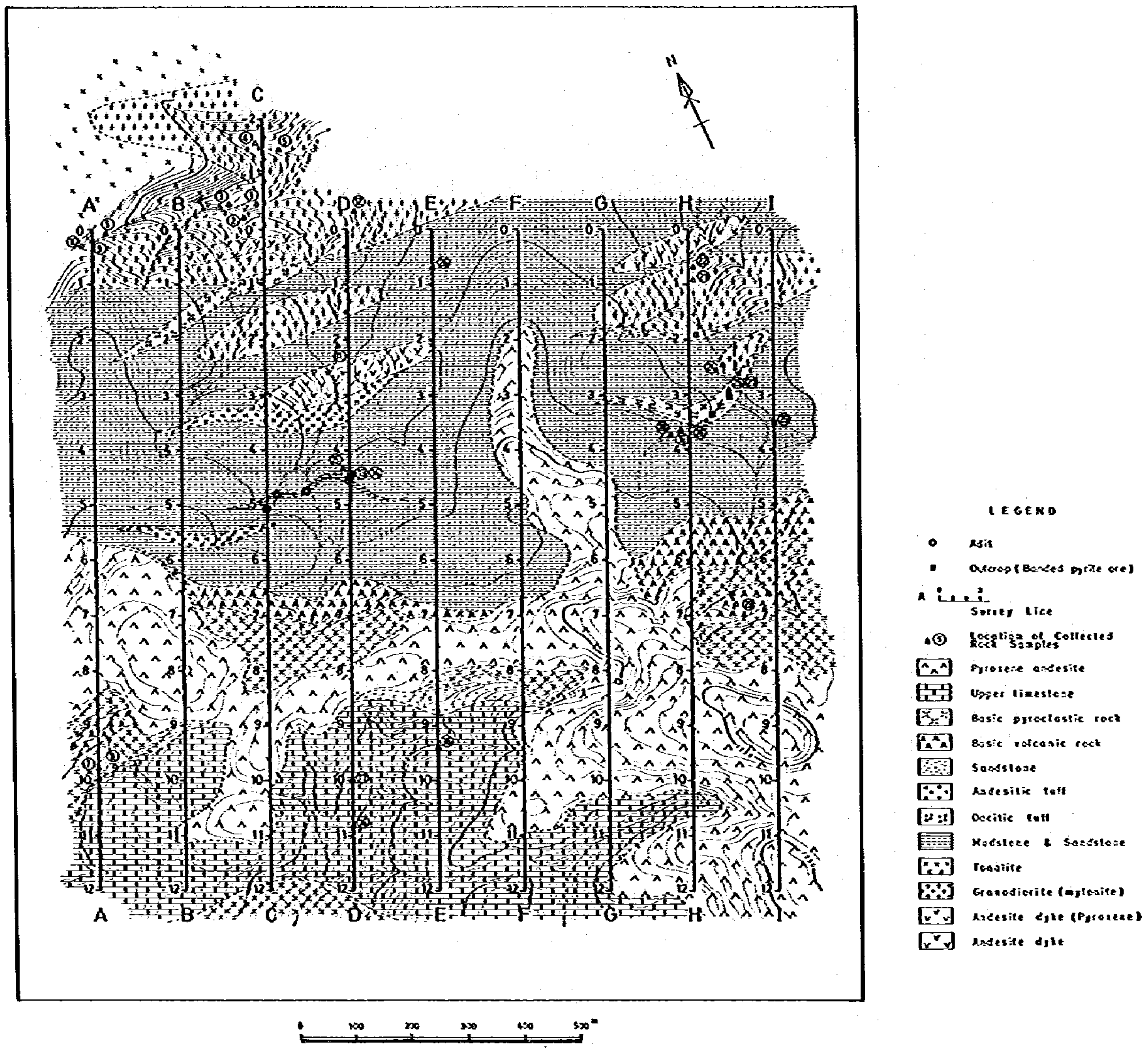

Fig. III-1-1 Location Map of Spectral IP Survey Lines

CHAPTER 2 SURVEY METHOD

The Spectral IP method gives the ability to survey the magnitude and phase, using a wide variety of frequencies from 0.001 to 1,000 Hz. This method has the advantage over the former method, as it has the ability to discriminate between the anomalous IP source from the frequency responses (spectral responses) of the stratum and the ore body. On the other hand, the conventional IP method only surveys the resistivity of the two frequencies. The frequency range most often used is from 0.1 to 100 Hz for all practical reasons. In this present survey a system of the Zongé Engineering & Research Organization, which is the manufacturer of the equipment were used whose frequency range is from 0.125 - 88 Hz. In this survey, three fundamental frequencies of 0.125 Hz, 1 Hz, and 8 Hz were adopted. A Fourier analysis of these frequencies, and also their third, fifth, seventh, ninth and eleventh harmonics were surveyed, to check the IP responses.

2-1 SURVEY METHOD

The survey technique for the Spectral IP method is basically not so different than the technique for the conventional IP method, in that they both use dipole-dipole electrode configurations in the frequency domain. However, in the Spectral IP method it is necessary to record the same period in time of the signals, in both the transmitter and receiver, as the Spectral IP survey uses the magnitude and phase in higher frequencies. In order to accomplish this timing of the signals, a "communication wire" connecting the transmitter and receiver, is laid parallel to the survey line. The layout of these lines is shown in Figure III-2-1.

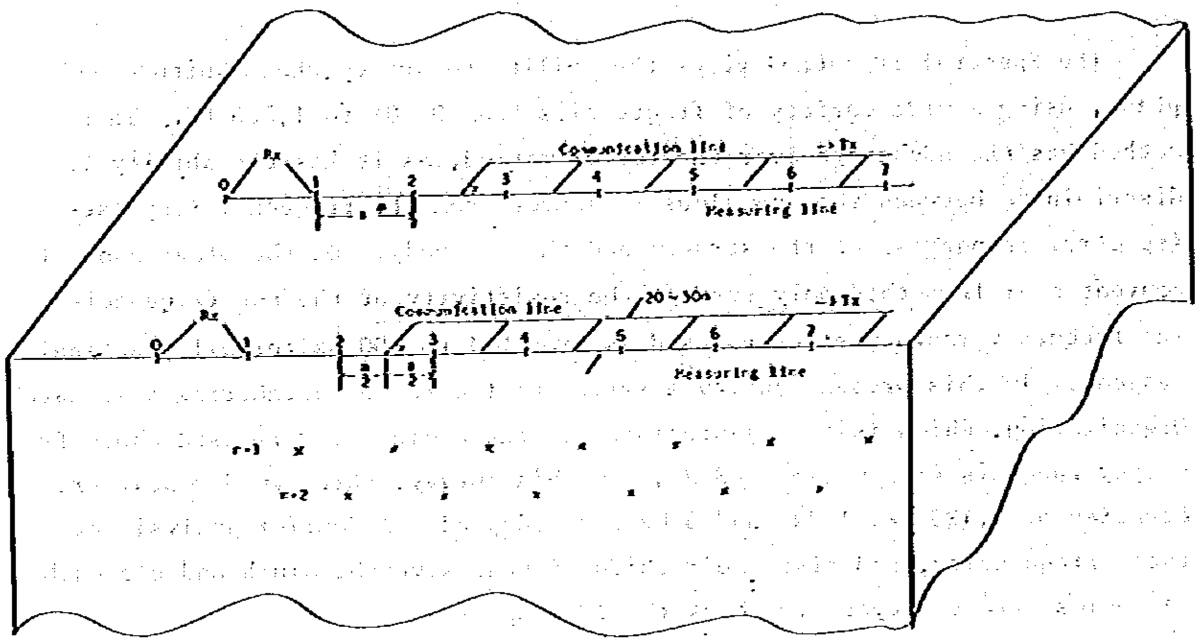

Fig. III-2-1 Spectral IP Survey Lines

The Layout of the Potential Electrodes

In this survey, non-polarizable potential electrodes were used. These electrodes consist of a saturated copper sulphate solution, contained in a porous pot with a copper conductor. Three electrodes are placed together, this is different from the ordinary IP method. (see Figure III-2-2).

This arrangement enables better noise rejection in the differential preamplifier, as a zero electric potential point is established at point (B), exactly the same distance between points (A) and (C).

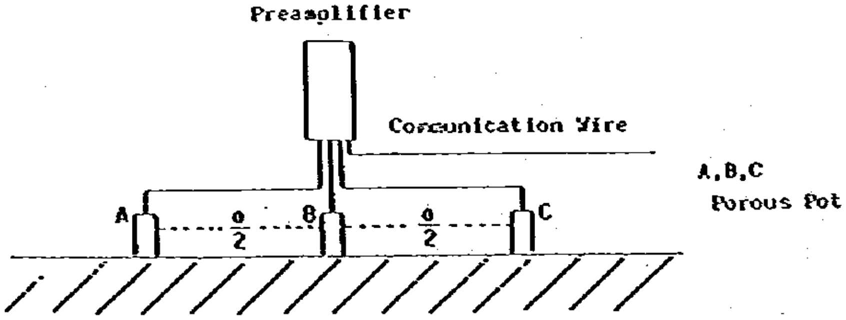

Fig. III-2-2 Arrangement of Potential Electrodes & Preamplifier

The Layout of the Current Electrodes

When the current electrodes are laid out, the future mobility and operational efficiency of the electrodes are taken into consideration. Normally, 7 or 9 electrodes are placed ahead of time, and the connections are changed at the transmitter, as required. In this survey a 9 electrode configuration was used. This arrangement is shown in Figure III-2-3.

The electrodes consist of 8 Stainless Steel wires, with a diameter of 5 mm, they are 0.60 meters long. If the resistance to earth is very high, the number of electrodes is doubled, to give a total of 16.

Fig. III-2-3 Arrangement of Current Electrode & Wires

2-2 MEASURING EQUIPMENT

The equipment used in this survey is manufactured by Zonge Engineering and Research Organization Co., from Tucson, Arizona, U.S.A. The component parts of this equipment are described in Table III-2-1, and a typical measurement configuration is shown in Figure III-2-4.

Table III-2-1 Survey Equipments

Data processor	GDP-12/2G	1
Pre-amplifier	PP-12	2
Isolation amplifier	ISO/1	2
Cassette-printer	CAP-12	1
Oscilloscope	Tektronix 212	1
Transmitter	FT-1 Geotronics	1
Engine generator	ZMG-5	1
Voltage regulator	VR-1	1

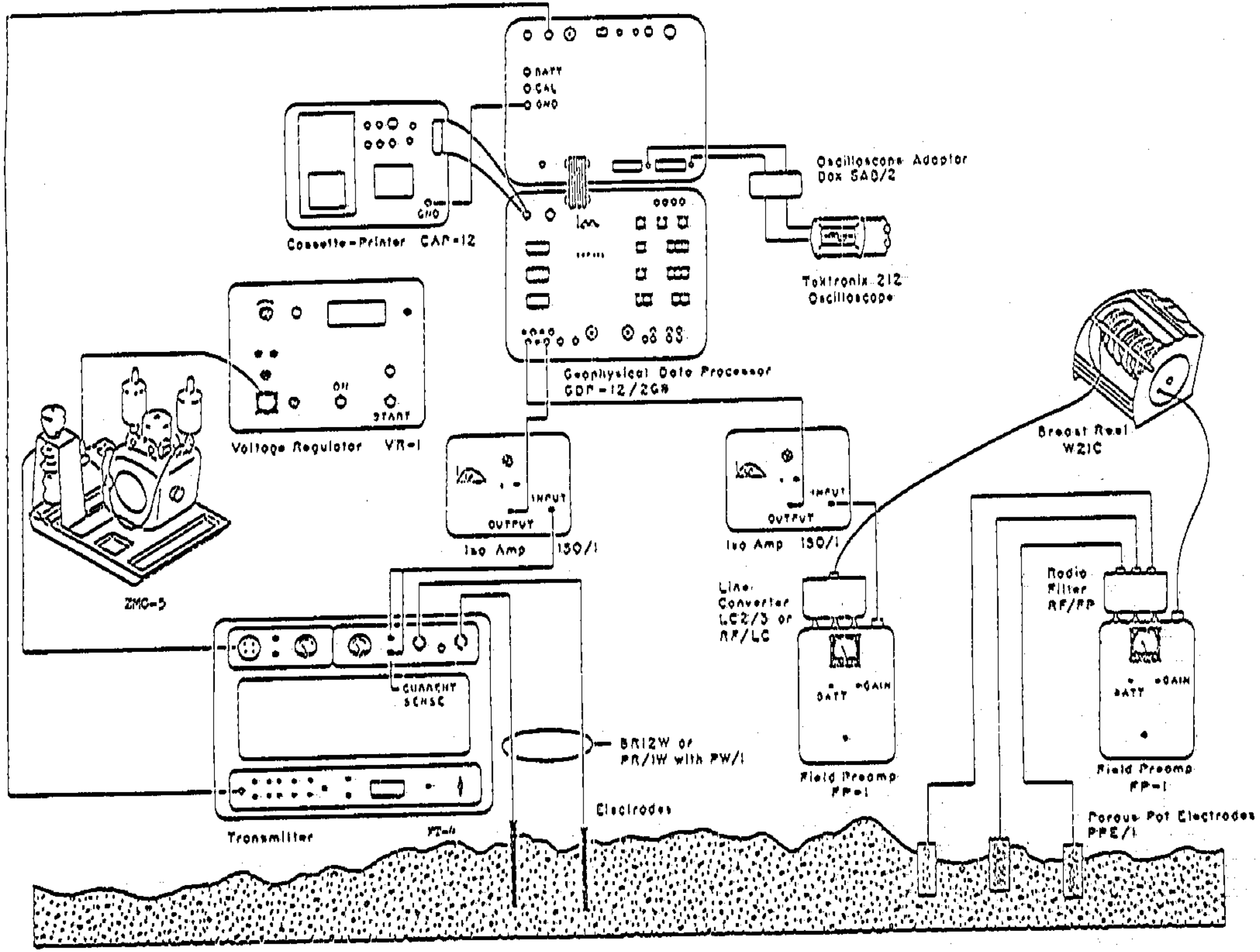

Fig. III-2-4 Block Diagram of Spectral IP Survey Instruments

In the Spectral IP method, the magnitude and the phase of the signal are measured, the results are plotted as the spectrum versus the frequency, or the Cole-Cole diagram, as it is called. Apparent resistivity, 3 point de-coupled phase, and so on are shown as a pseudo-section, which is the same as the former IP method.

The Conception of Spectral IP

The conception of spectral IP is shown in Figure III-3-1, where (a), shows a small section of a mineralized rock, which has both blocked and un-blocked pore pasages. If this is depicted in an equivalent circuit, then it appears like (b). (c) shows the time domain responses, while (|Z|) and (ϕ) are the measuring value in spectral IP.

In Figure III-3-2, the concept of in-phase and out-of-phase are shown. When the arbitrary amplitude rectangular waveforms are transmitted, the signals, which phase-shift, are (ϕ), with an amplitude of (V) obtained at the receiver.

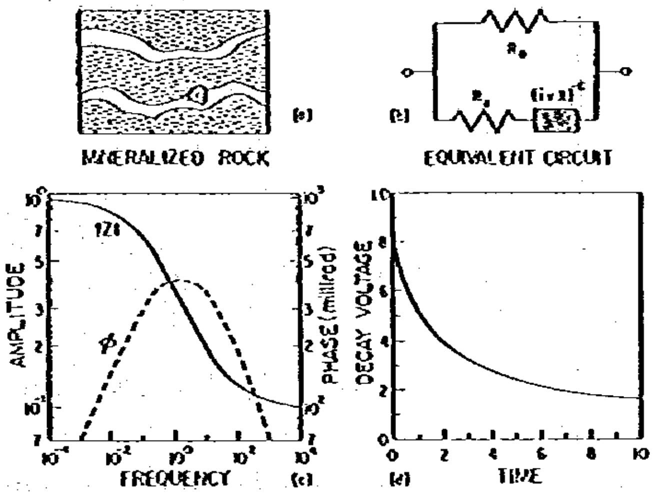

Fig. III-3-1 Spectral IP Effect

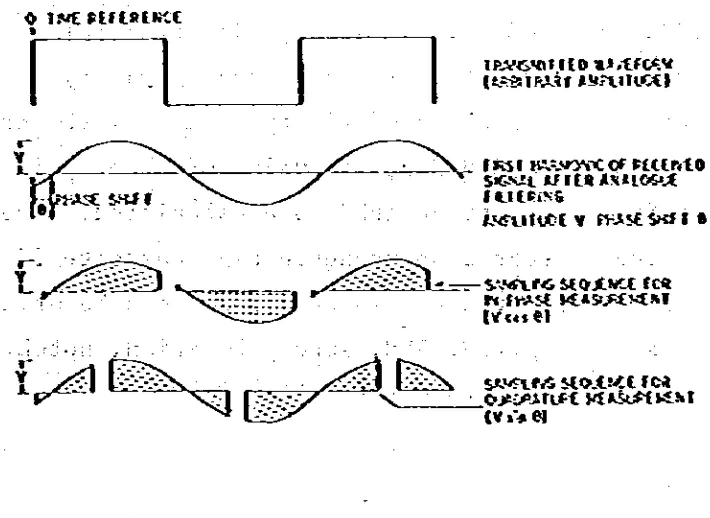

Fig. III-3-2 Transmitting & Receiving Wave-forms

The sampling sequences for in-phase and quadrature measurement are shown in the graphs in the loewr part of Figure III-3-2. The relation between frequency effect and phase angle is shown in Figure III-3-3, in this figure the Cole-Cole diagram is adopted, with the Vertical axis showing negative out-of-phase factors, and the horizontal axis showing positive in-phase factors. The magnitude (M_1) is at 0.1 Hz, and (M_2) is at 1 Hz, the phase angle is (ϕ_1) and (ϕ_2). Frequency effects and in-phase factors are approximately directly proportional to each other, and the phase angle and out-of-phase factors are directly proportional to each other. The black dotted line in the figure shows the results of the measurement, with the lower frequencies occurring to the right, and the higher frequencies occurring to the left.

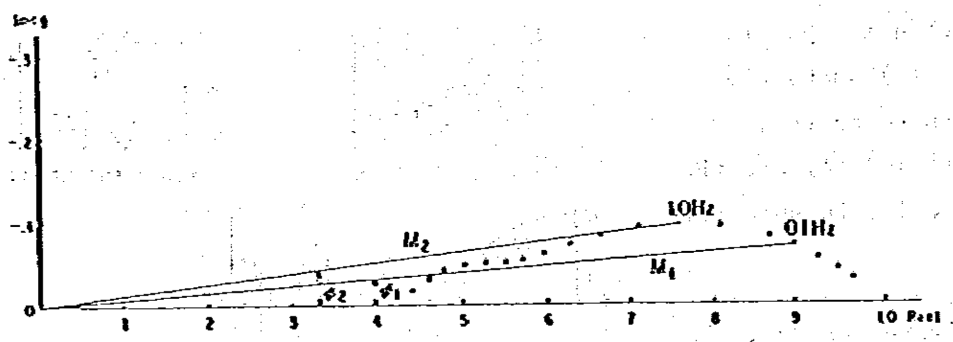

$$PFE = \frac{M_1 - M_2}{M_2} \times 100\% \quad \text{(0.1 to 10 Hz decade)}$$

Fig. III-3-3 Relation between Frequency Effect & Phase Shift

3-1 DATA MANIPULATION

Data from field measurements give phase shift and amplitude of eighteen frequencies, from 0.125 Hz to 88 Hz. These signals are recorded and inputted to the data Processor (GDP-12G), where the real and imaginary part of each frequency are calculated, as are the resistivity values of the three fundamental frequencies (0.125, 1, and 8 Hz), the value of three point de-coupled phase and the percent frequency effect (PFE) are calculated. The results are printed out, and can also be stored on magnetic tape cassette if necessary. Other data relevant to the survey are also stored and can be printed out, these include; the current supplied, SEM, survey location, notch filter setting, and stacking number, (see Figure III-3-4).

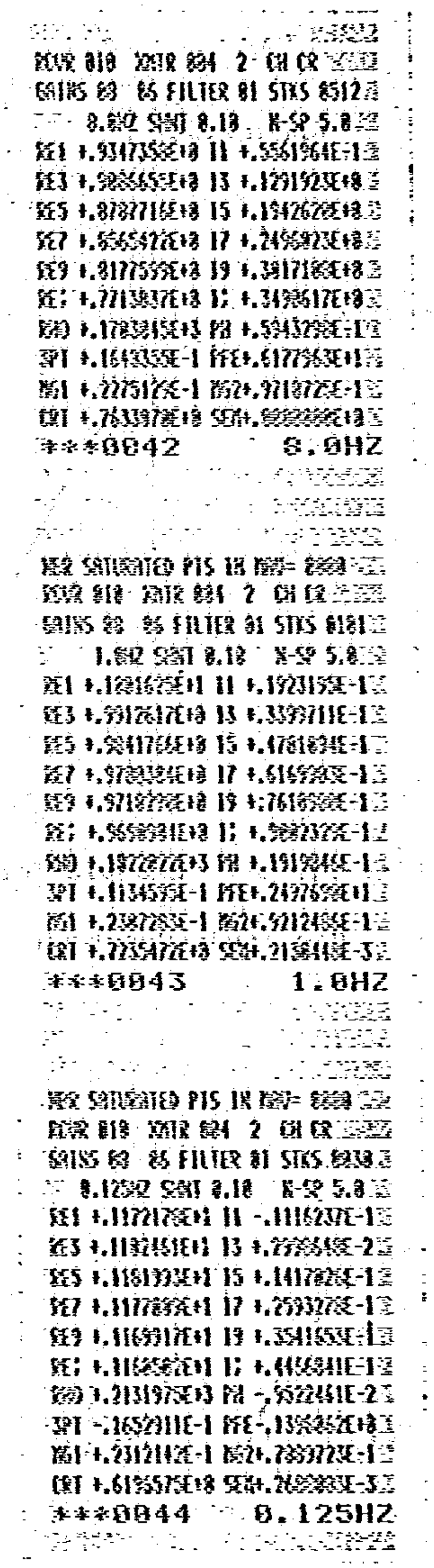

Index

RCVR ; Receiver position
XMTR ; Transmitter position
2 CH CR ; 2channel Spectral IP
Gains ; Gain of channel 1,2
Filter 01 ; Notch filter "ON"
STKS ; Number of stucking
8.0 Hz ; Transmitted frequency
SHNT ; Shunt resistor
N-SP; Electrode spacing factor
RE1: ; Real part (left side)
I1 ; Imaginary part (right side)
RHO ; Apparent resistivity
PH ; Raw phase
3PT ; 3 point decoupled phase
MG1, MG2 ; Magnitude of channel 1,2
CRT ; Transmitted current
SEM ; Standard error mean

Fig. III-3-4 Example of field data print out

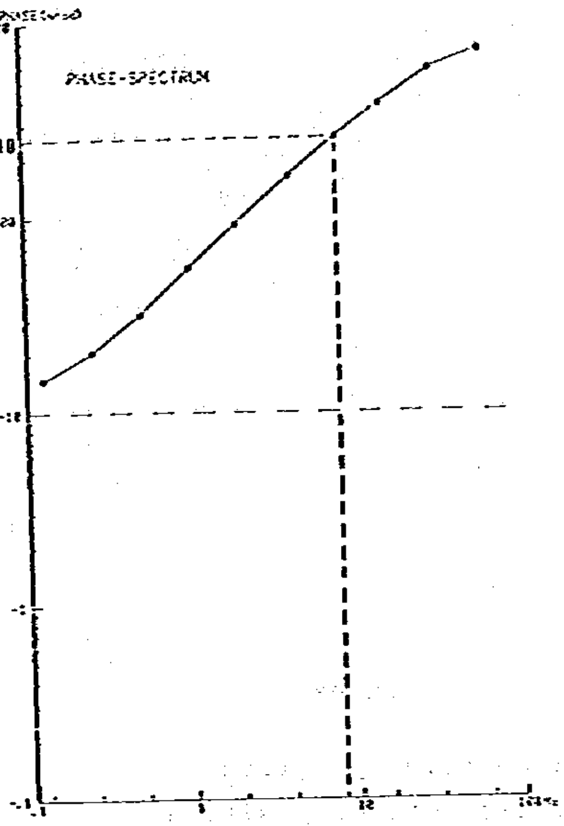

Fig. III-3-5 Example for

Phase Spectrum

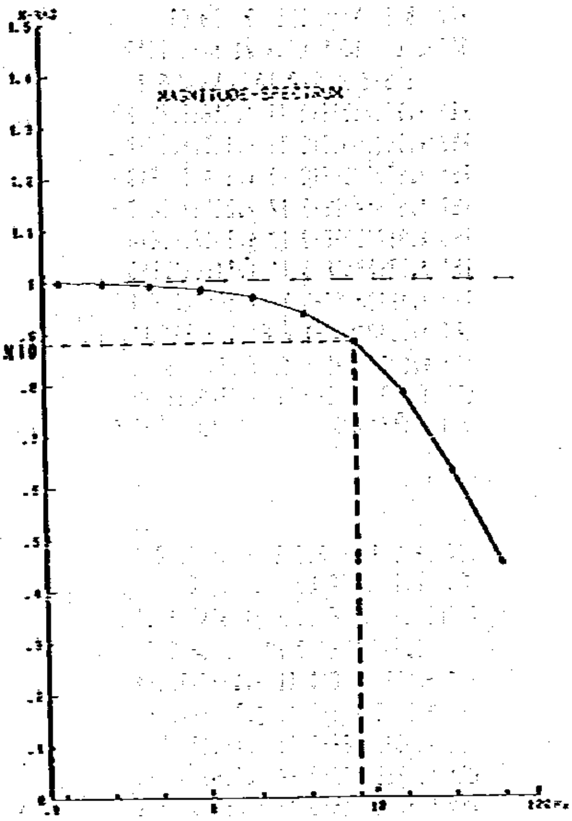

Fig. III-3-6 Example for

Magnitude Spectrum

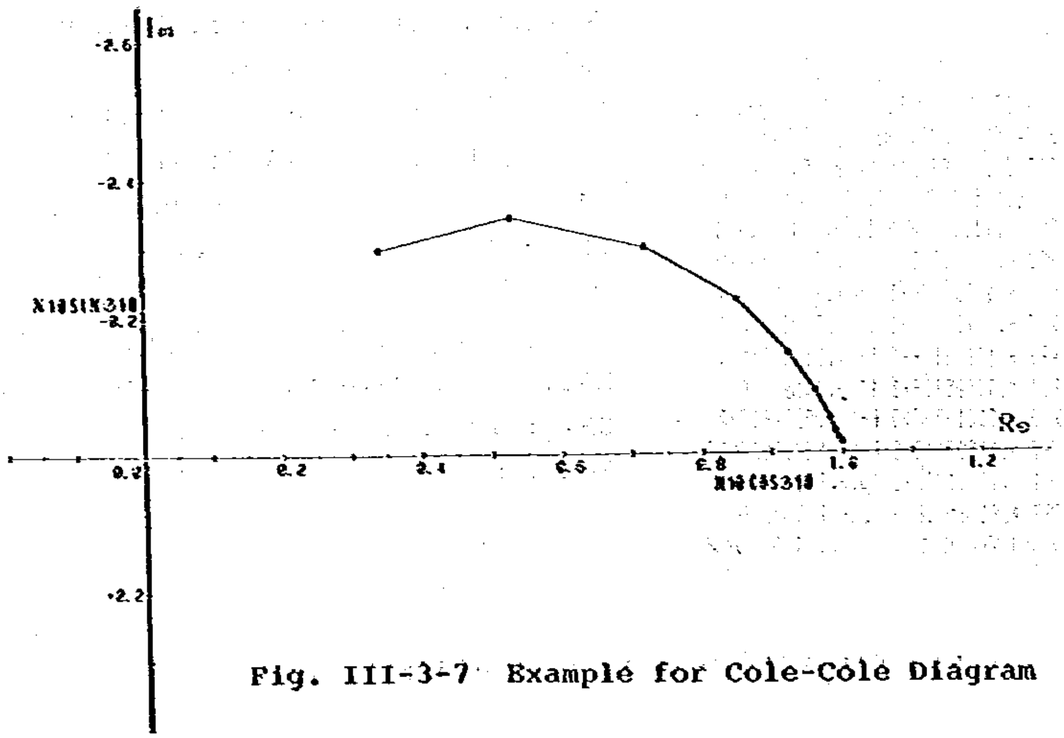

Fig. III-3-7 Example for Cole-Cole Diagram

As data manipulation occurs, a pseudo-section is normalized, also a calibration correction and any topographic corrections are applied if necessary, to the resistivity curves.

Calibration Correction

A daily calibration measurement was taken, prior to any field measurements, the values received in this measurement were then removed from subsequent signal measurements at each point, in order to be sure that only the correct earth signal was being calculated. Phase spectrum (Figure III-3-5), magnitude spectrum (Figure III-3-6), and a Cole-Cole diagrams (Figure III-3-7), were made for the surveyed values, after the calibration.

3-2 TOPOGRAPHIC CORRECTIONS

Generally, when a dipole-dipole electrode array is used, then the topography strongly effects the apparent resistivity values. The tendency is that topographic highs produce correspondingly higher apparent resistivity values, and topographic lows produce correspondingly lower apparent resistivity values. As this survey was in a mountainous region, then corrections for these elevation changes were made, especially to the south, on survey lines B, D, E and G. The topographical section was measured for each of these survey lines, these measurements were inputted in the computer, which then calculated the effects of the topography to the apparent resistivity. These calculated effects were then used to correct the observed results from the survey lines.

3-3 ROCK SAMPLE MEASUREMENT

In order to evaluate the observed results of the resistivities and spectral responses of magnitude and phase of the rocks which are found in the survey area, a total of 29 rocks and ore samples were collected from the surface of the survey area. These samples were sent to Japan to be analyzed for their properties, Figure III-3-8 shows the test measurement installation.

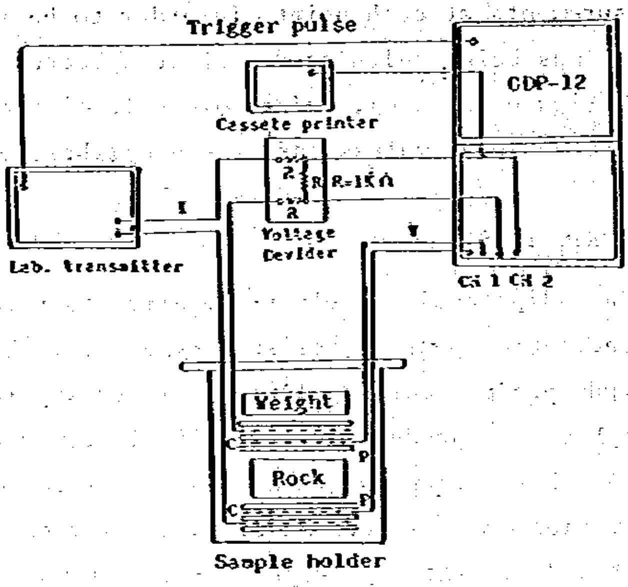

Fig. III-3-8 Block Diagram for Sample Measurement

It seems dangerous and limited to try to represent the resistivity and spectral responses for phase and magnitude of these surface samples as being the same as the sub-surface rocks in the same area; however, it is important to know the types and qualities of the local rocks, and especially for the anormalous rocks by Spectral IP method.

The results from these samples can be categorized by their spectrum which fall into four groups, as follows:

Type A : The spectrum which decreases slowly as the frequency decreases.

Type B : The spectrum which shows the minimum vlaue in the 3 - 5 Hz range, and increases in the low and high frequencies.

Type C : The spectrum which shows almost a horizontal line.

Type D : The spectrum which increases as the frequency increases.

Table III-3-1 Results of Rock Sample Measurement

Sample No.	Rock Name	Block No. of Print Out	Resistivity (Ω-m)	Raw Phase (-mrad)	3 point Decoupled Phase (-mrad)	PFE (%)	Spectral Type of Phase	Remarks
1	Muscovite granodiorite (Mylonite)	69∼74	542	26.0	32.8	2.08	A	Py-diss
2	Muscovite granodiorite (Mylonite)	58∼63	457	21.3	25.0	2.10	B	
3	Muscovite granodiorite (Mylonite)	52∼57	1840	17.7	18.0	2.23	D	Py-diss
4	Muscovite granodiorite (Mylonite)	81∼85	414	27.2	30.4	2.83	B	Fine Py vein
5	Muscovite granodiorite (Mylonite)	39∼44	722	17.9	20.6	1.64	B	
6	Quartz vein	63∼68	2690	20.5	20.5	2.57	C	Py network
7	Fine grain Andesite	70∼75	2200	4.98	4.87	0.67	D	
8	Basic tuffacious sandstone	33∼38	5020	16.2	16.3	2.01	D	
9	Muscovite granodiorite	21∼26	1090	25.6	27.4	3.07	B	Py network
10	Meta andesite	82∼87	3310	10.2	10.3	1.43	D	Py-Imp
11	Silicious mudstone	15∼20	6360	6.17	6.00	0.73	C	
12	Muscovite granodiorite	87∼90	644	15.4	17.3	1.62	C	Py network
13	Black ore (Pb + Zn + Py)	34∼39	130	93.0	111	9.28	A	
14	Black ore (Limonitized) (Pb + Zn)	13∼18	163	133	150	13.2	A	
15	Black ore (Pb + Zn + Py)	27∼32	61.0	436	456	69.5	A	
16	Andesitic tuff	31∼33	2370	9.50	11.3	0.92	B	
17	White limestone	1∼6	7630	5.24	4.83	0.75	D	
18	White limestone	57∼62	24300	4.90	4.93	0.59	D	
19	Sandstone	2∼4, 6.7	1230	16.0	20.1	1.34	B	
20	Sandstone	76∼81	1230	10.5	13.4	0.82	A	Quartz vein
21	Muscovite granodiorite	9∼14	2340	15.4	16.0	1.58	D	
22	Silicious andesite	25∼30	7730	23.3	24.7	4.47	D	Py-Imp
23	Altered andesite	46∼51	45.9	90.3	130	4.65	A	
24	Muscovite granodiorite	45∼50	433	38.8	49.5	3.23	A	
25	Banded pyrite ore	64∼69	45.3	428	437	75.3	A	
26	Limonite gossan	7∼12	831	28.0	31.9	2.99	C	Porous, Py-Imp
27	Banded pyrite ore	18∼24	168	435	429	61.7	A	
28	Dacitic tuffacious sandstone	51∼56	2550	60.7	62.6	7.63	A	Py, Pb + Zn-Imp
29	Dacitic tuffacious sandstone	75∼80	1810	11.2	11.9	1.28	C	

Sample NO.1

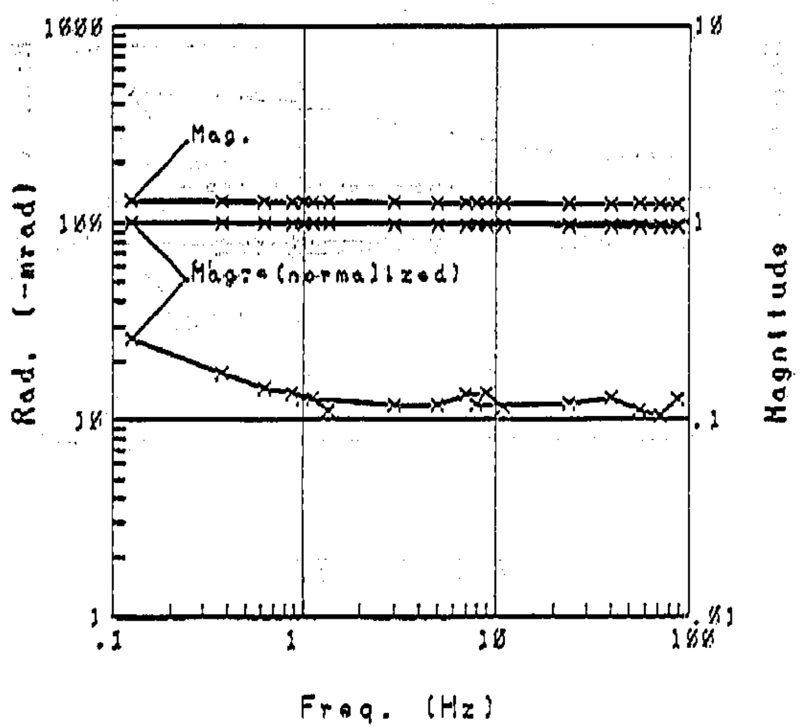

Fig.III-3-9.1 Spectrum of phase & Magnitude
(Sample No.1)

Sample NO.2

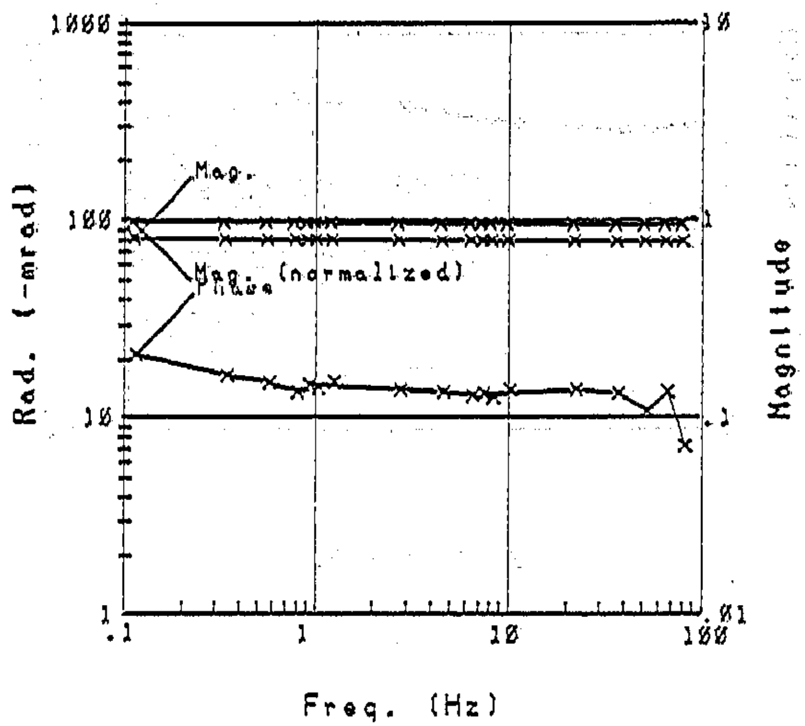

Fig.III-3-9.2 Spectrum of phase & Magnitude
(Sample No.2)

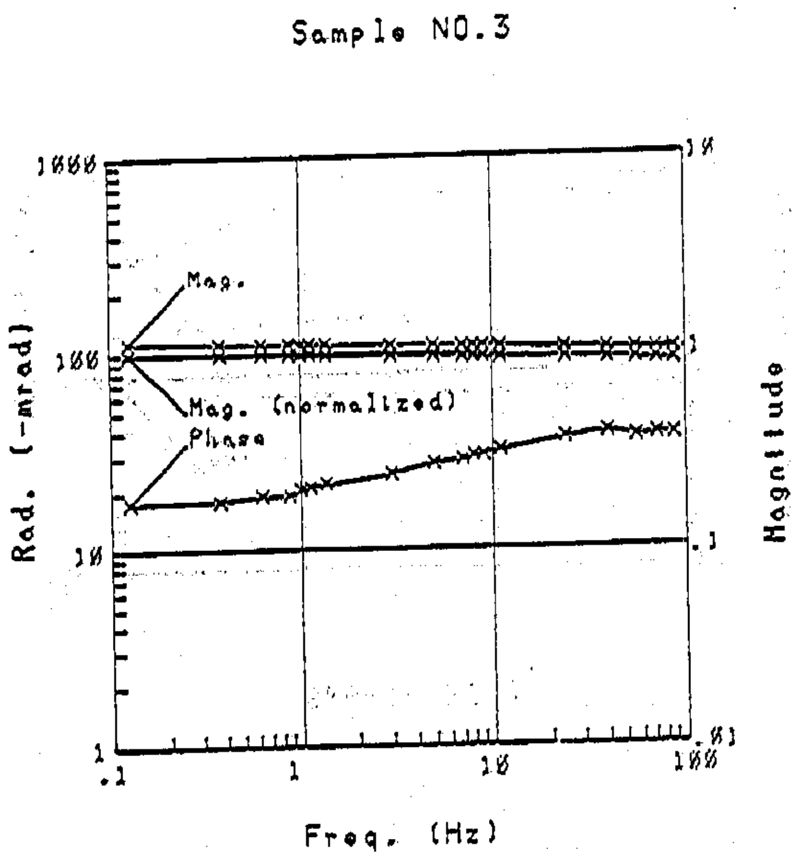

Fig.III-3-9.3 Spectrum of phase & Magnitude (Sample No.3)

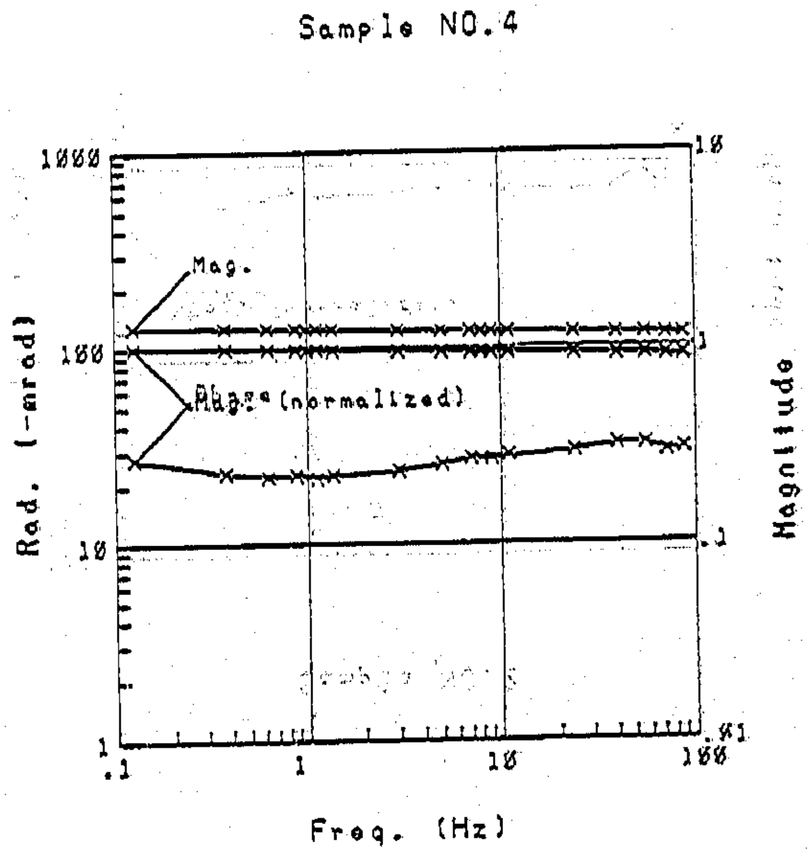

Fig.III-3-9.4 Spectrum of phase & Magnitude (Sample No.4)

Sample NO.5

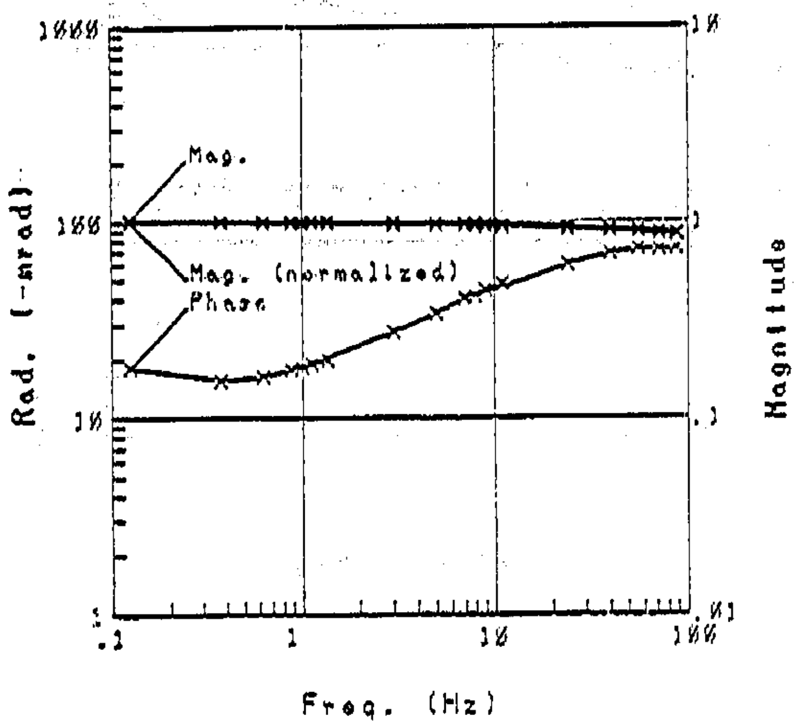

Fig.III-3-9.5 Spectrum of phase & Magnitude

(Sample No.5)

Sample NO.6

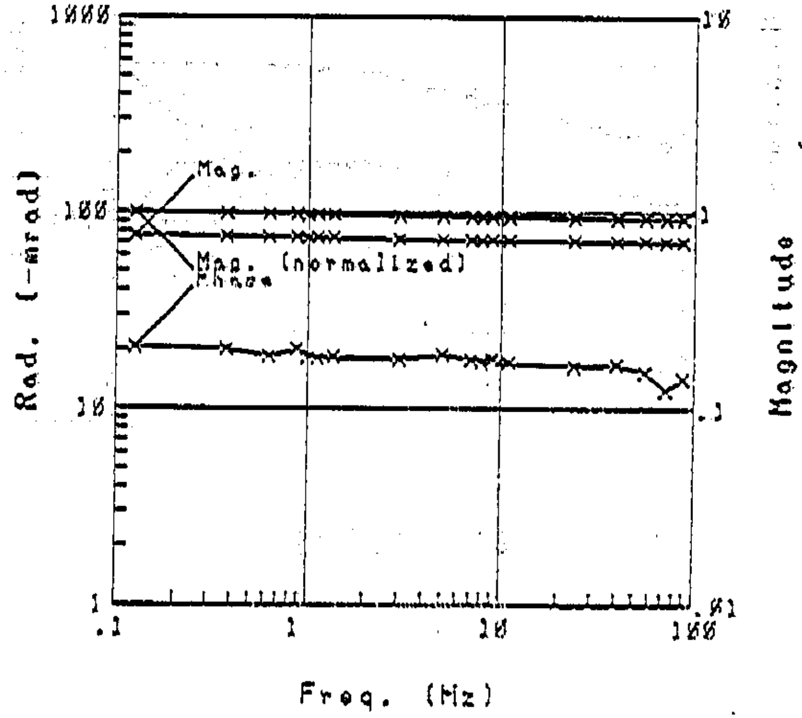

Fig.III-3-9.6 Spectrum of phase & Magnitude

(Sample No.6)

Sample NO.7

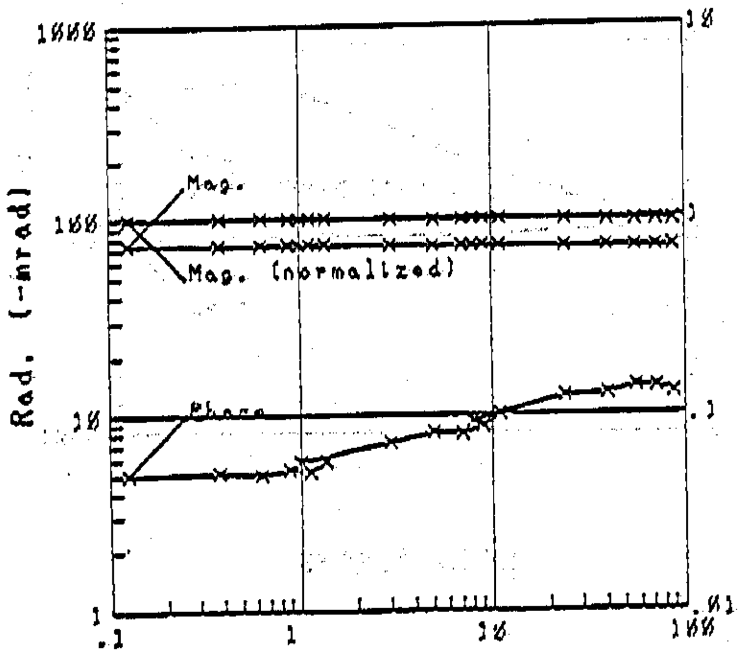

Fig.III-3-9.7 Spectrum of phase & Magnitude
(Sample No.7)

Sample NO.8

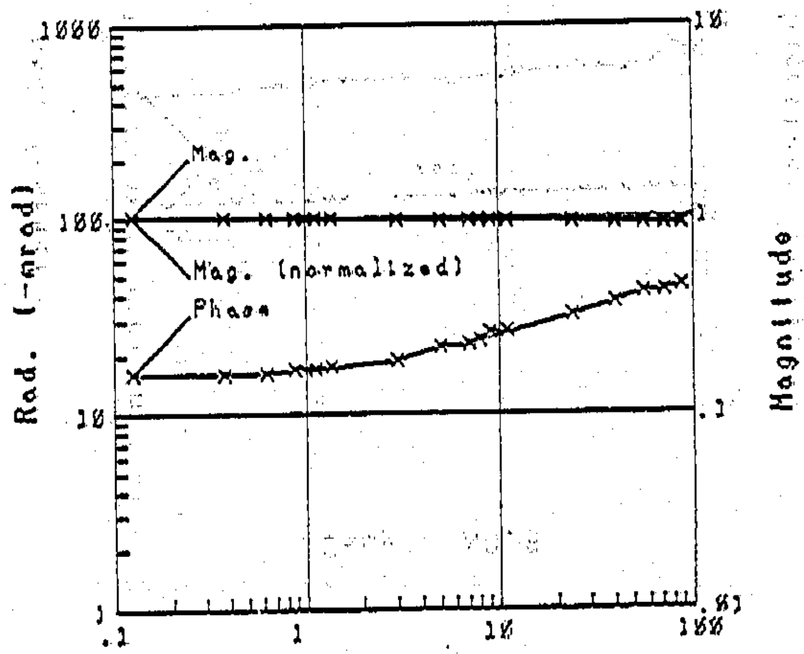

Fig.III-3-9.8 Spectrum of phase & Magnitude
(Sample No.8)

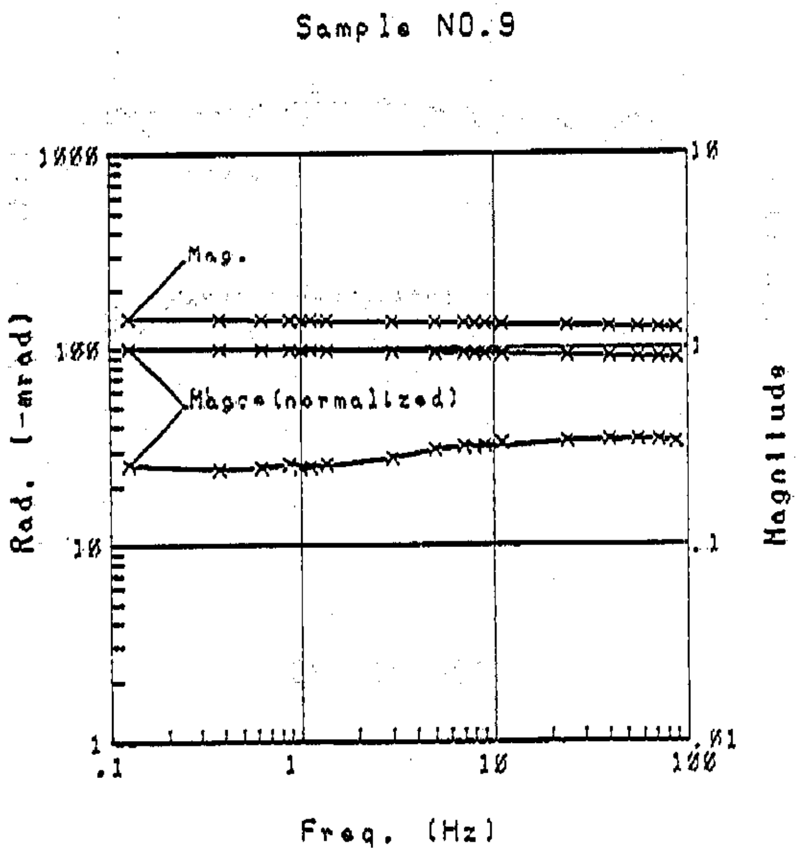

Fig.III-3-9.9 Spectrum of phase & Magnitude (Sample No.9)

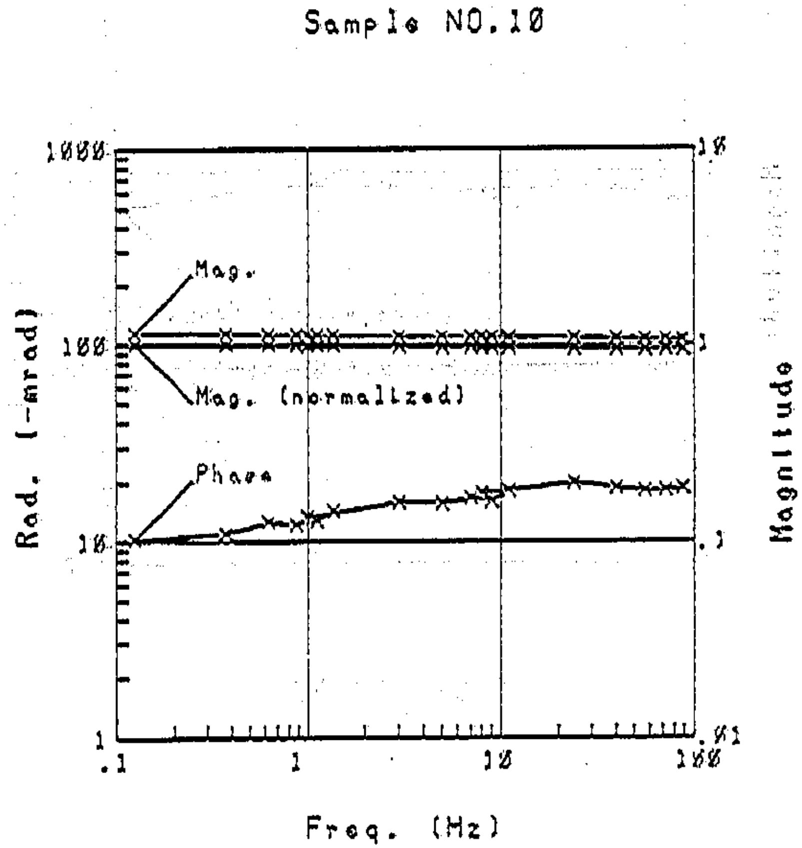

Fig.III-3-9.10 Spectrum of phase & Magnitude

(Sample No.10)

Sample NO.11

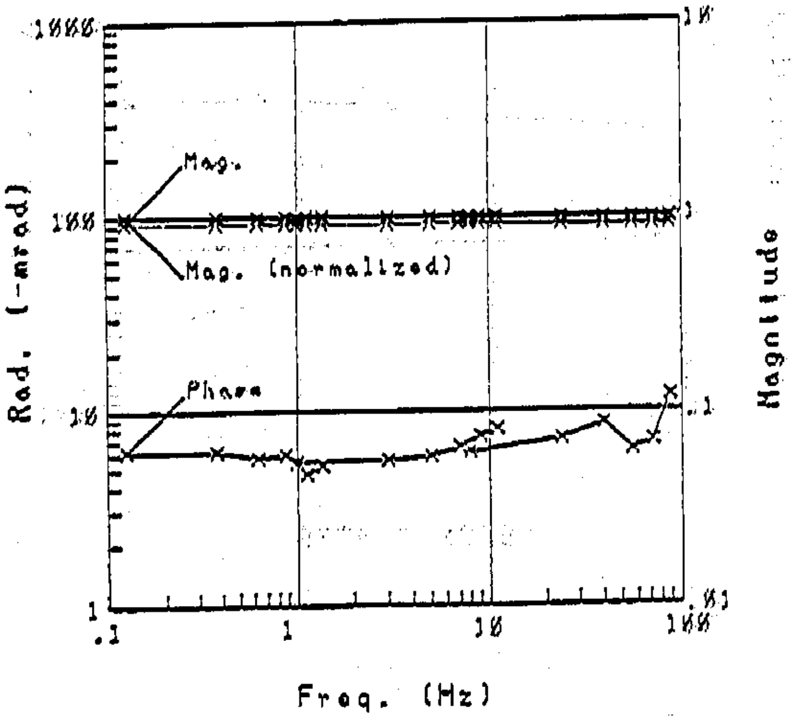

Fig.III-3-9.11 Spectrum of phase & Magnitude

(Sample No.11)

Sample NO.12

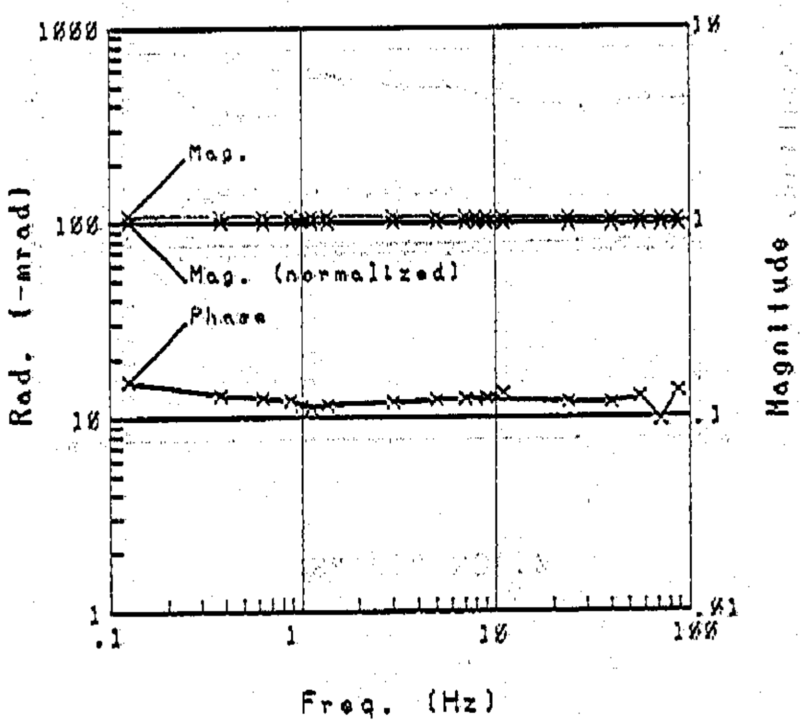

Fig.III-3-9.12 Spectrum of phase & Magnitude

(Sample No.12)

Sample NO.13

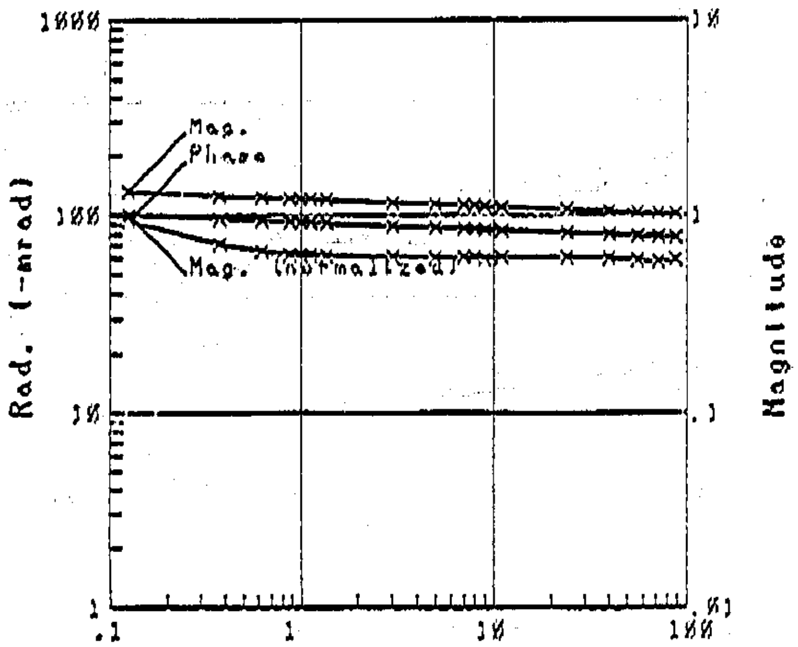

Fig.III-3-9.13 Spectrum of phase & Magnitude
(Sample No.13)

Sample NO.14

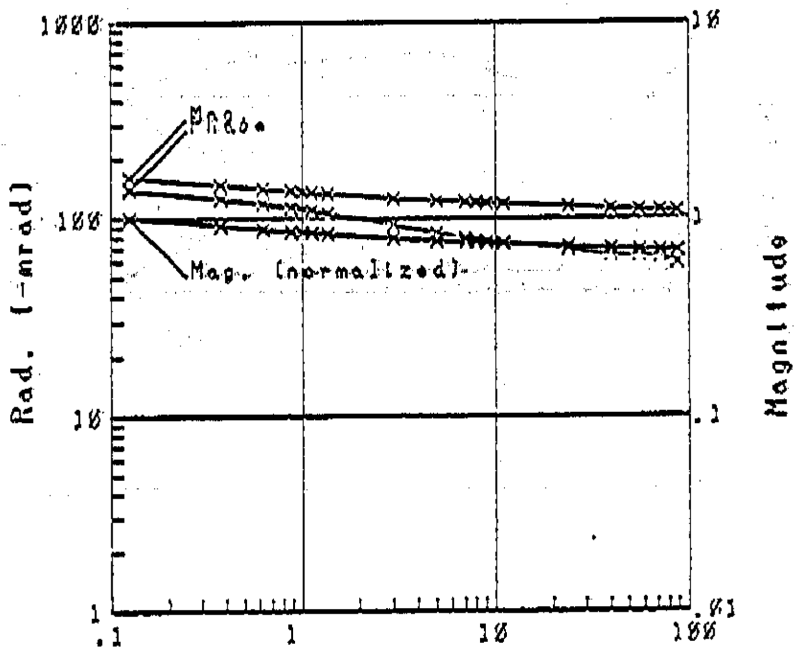

Fig.III-3-9.14 Spectrum of phase & Magnitude
(Sample No.14)

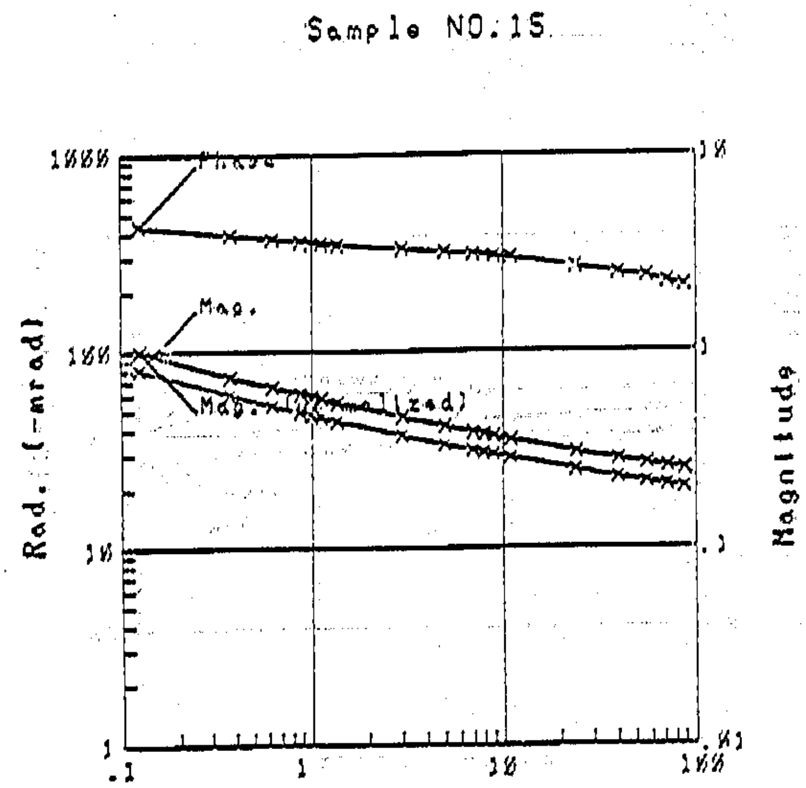

Fig.III-3-9.15 Spectrum of phase & Magnitude
(Sample No.15)

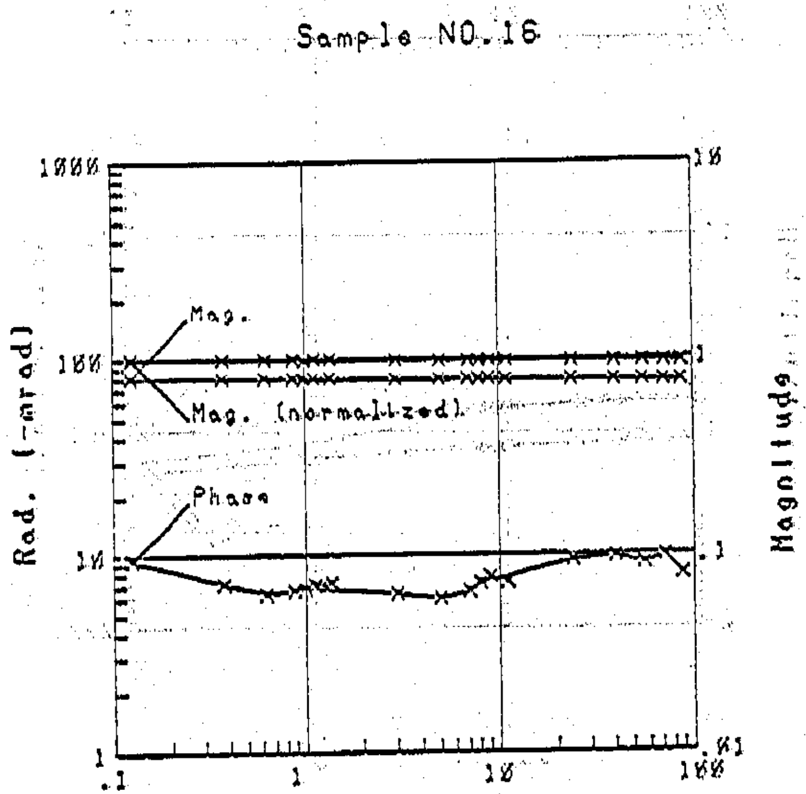

Fig.III-3-9.16 Spectrum of phase & Magnitude
(Sample No.16)

Sample NO.17

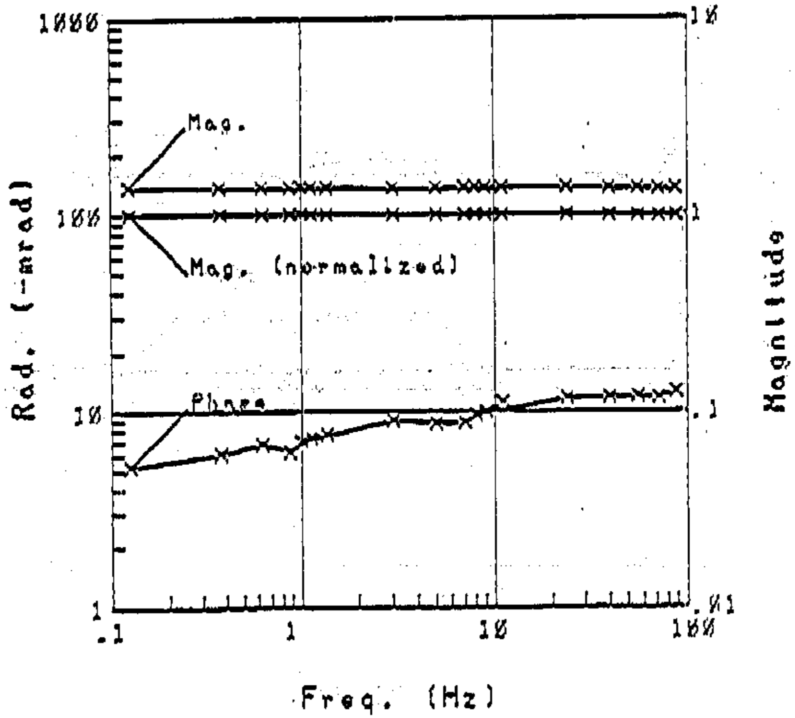

Fig.III-3-9.17 Spectrum of phase & Magnitude
(Sample No.17)

Sample NO.18

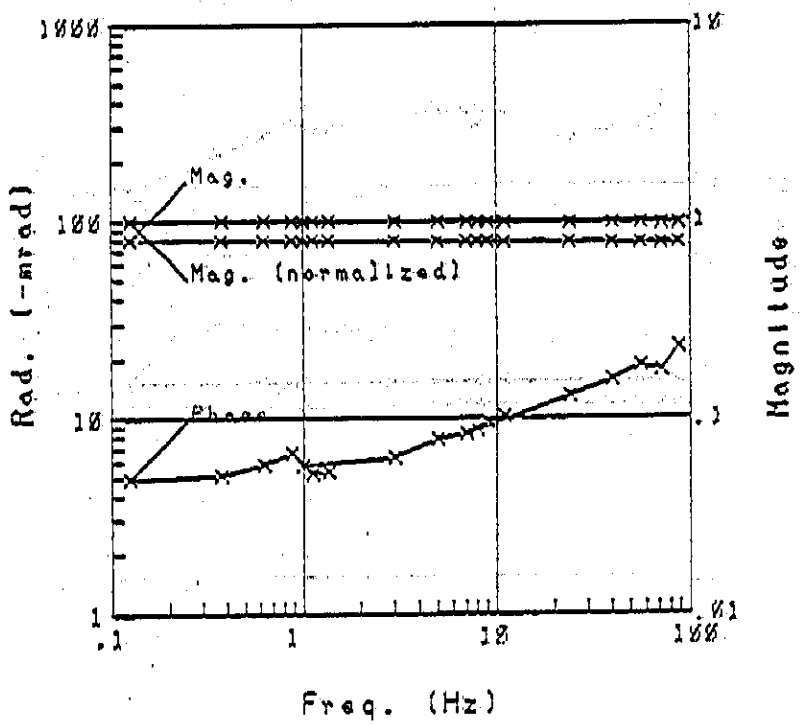

Fig.III-3-9.18 Spectrum of phase & Magnitude
(Sample No.18)

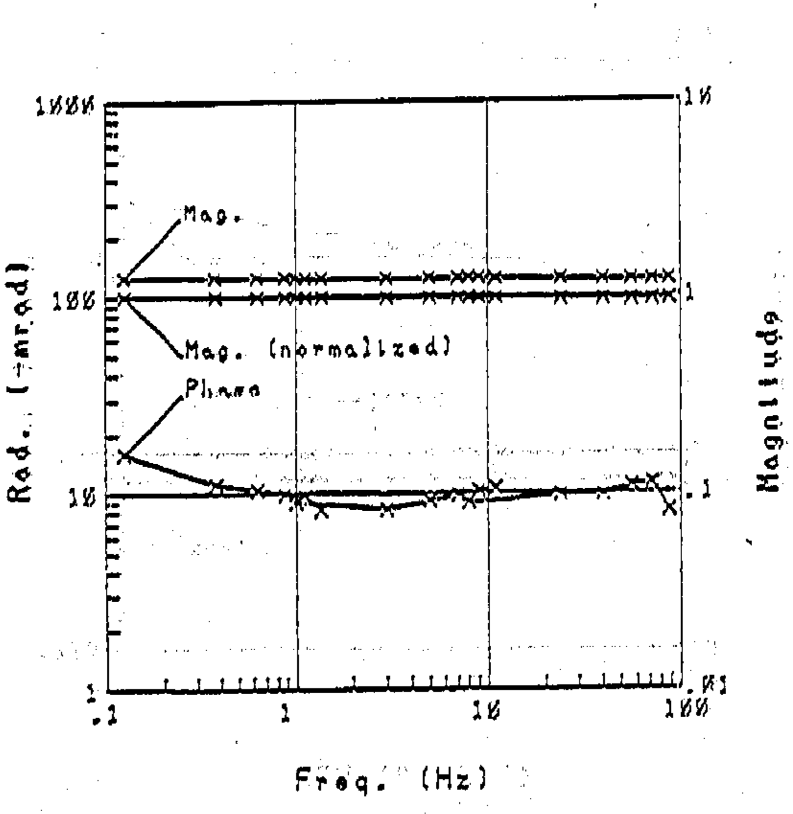

Fig.III-3-9.19 Spectrum of phase & Magnitude
(Sample No.19)

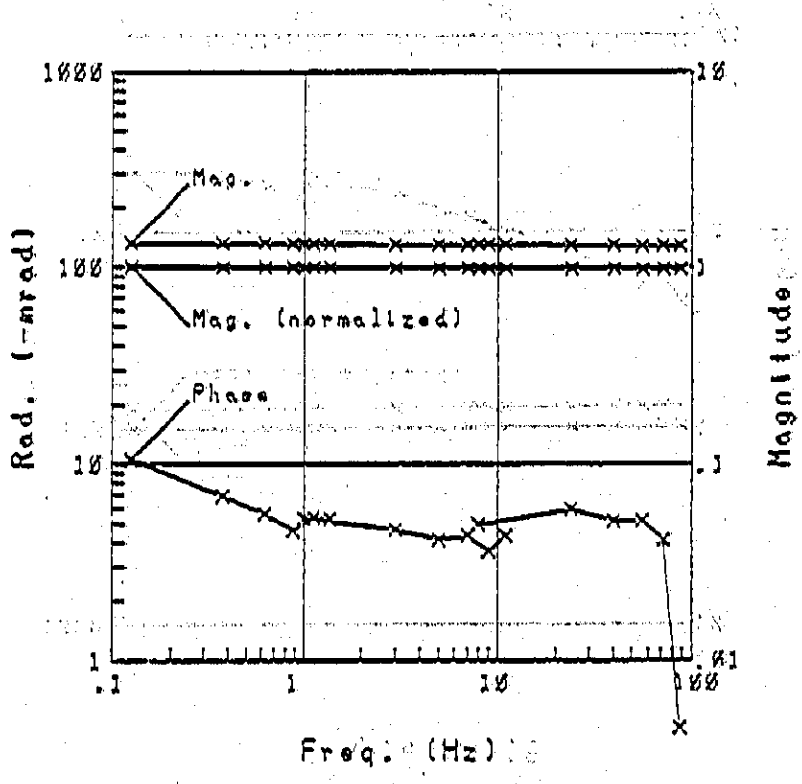

Fig.III-3-9.20 Spectrum of phase & Magnitude
(Sample No.20)

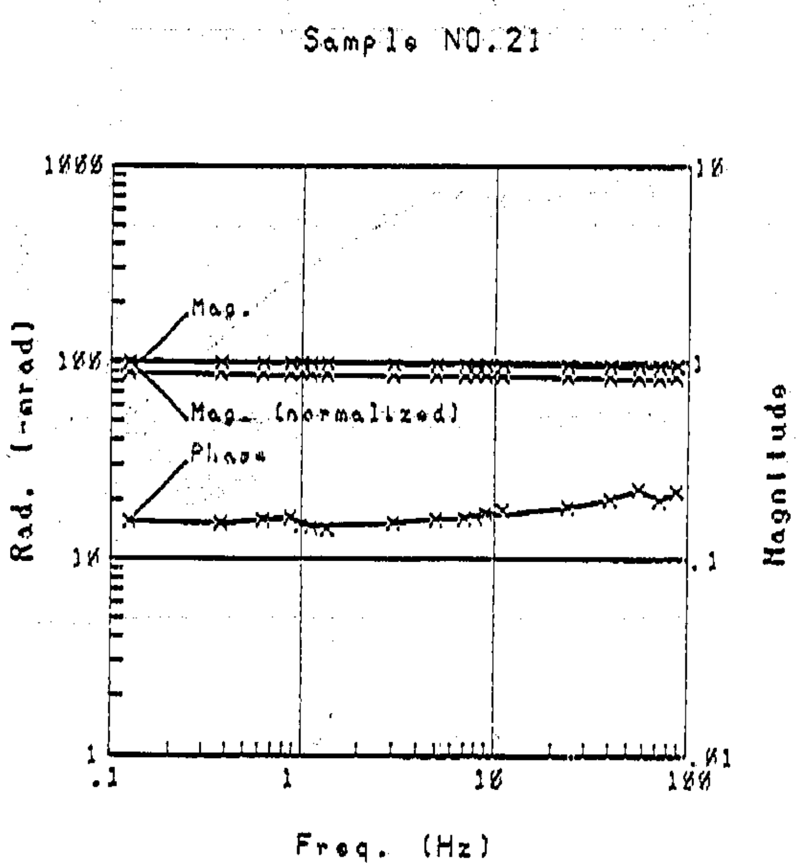

Fig.III-3-9.21 Spectrum of phase & Magnitude (Sample No.21)

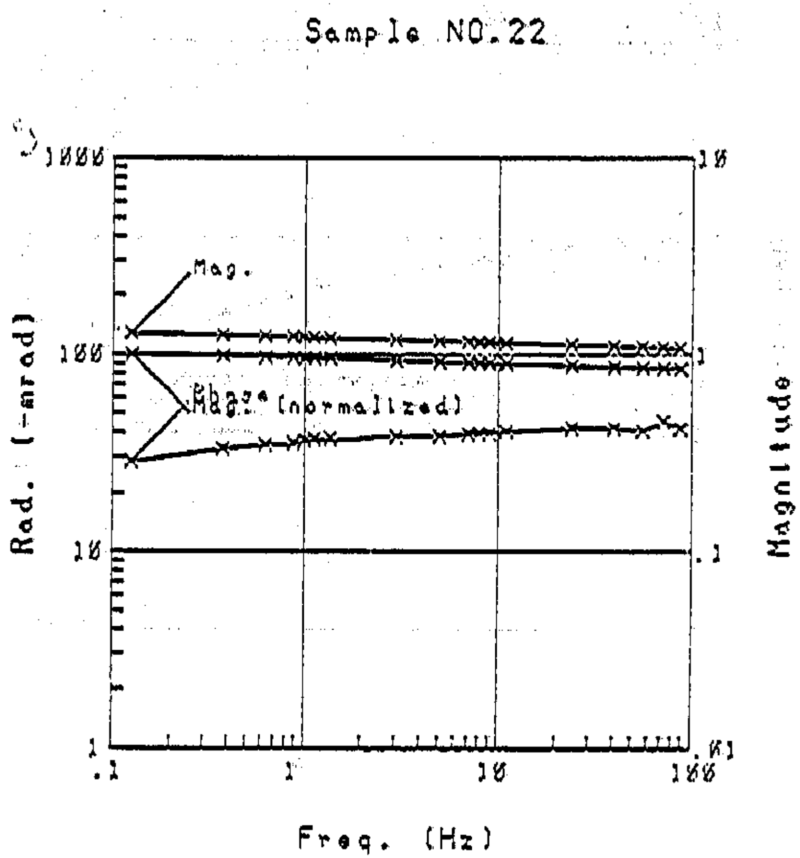

Fig.III-3-9.22 Spectrum of phase & Magnitude (Sample No.22)

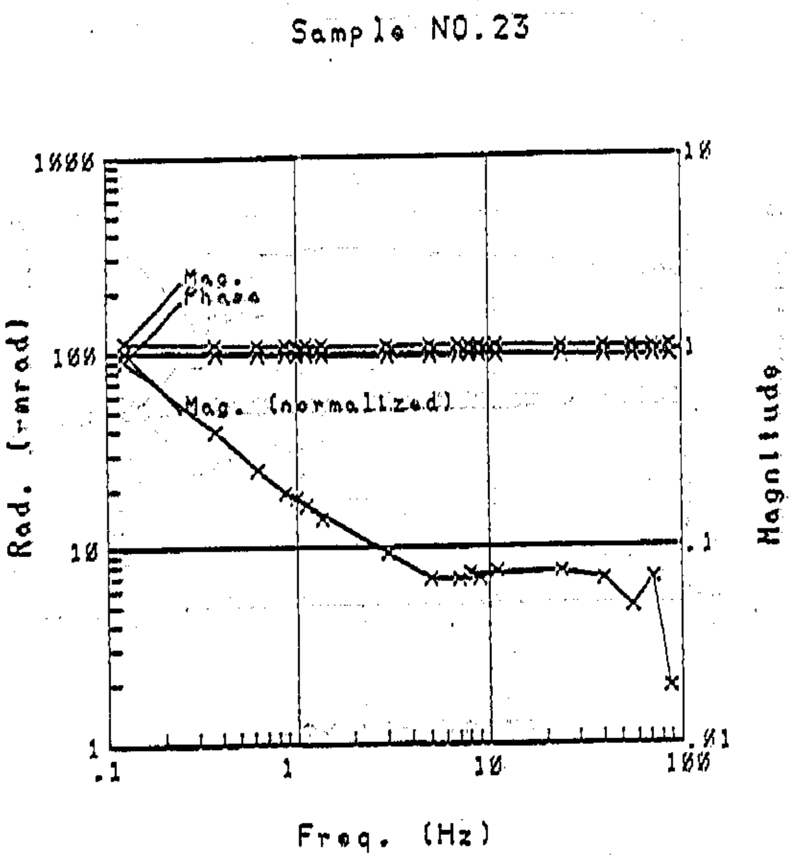

Fig.III-3-9.23 Spectrum of phase & Magnitude
(Sample No.23)

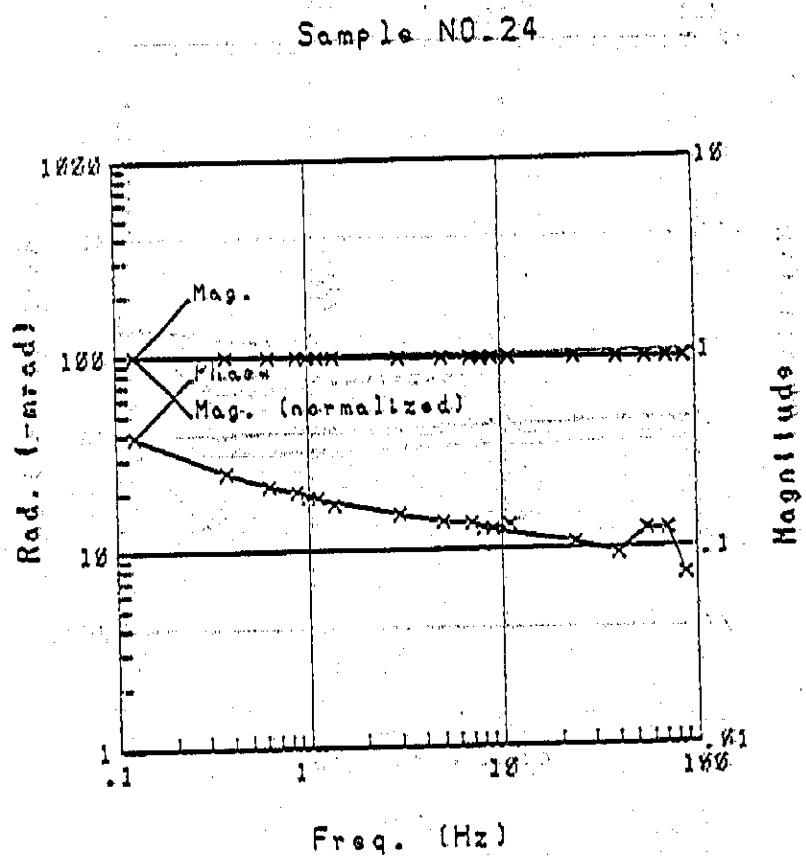

Fig.III-3-9.24 Spectrum of phase & Magnitude
(Sample No.24)

Sample NO.25

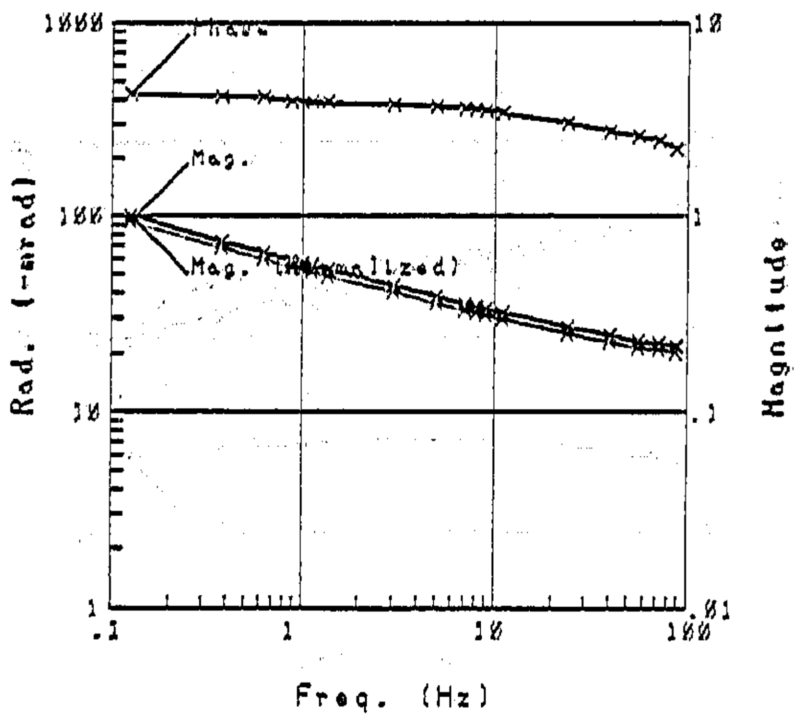

Fig.III-3-9.25 Spectrum of phase & Magnitude (Sample No.25)

Sample NO.26

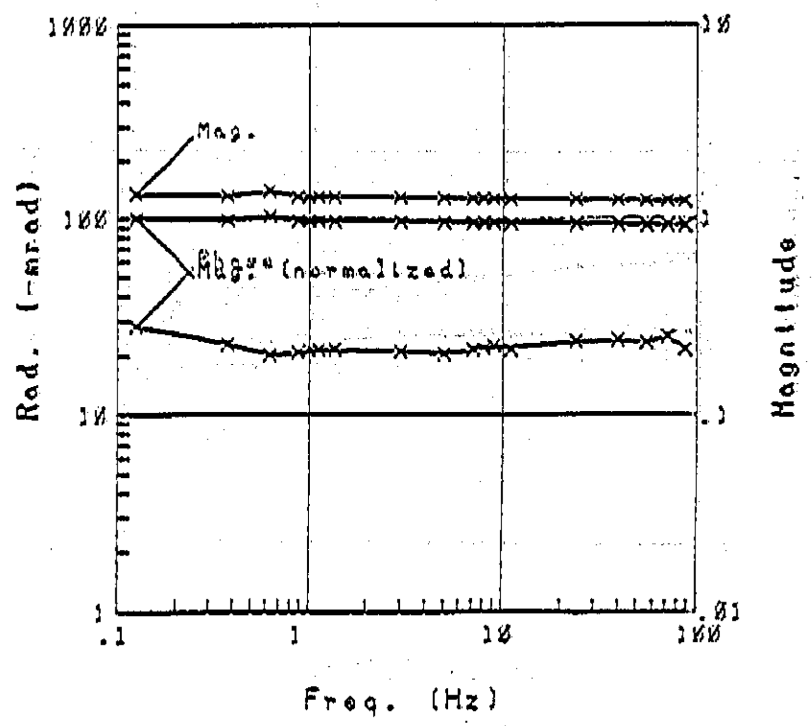

Fig.III-3-9.26 Spectrum of phase & Magnitude (Sample No.26)

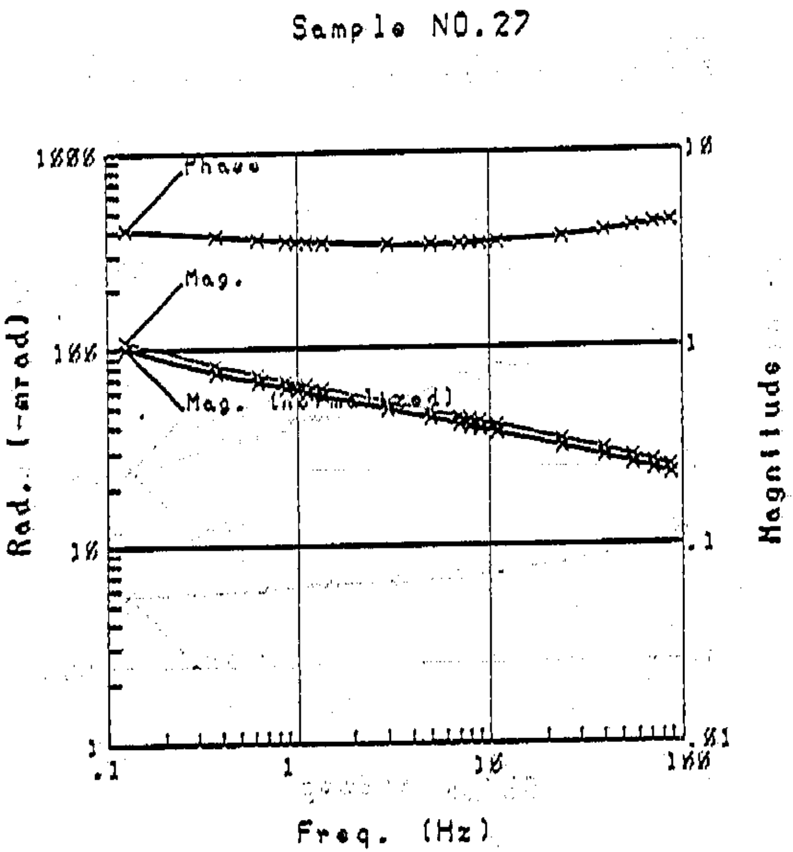

Fig.III-3-9.27 Spectrum of phase & Magnitude
(Sample No.27)

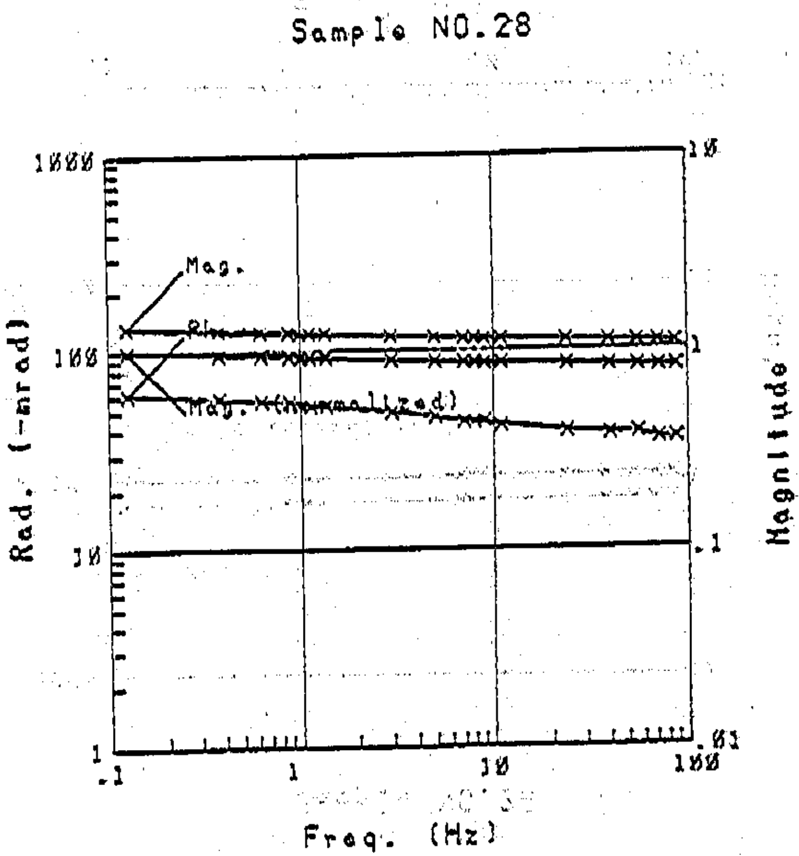

Fig.III-3-9.28 Spectrum of phase & Magnitude
(Sample No.28)

Sample NO.29

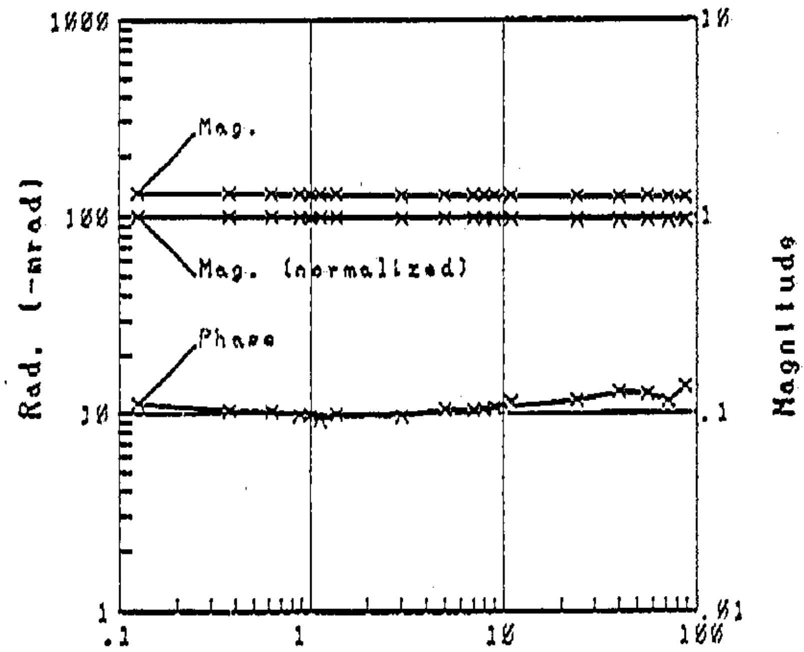

Fig.III-3-9.29 Spectrum of phase & Magnitude
(Sample No.29)

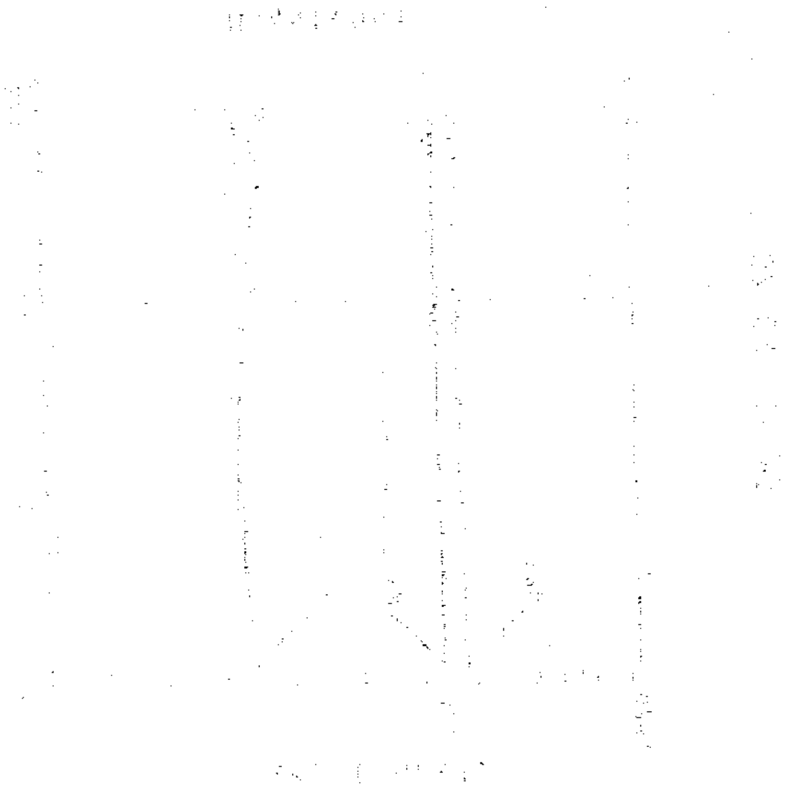

The resistivity (0.125 Hz), phase (0.125 Hz), 3 point decoupled phase, and PFE (0.125 ~ 1 Hz), are classified of these four types in Table III-3-2. The mean values in this table were obtained by excluding the maximum and minimum values. Resistivity in the table is shown when the frequencies were at 0.125 Hz.

Table III-3-2 Classification of Phase Spectrum

	Type	Maximum	Minimum	Average
Resistivity (Ω-m)	A	2,650	45.3	356
	B	2,370	414	876
	C	6,360	644	1,870
	D	24,300	1,840	4,710
Phase (-mrad)	A	436	10.5	172
	B	27.2	9.50	20.8
	C	28.0	6.17	15.8
	D	28.3	4.90	11.7
3 point decoupled phase (-mrad)	A	466	13.4	175
	B	30.4	11.3	22.6
	C	31.9	6.0	16.5
	D	24.7	4.87	11.7
PFE (%) (0.1 - 1.0 Hz)	A	75.3	0.82	22.5
	B	3.07	0.92	1.99
	C	2.99	0.73	1.82
	D	4.47	0.59	1.52

The Type A rocks show the lowest resistivity, then come B, C, and D, the reason for the low resistivity of the Type A rock is the presence of large amounts of disseminated pyrite. The phase (0.125 Hz), 3 point decoupled phase, and PFE (0.125 - 1 Hz), a Type A spectrum shows that a large value makes a big difference to the mean values of the B, C and D Types. A conclusion from these facts assumes that if ore or pyrite dissemination exists, the resistivity value becomes approximately 300 ~ 400 Ω-meters, and the phase spectrum decreases as the frequency increases, this is what was observed with the Type A.

When samples with phase spectrum characteristics of a Type A (10 samples), and Type B (6 samples), were examined with the naked eye, they were seen to contain a large quantity of pyrite. There are no differences of the spectra, betweem the samples which contain galena, and zinc-blend (sample numbers 13, 14 and 15) and those samples containing pyrite dissemination only. This is because sample number 13, 14 and 15 also contain quite a bit of pyrite. The difference between the spectra of the samples containing pyrite dissemination and banded pyrite ore is as follows; if there is a large amount of pyrite, then it is a Type A rock, if it is low, then it is a Type B or C.

3-4 THE ANALYSIS METHOD

Topographic and calibration corrections were applied to the field data, then section, plane and spectrum diagrams were drawn, and the results analyzed for IP anormalies, as follows;

(1) Plane and section map of apparent resistivity (0.125 Hz).
(2) Plane and section map of PFE (0.125 - 1 Hz, and 0.375 - 3 Hz).
(3) Section diagram of Phase (15 frequencies).
(4) Cole-Cole diagram.
(5) Phase spectral response diagram.
(6) Magnitude spectral response diagram.
(7) Three point decoupled phase diagram.

Ordinary method of analyses were used for (1) and (2), as these are the same kind of apparent resistivity and PFE by the conventional IP method. The (3 - 7) are the special case of spectral IP, and can be identified through their abnormal spectral response.

The (7) is the method through which we can require the phase in direct current, using 0.125, 0.375 and 0.625 Hz. If we assume that frequency and phase have quadratic relationship, and let phase (ϕ) be an ordinate, frequency (f) be an abscissa, it then becomes a quadratic function $y = ax^2 + bx + C$, this "C" is the phase which can become a frequency close to a direct curent, and it is called the three point decoupled phase. To solve "C", 0.125, 0375 and 0.625 Hz are put in for frequency (x), and phase (y) becomes $\phi_{0.125}$, $\phi_{0.375}$, $\phi_{0.625}$.

where:

$$\phi_{0.125} = a(0.125)^2 + b(0.125) + C$$
$$\phi_{0.375} = a(0.375)^2 + b(0.375) + C$$
$$\phi_{0.625} = a(0.625)^2 + b(0.625) + C$$

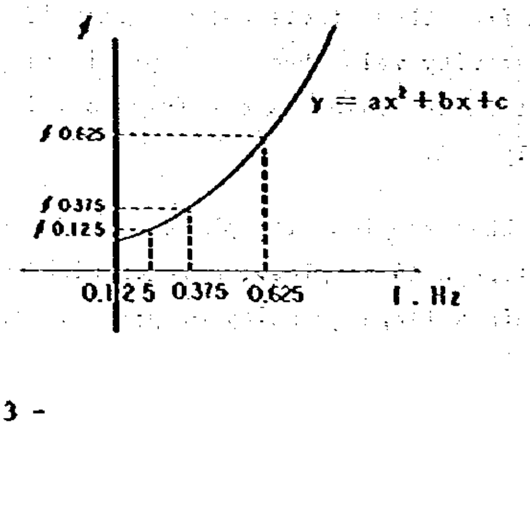

From this, "C" can be driven by the following equation.

$$C = \frac{15}{8}\phi_{0.125} - \frac{10}{8}\phi_{0.375} + \frac{3}{8}\phi_{0.625}$$

CHAPTER 4 RESULTS OF INTERPRETATION AND CONSIDERATION

4-1 RESULTS OF INTERPRETATION

4-1-1 Cole-Cole, Phase and Magnitude Spectrums

Cole-Cole diagram was proposed by Cole and Cole in 1941 with the purpose to examine the measurement results of rock samples. The measurement results are plotted with every frequency by setting the negative out-of-phase (imaginary) on vertical axis and the positive in-phase (real) on horizontal axis (Fig. III-3-3). Frequency effect is very proportional to in-phase, while phase angle is proporitonal to out-of-phase.

Cole-Cole diagram is expressed on the sections of survey lines A ~ I and is shown in Figure III-4-1. Cole-Cole diagram generally shows a simple ascent to the left; however, in south of survey lines G ~ I, there is small out-of-phase with small anomaly. Southern end of survey lines A ~ F with no IP phenomenon shows perpendicular pattern, and northern part of survey lines indicates the pattern of the ascent to the left.

Concerning the phase spectral, steady increase caused by electro magnetic coupling can be seen at high frequency range (harmonic of 8 Hz), and some patterns reflecting characteristics of the anomaly source can be seen at low resistivity range (harmonic of 0.125 Hz).

First one of the patterns is the anomaly which is recognized at n = 3 ~ 5 at northern end of survey lines A, B, D and E. There is the anomaly of flat and of more than -50 milliradian at harmonic of 0.125 Hz. This can be considered as the effect of disseminated sulfide.

Second one of characteristic patterns is the V-shape spectral in the center of survey line C. This spectral is the one whose harmonic of 0.125 Hz decreases as frequency increases. This type of spectral can be observed at survey lines B and D. This anomaly has the value of less than -40 milliradian at 0.125 Hz is not much remarkable than the above-mentioned one. This pattern is normally seen for big mineral grain size. For a case as this, it is probably caused by massive sulfide.

Furthermore, as for the third pattern, there is steady increasing spectral with the ascent to the right as seen at southern end of survey line A, where there is anomaly caused only by electro magnetic coupling without any phase in low frequency range.

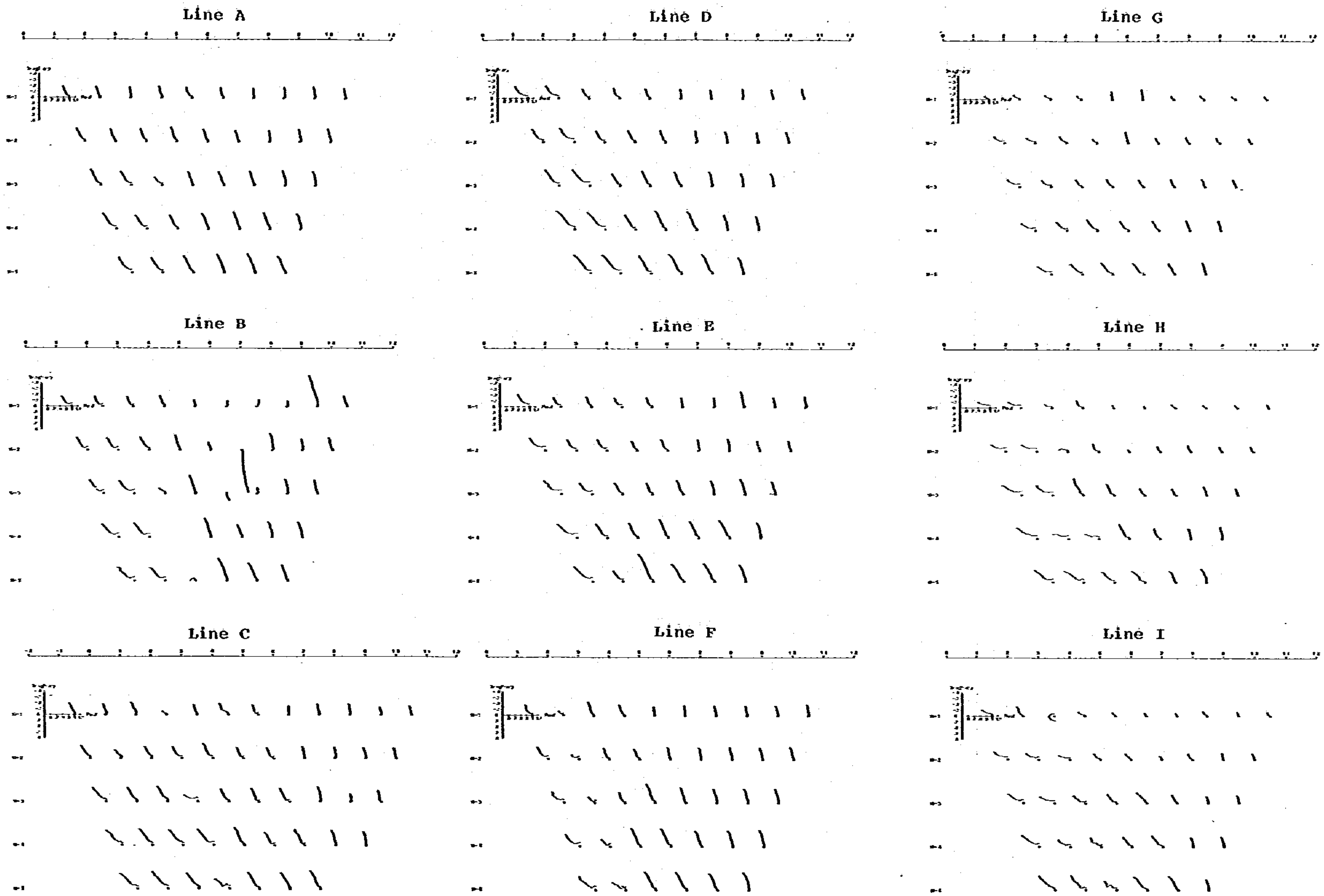

Fig. III-4-1 Cole-Cole Diagram

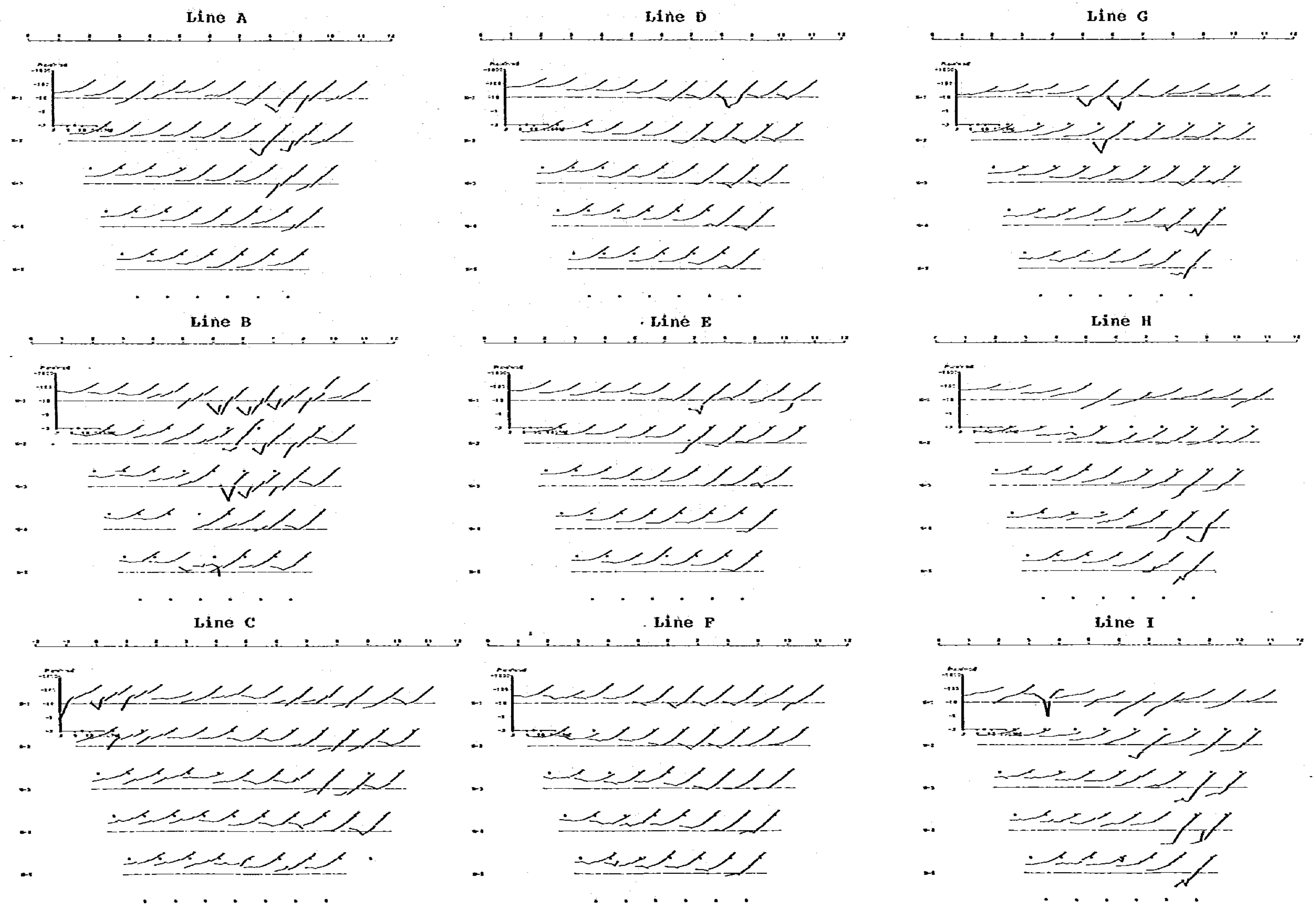

Fig. III-4-2 Phase Spectrum

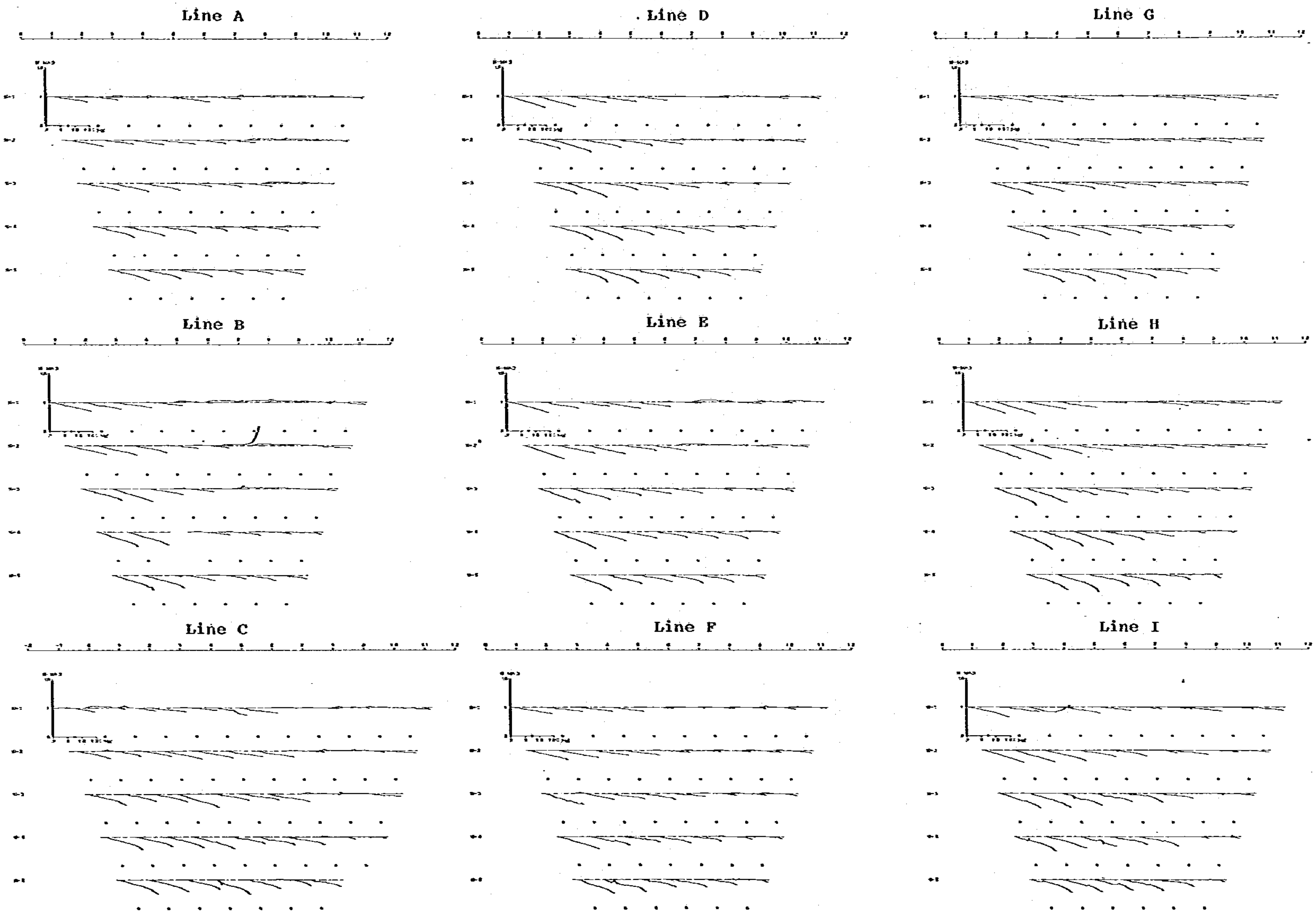

Fig. III-4-3 Magnitude Spectrum

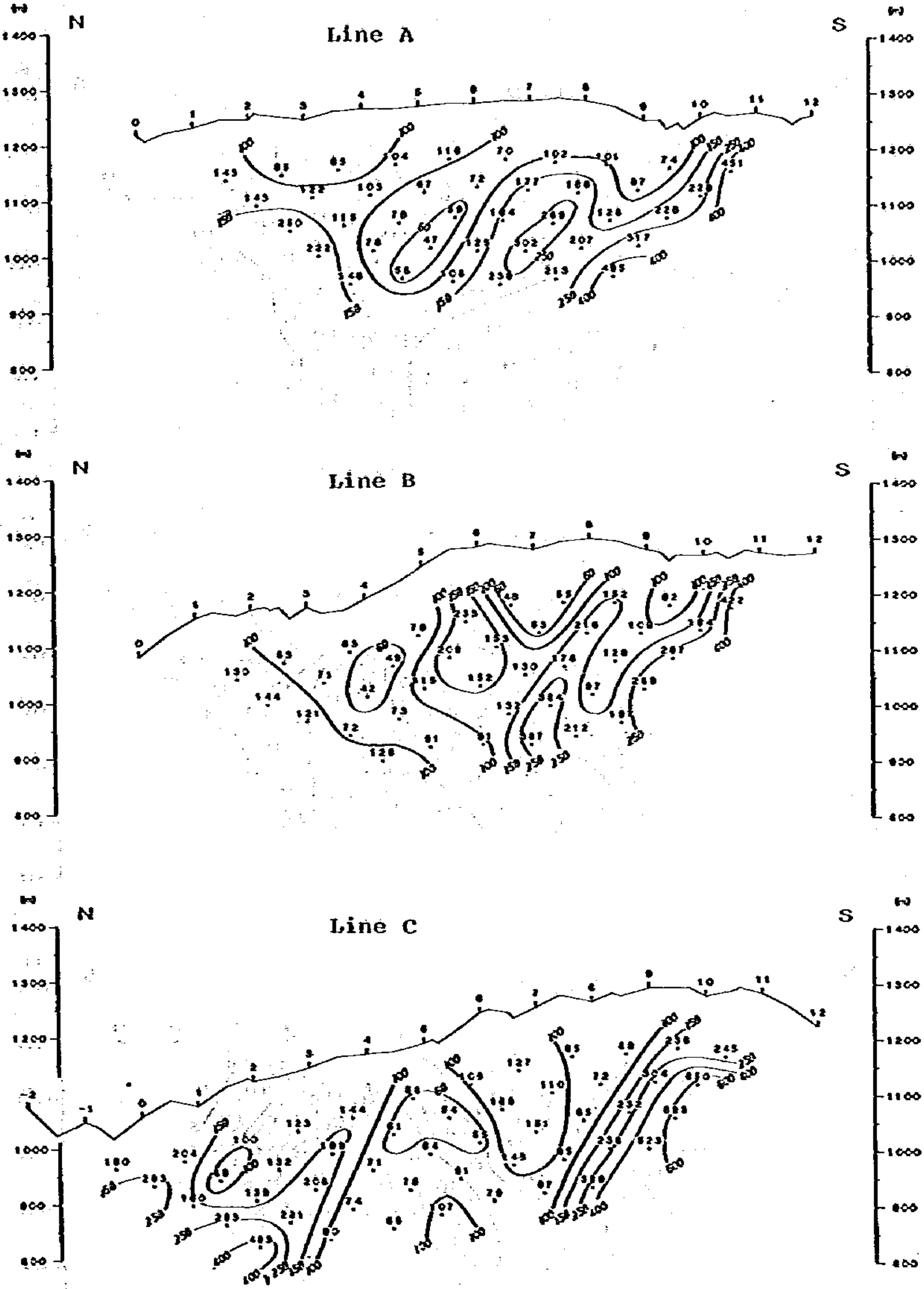

Fig. III-5-1.1 Spectral IP Pseudo-Section
Apparent Resistivity (Line A, B, C)

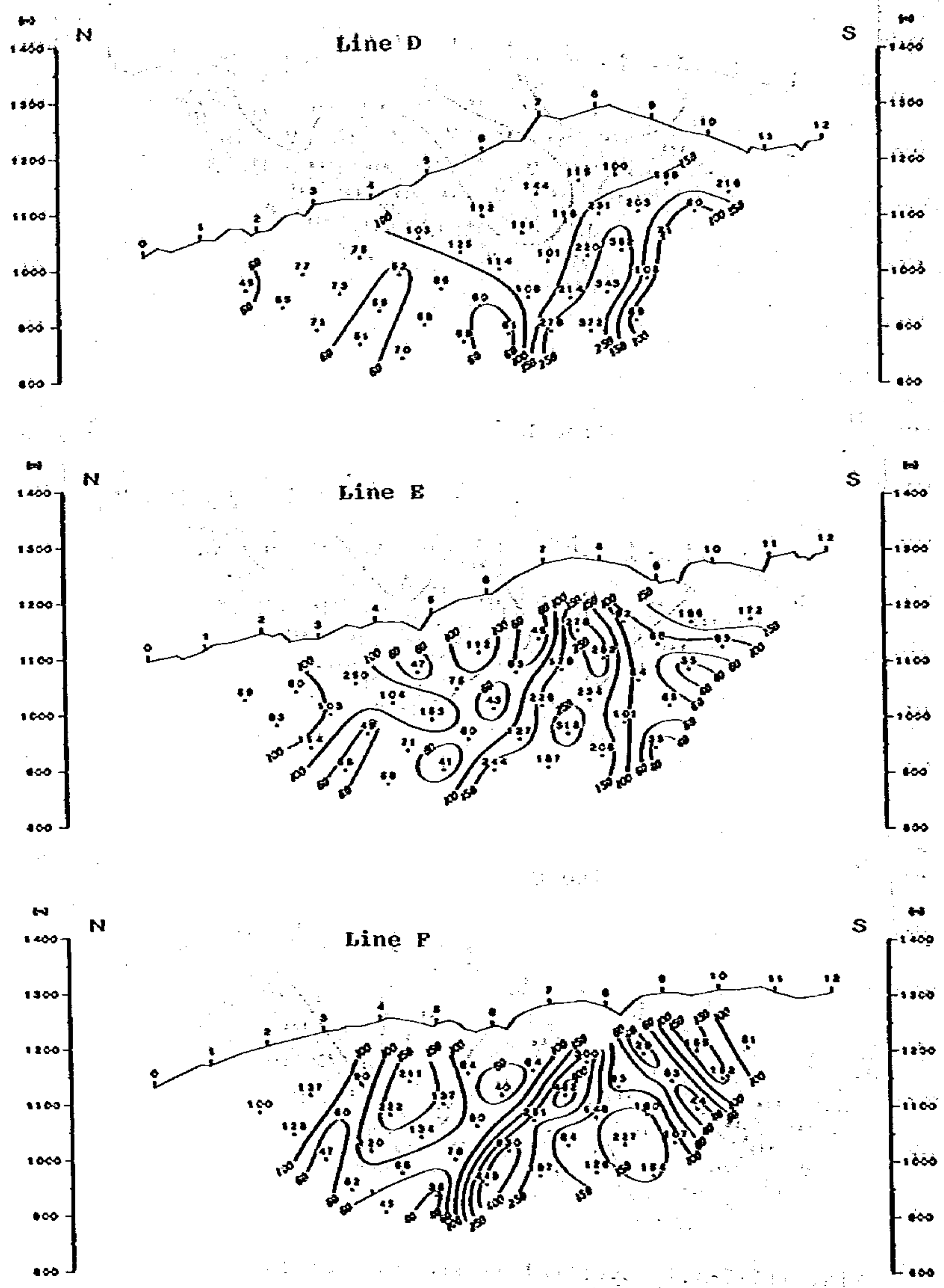

Fig. III-5-1.2 Spectral IP Pseudo-Section
Apparent Resistivity (Line D, E, F)

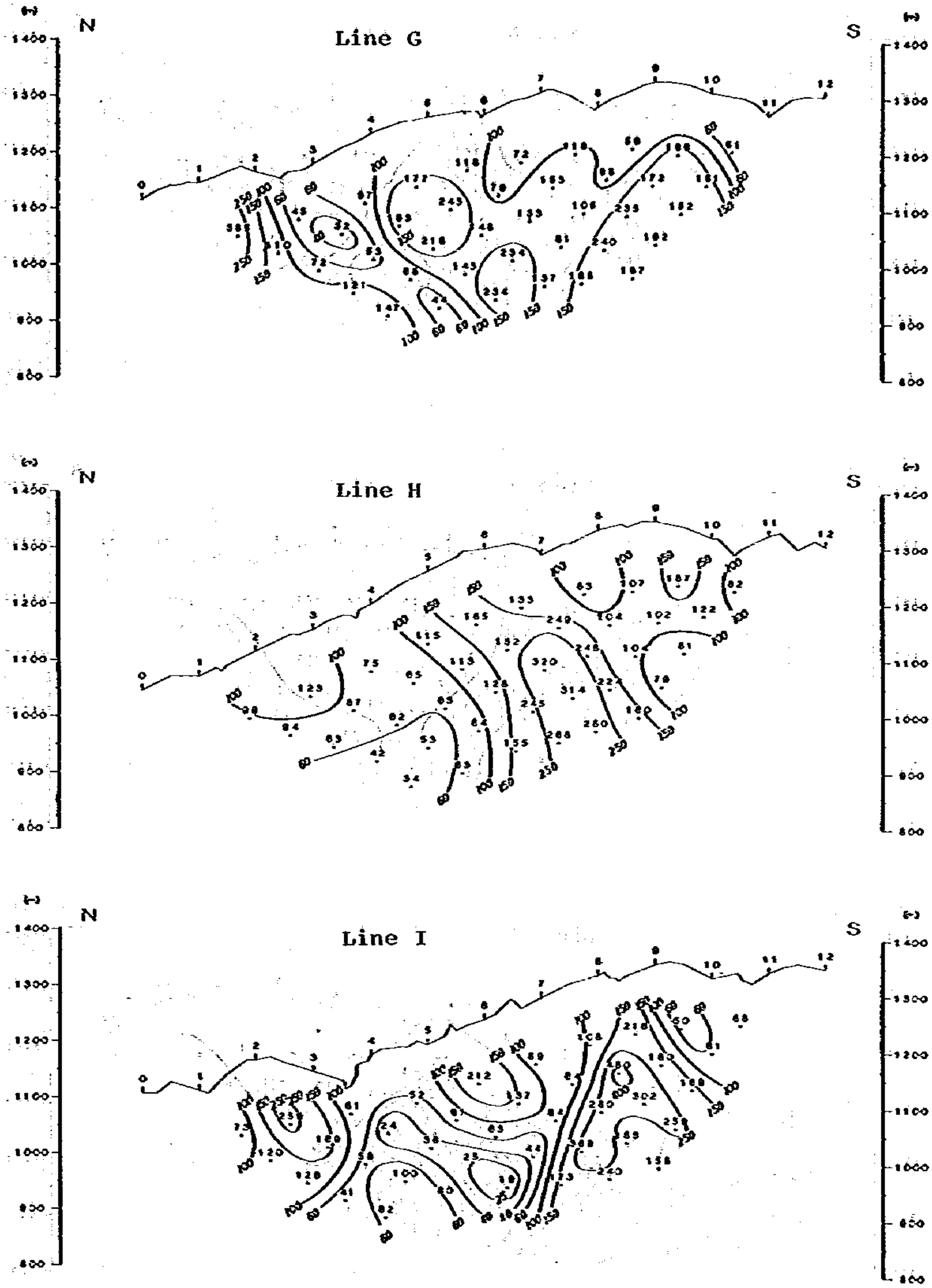

Fig. III-5-1.3 Spectral IP Pseudo-Section
Apparent Resistivity (Line G, H, I)

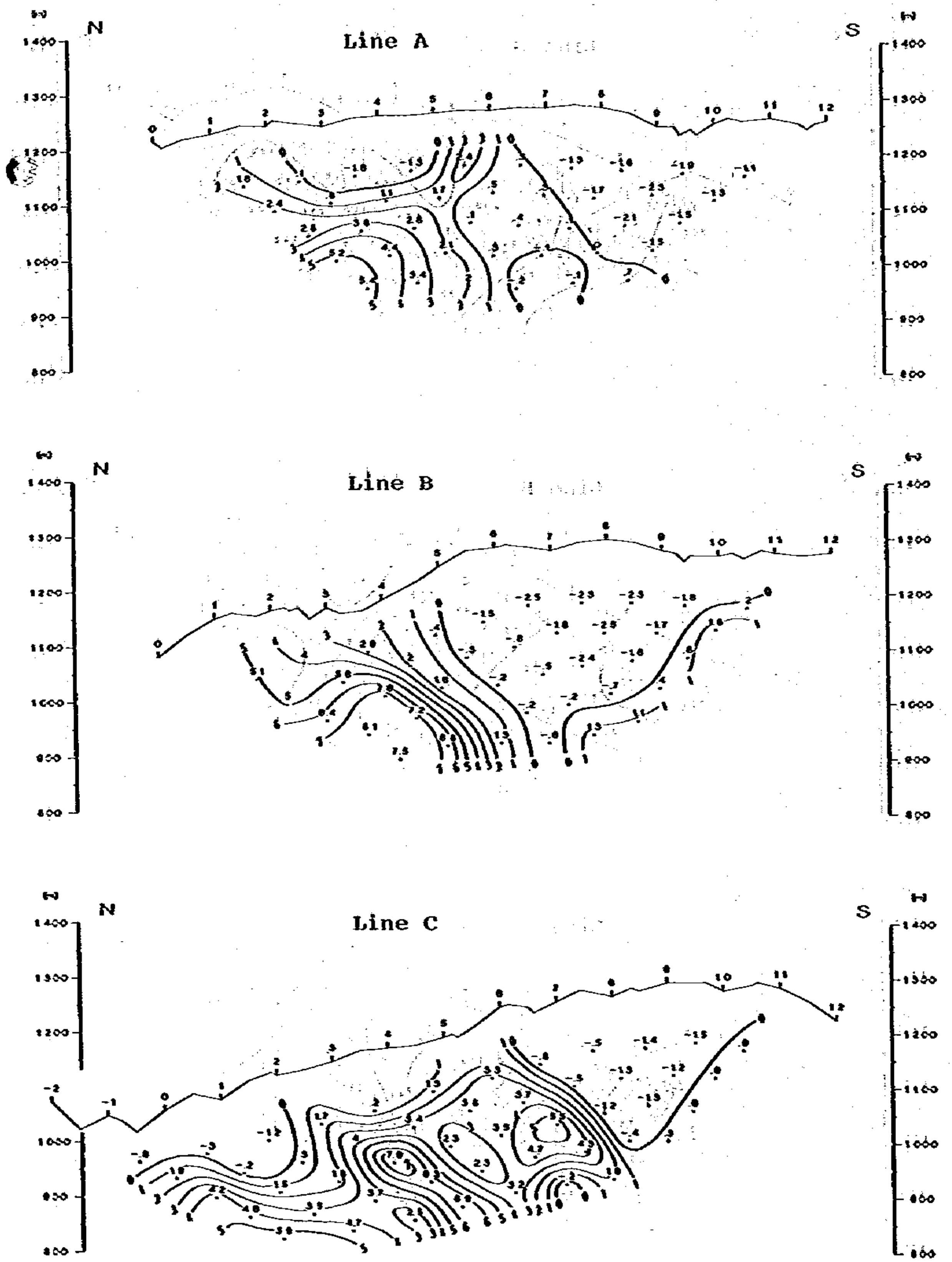

Fig. III-6-1.1 Spectral IP Pseudo-Section
Percent Freqency Effect [0.125 ∿ 1.0 Hz] (Line A, B, C)

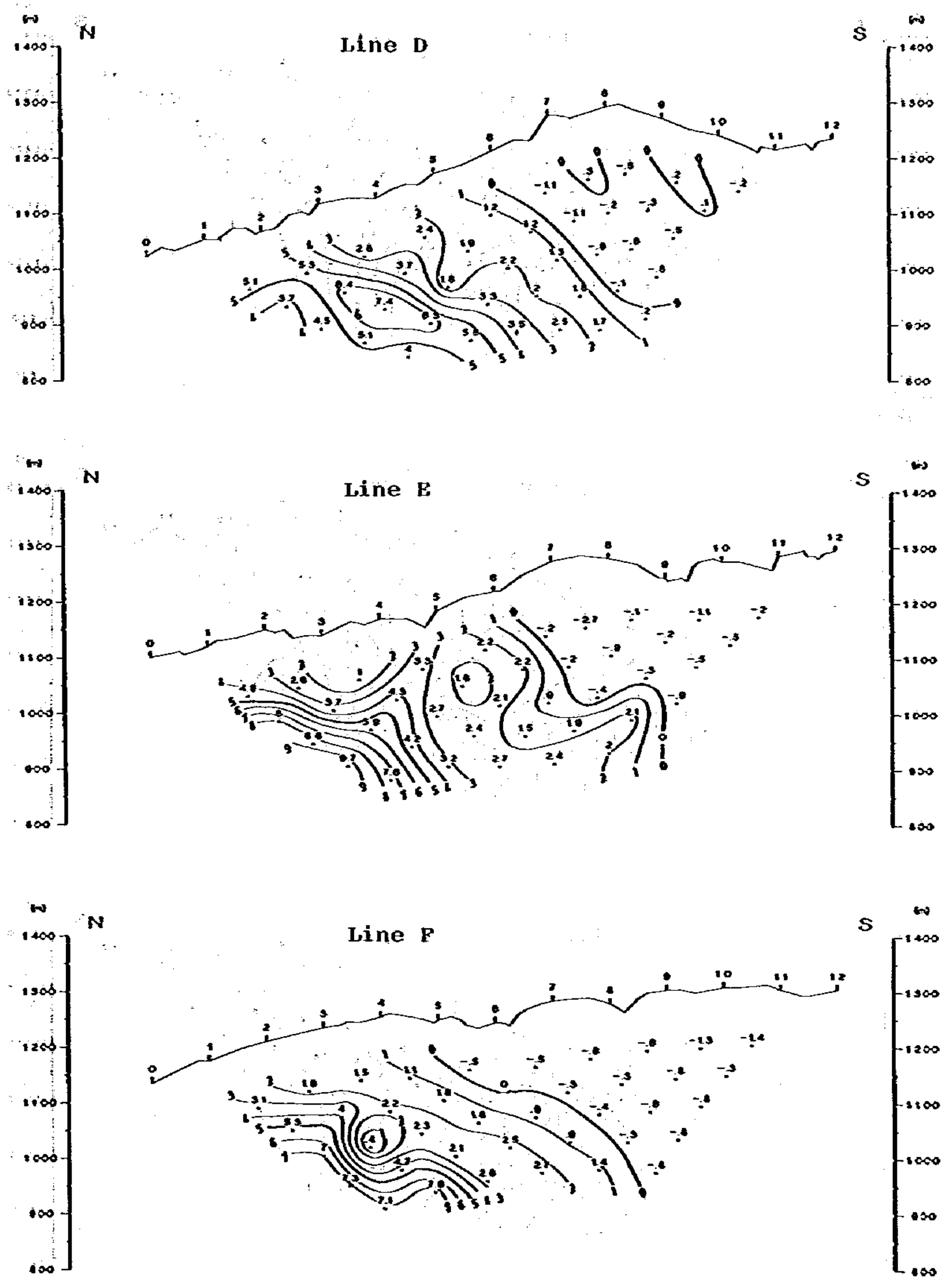

Fig. III-6-1.2 Spectral IP Pseudo-Section

Percent Freqency Effect [0.125 ∿ 1.0 Hz] (Line D, E, F)

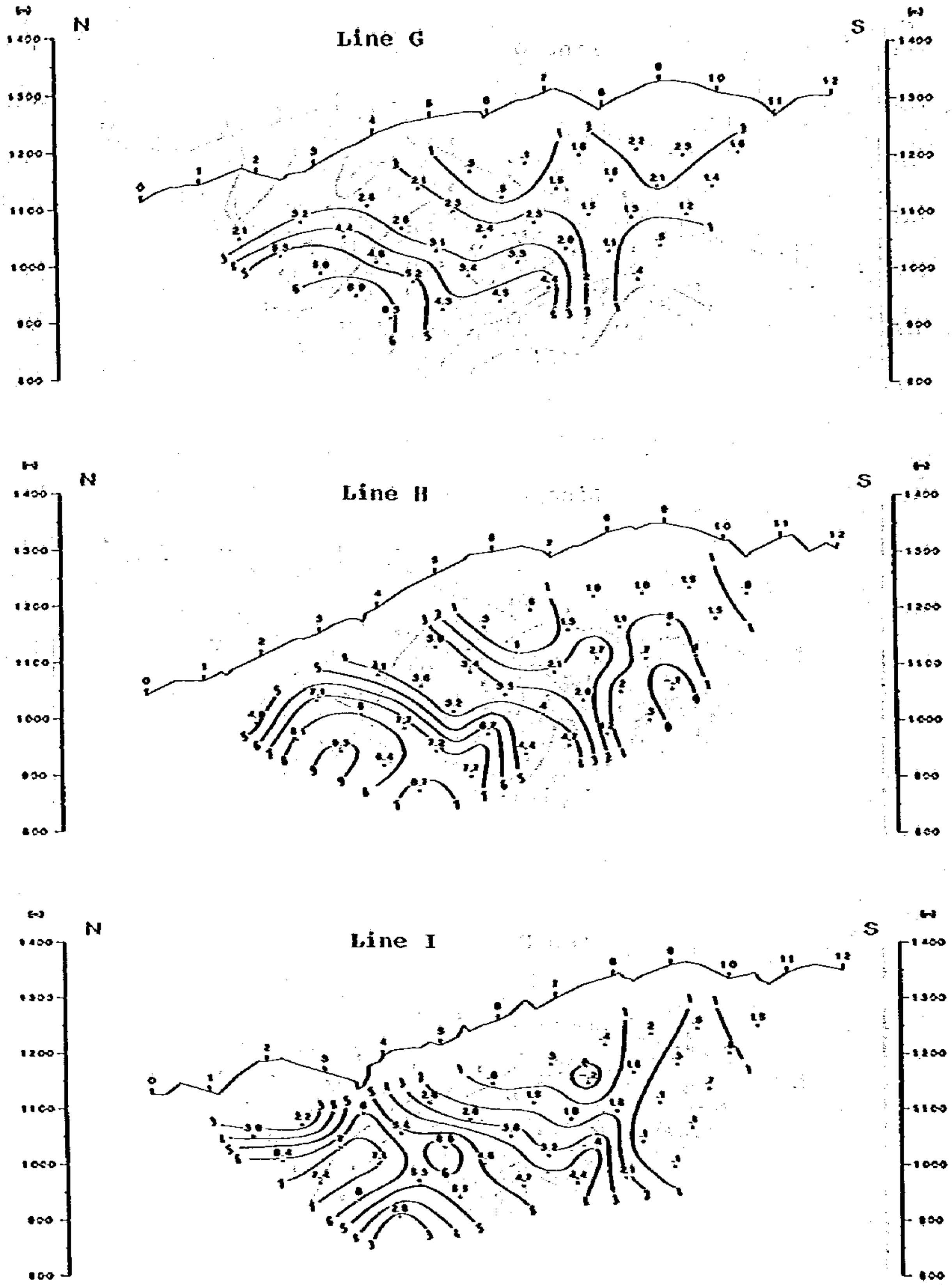

Fig. III-6-1.3 Spectral IP Pseudo-Section
Percent Freqency Effect [0.125 ∿ 1.0 Hz] (Line G, H, I)

Magnitude Spectral is normalized at 0.125 Hz and its magnitude decreases as frequency increases. It shows the pattern with descent to the right when IP effect is large. This kind of pattern seen in northern half of every survey line has the same significance with one of the Cole-Cole diagram ascending to the left; that means, in-phase decreases (frequency effect increases) as the frequency increases.

4-1-2 Apparent Resistivity

The geographical effects are accumulated in measured apparent resistivity. In order to remove them, two dimensional topographic correction was carried out by means of the computer with finite element method (Fig. II-5-1.1 - 1.3).

The correction is effective when the survey lines (such as A, D and so on) intersect at the right angle with topographic contour and/or when two dimensional geological change has taken its place. However, the correction may not be able to cover all of the effects along the mountain ridge (like as survey line F). For such case, distribution of resistivity is qualitatively considered by examining the surrounding topography.

Resistivity of this area generally shows low value of change within 40 ~ 200 Ω-m. As for resistivity change, it is understood that value with less than 100 Ω-m is as the low resistivity zone, and one with more than 200 Ω-m as high resistivity zone. Especially low resistivity shown at center part of survey line C with some outcrops around No. 5 shows the same anomaly zone with IP anomaly. Furthermore, high resistivity is shown at non-altered andesite dike and limestone.

It is needed to pay attention for spectral IP since the coupling phenomenon occurs in the area with low resistivity. By the calculation of electro magnetic coupling against two-layered structure model, phase change of 10 Ω-m with 10 m thickness of overburden and 100 Ω-m 2nd-layered models shows a value of -1 ~ -200 milliradian.

4-1-3 Frequency Effect

Besides 0.125 - 1 Hz frequency effect, 0.375 - 3 Hz frequency effect, which is the closest frequency effect to the conventional IP method, is calculated and shown as pseudo-section in Fig. III-6-1 ~ Fig. III-6-6. Both 0.125 - 1 Hz and 0.375 - 3 Hz FE show the same anomaly pattern with no predominant differences.

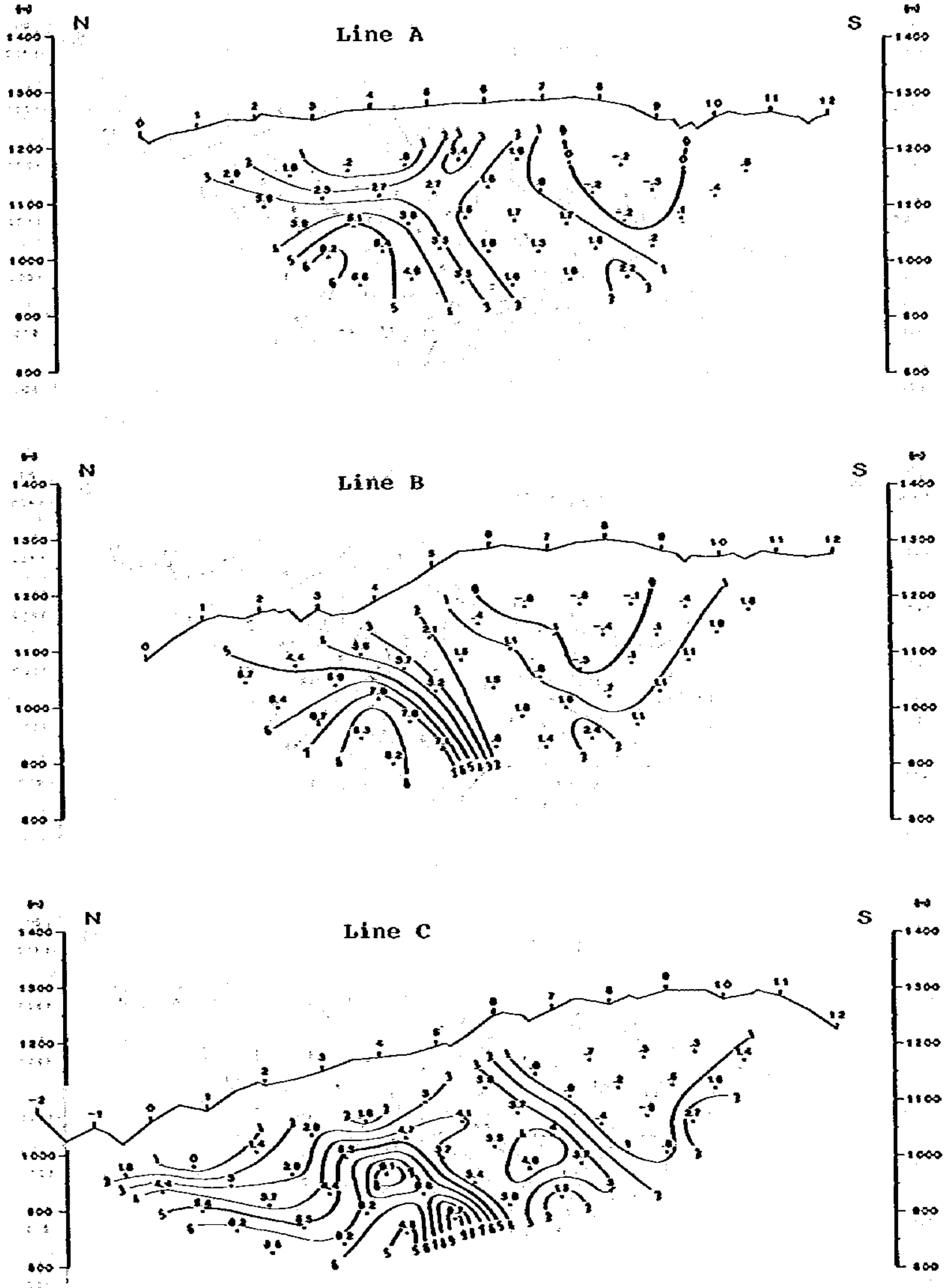

Fig. III-6-2.1 Spectral IP Pseudo-Section
Percent Freqency Effect (0.375 ∿ 3.0 Hz) (Line A, B, C)

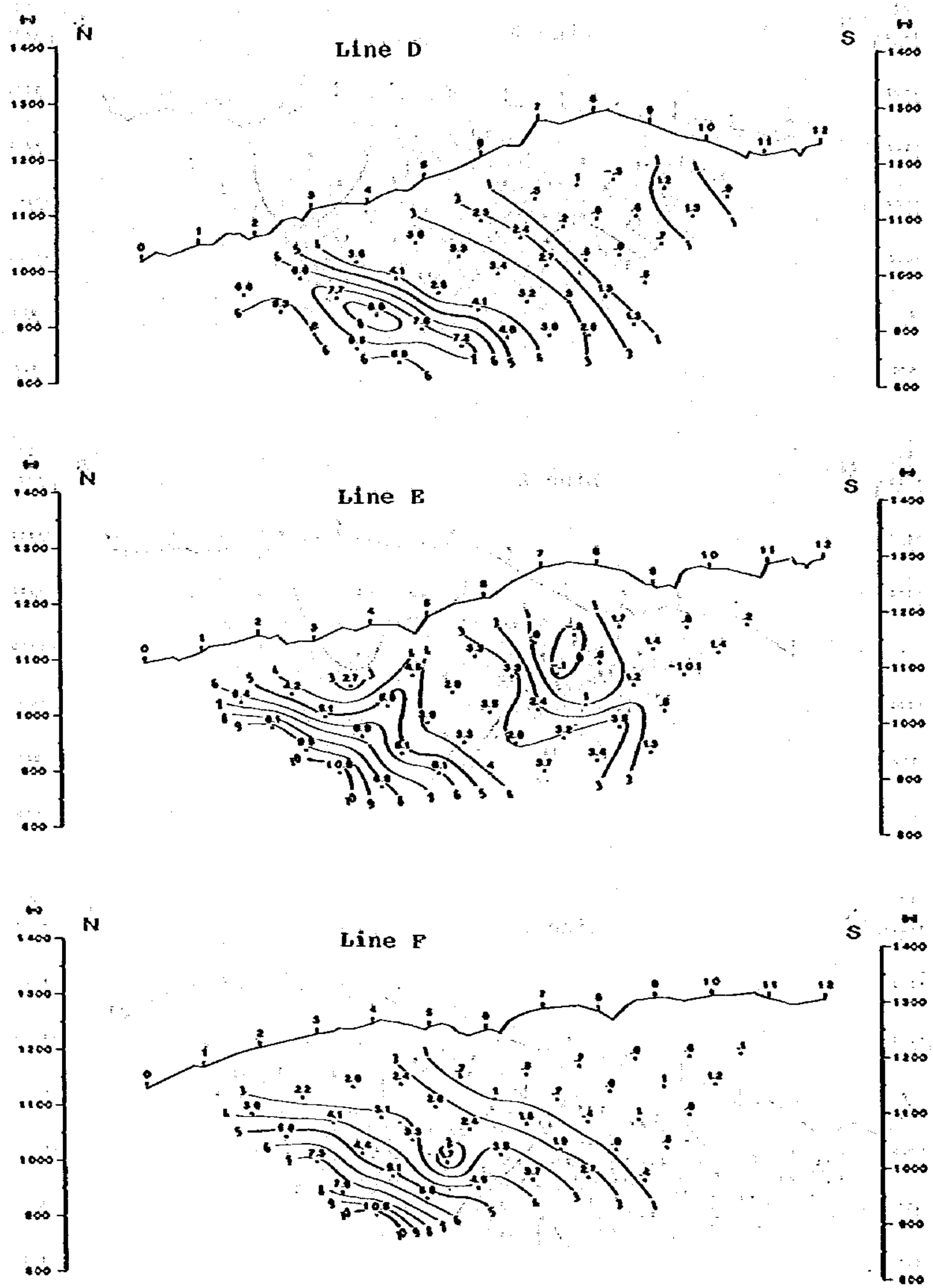

Fig. III-6-2.2 Spectral IP Pseudo-Section
Percent Freqency Effect [0.375 ∿ 3.0 Hz] (Line D, E, F)

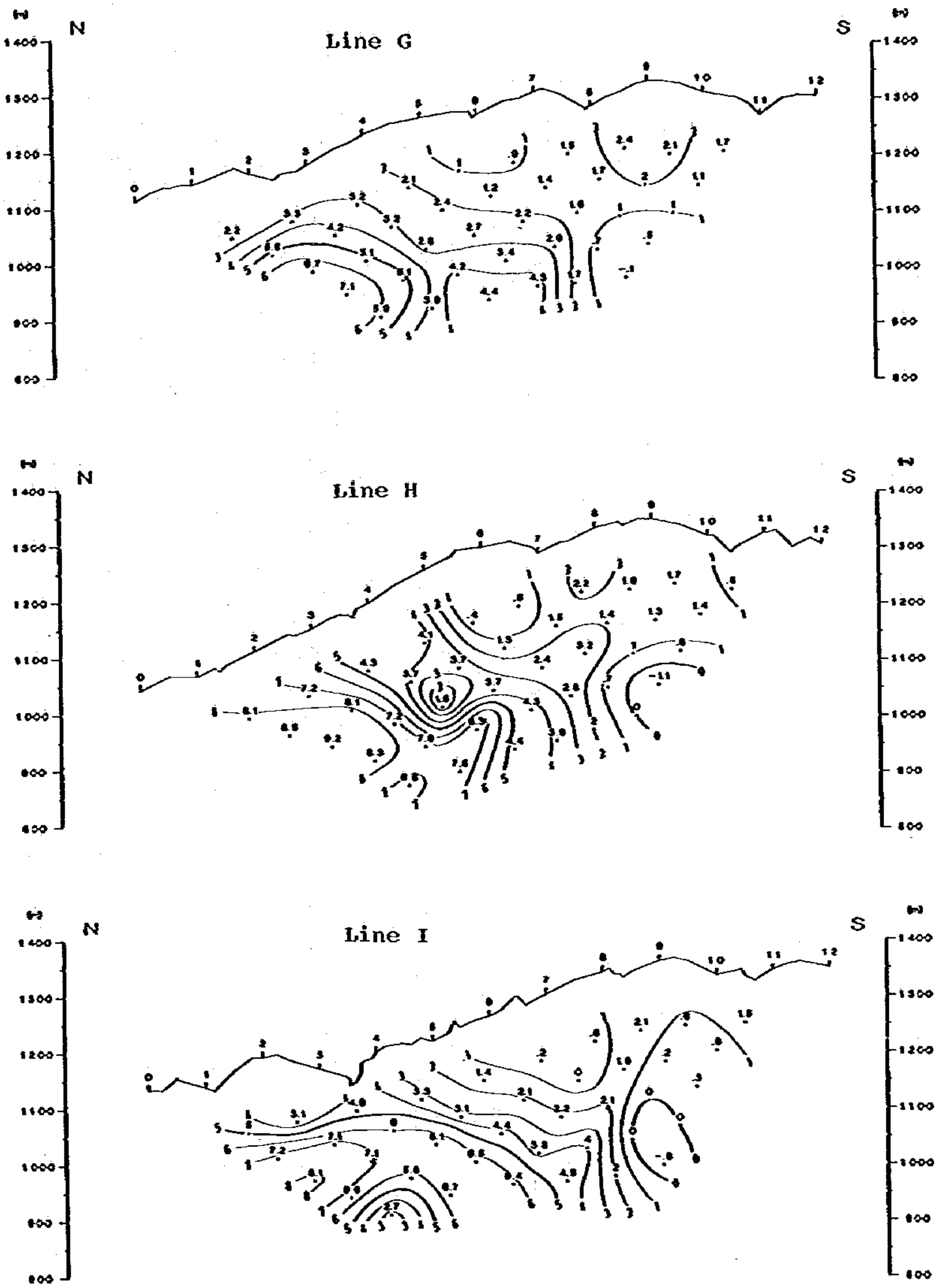

Fig. III-6-2.3 Spectral IP Pseudo-Section
Percent Freqency Effect [0.375 ∿ 3.0 Hz] (Line G. H. I)

Moreover, these anomalies shows good correlation with phase. Taking the correlation between phase and FE with total of 54 pairs of IP anomalies for A ~ F sections, they show the arrangement as shown in Fig. III-6-3, and its coefficient of correlation is calculated as γ = 0.945.

FE of each survey line indicates anomalous zone if more than 3% is anomalous. (This is equivalent to phase anomaly with value of more than -30 milliradian)

Northern end of survey line A at around 200 m deep has 3 ~ 6% of anomalous source. There is shallower anomalous source for survey line B.

About survey line C, FE anomalies are detected in the wide range. Especially the anomaly of the south dipping source of more than 4% caused by anomalous source, spreading from No. 5 ~ 6, is considered to be due to the effect of massive sulfide even though its value of anomalies are less than the ones detected at the northern end of the line. Generally FE anomaly of the disseminated sulfide is normally larger than that of the massive sulfide, but it is needed to note that the strong IP anomaly might be caused by pyrite for some of the cases.

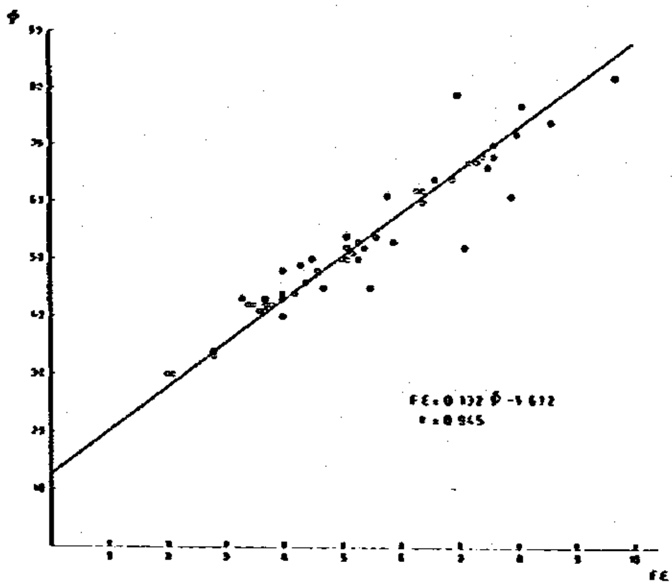

Fig. III-6-3
Correlation of Phase (ϕ) & PFE

Anomaly zone at the northern end of survey lines D, E, F and G successively distributes toward East-West with gentle south dipping. It is understood as that disseminated sulfide is latent in souther side of the boundary of andesite and sedimentary rocks.

For survey line H, this type of anomaly is recognized near the ground surface, and width of dissemination widely distributes toward north of No. 3 ~4. In addition, the biggest value of FE anomaly is 9.3% detected at deep part of No. 3.

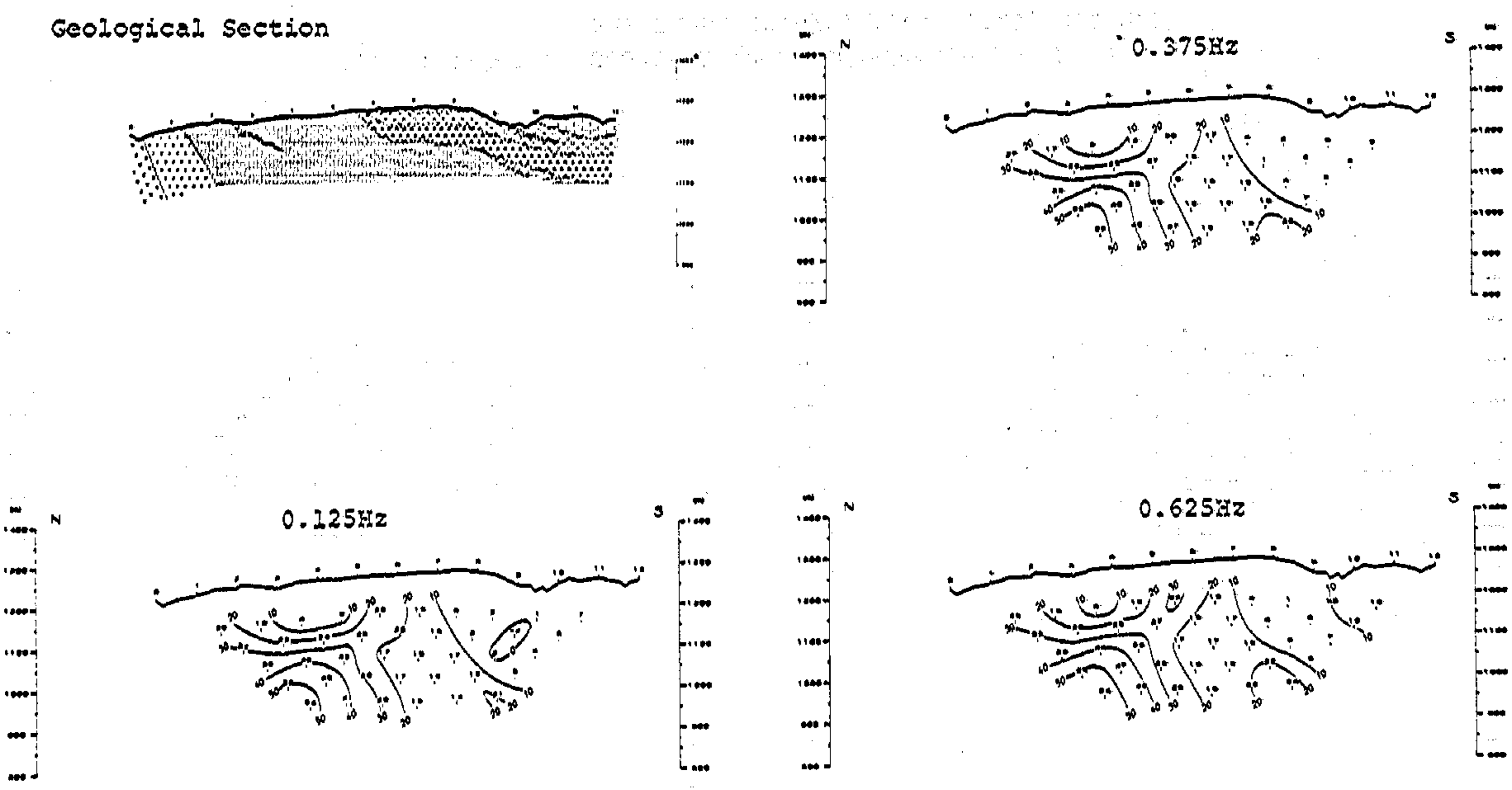

Fig. III-7-1.1 Spectral IP Pseudo-Section of Line A
Raw Phase (G. Sec., 0.125, 0.375, 0.625 Hz)

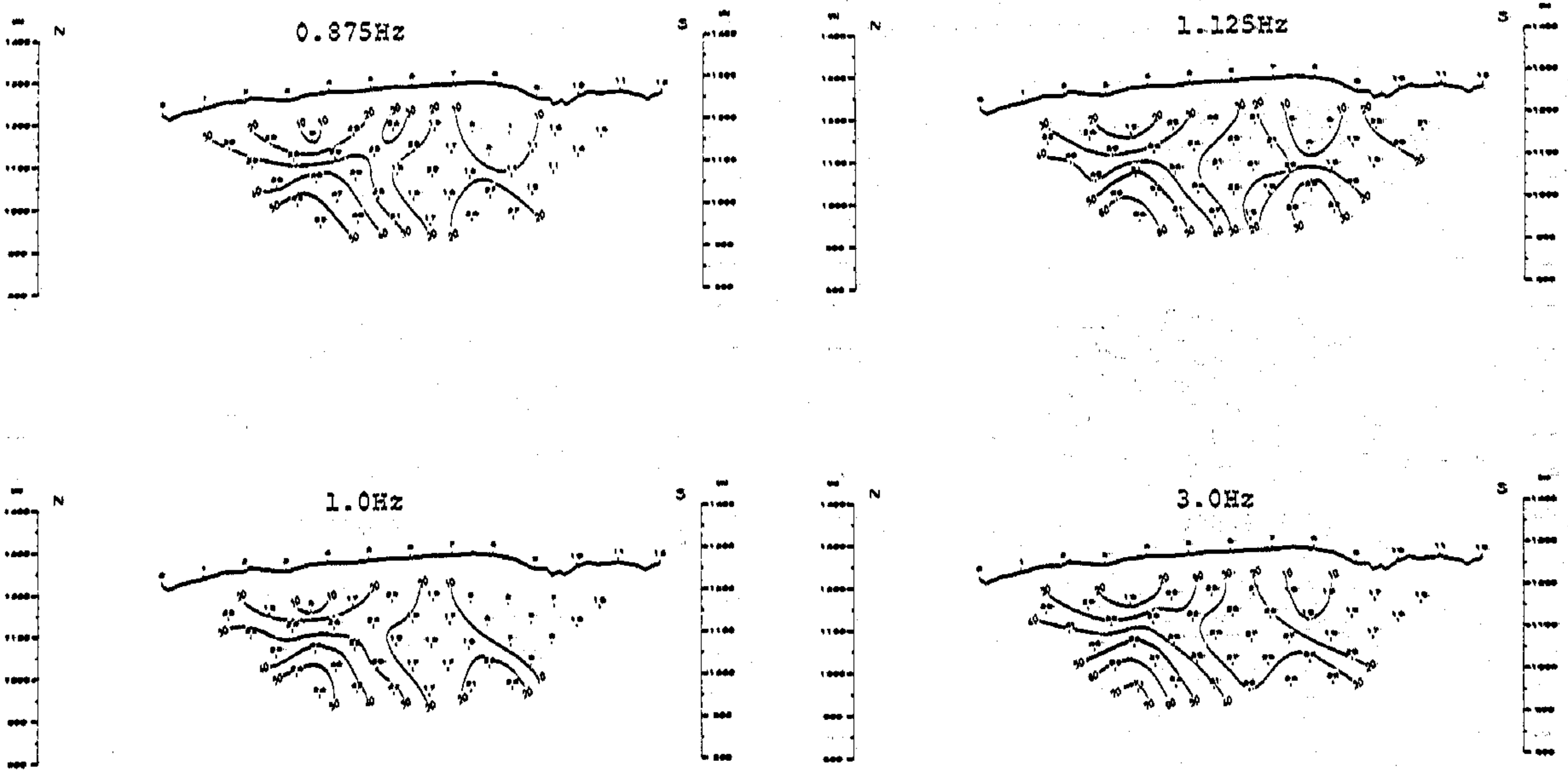

Fig. III-7-1.2 Spectral IP Pseudo-Section of Line A
Raw Phase (0.875, 1.0, 1.125, 3.0 Hz)

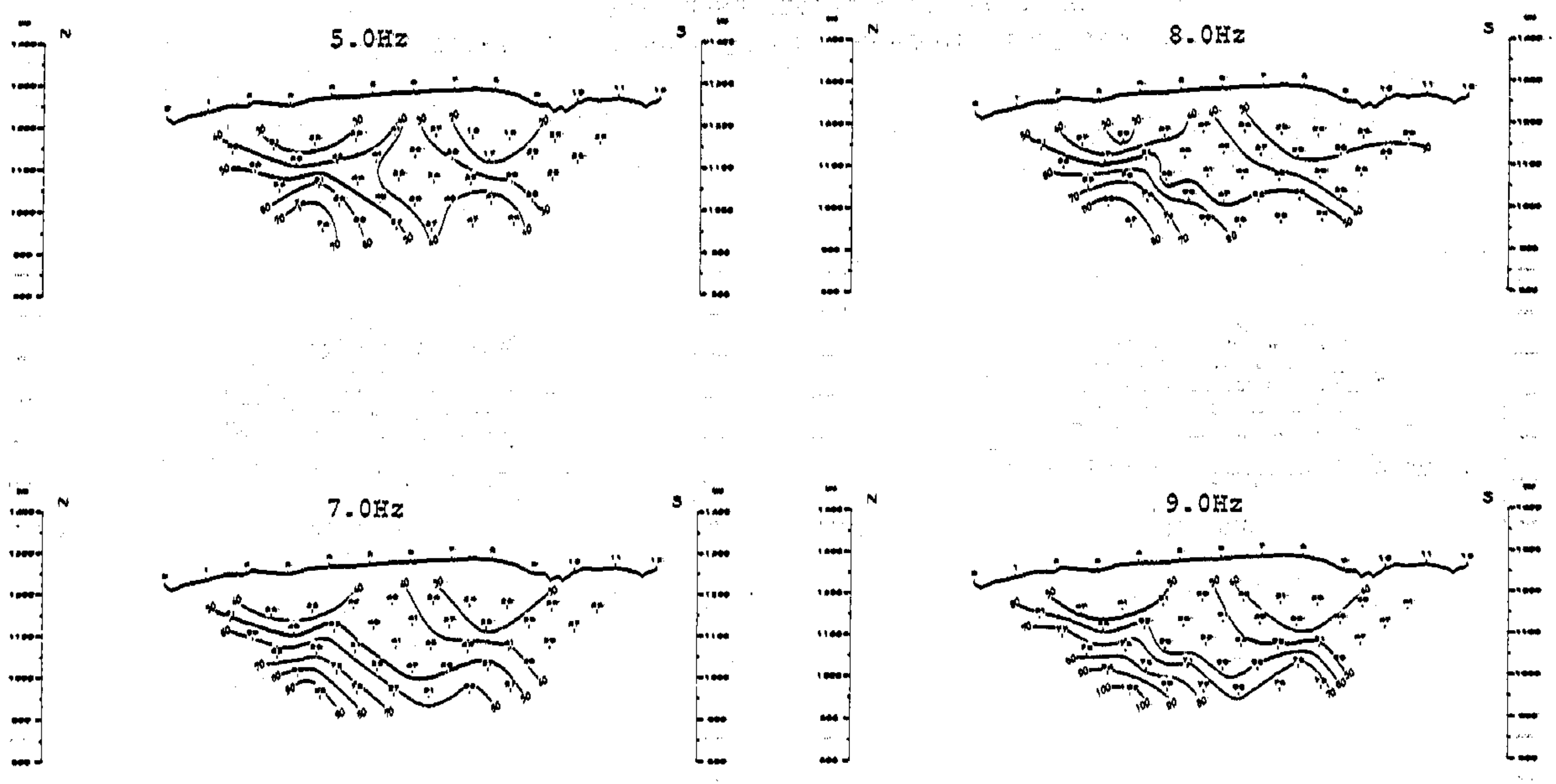

Fig. III-7-1.3 Spectral IP Pseudo-Section of Line A
Raw Phase (5,0, 7.0, 8.0, 9.0 Hz)

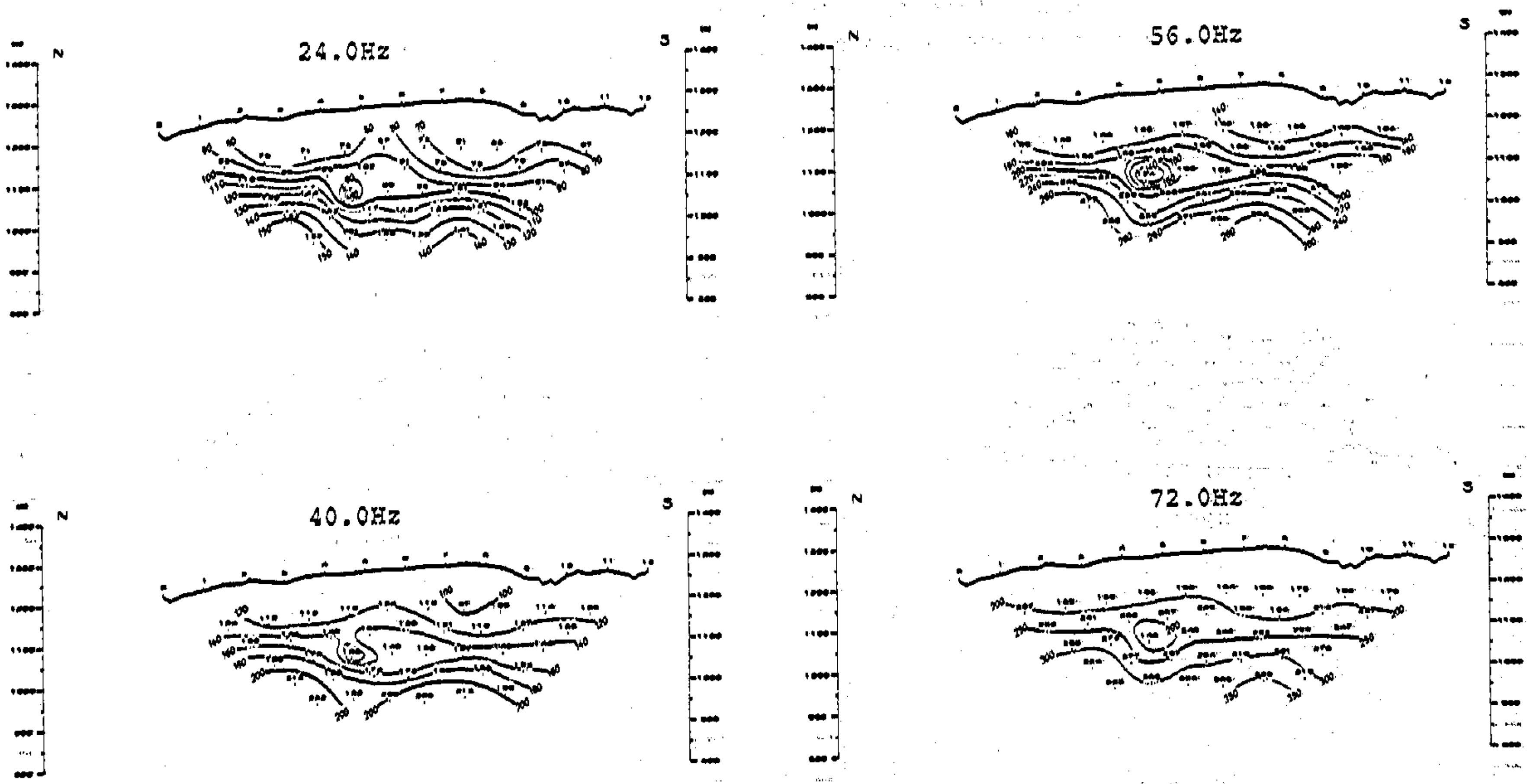

Fig. III-7-1.4 Spectral IP Pseudo-Section of Line A
Raw Phase (24.0, 40.0, 56.0, 72.0 Hz)

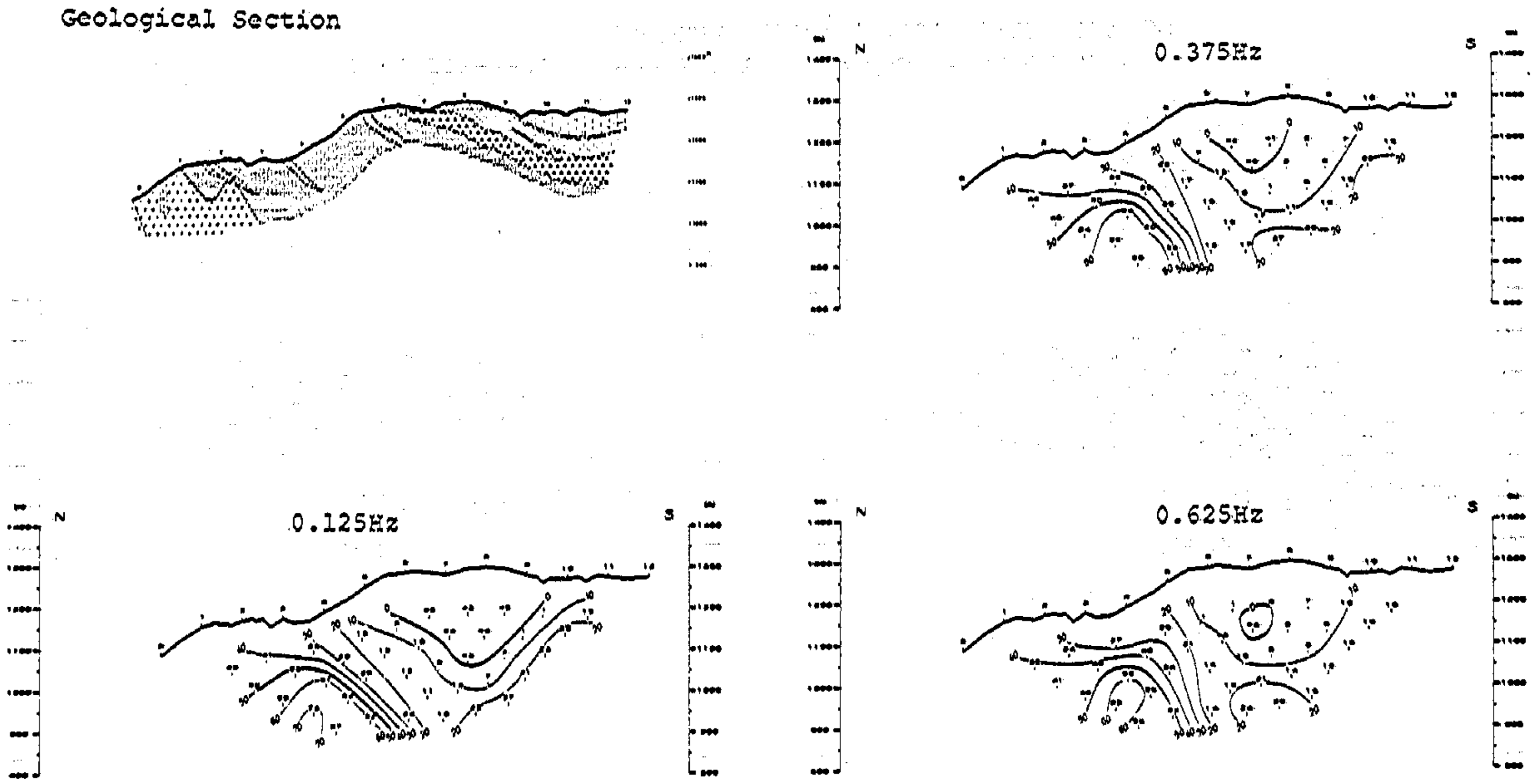

Fig. III-7-2.1 Spectral IP Pseudo-Section of Line B
Raw Phase (G. Sec., 0.125, 0.375, 0.625 Hz)

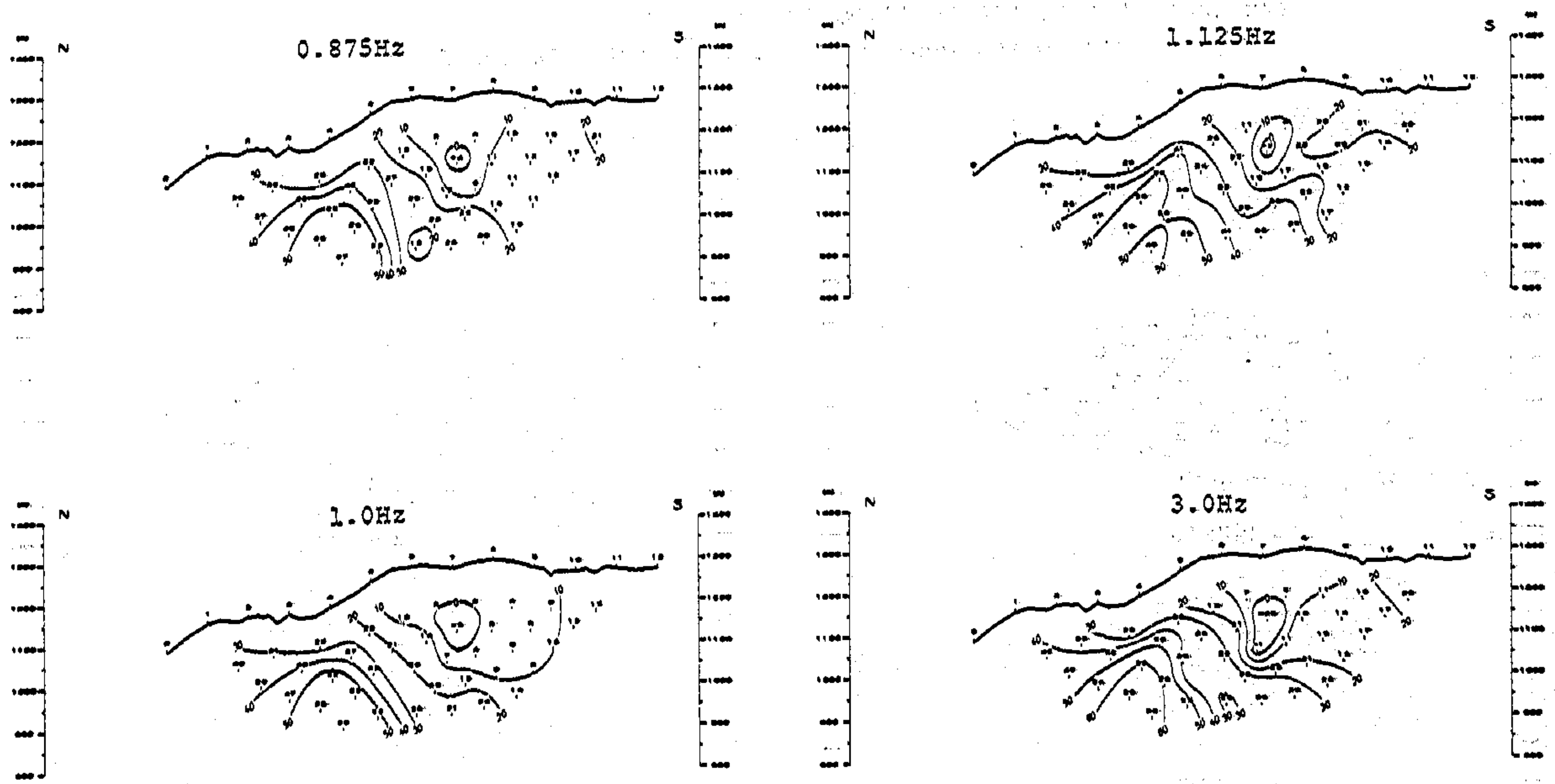

Fig. III-7-2.2 Spectral IP Pseudo-Section of Line B
Raw Phase (0.875, 1.0, 1.125, 3.0 Hz)

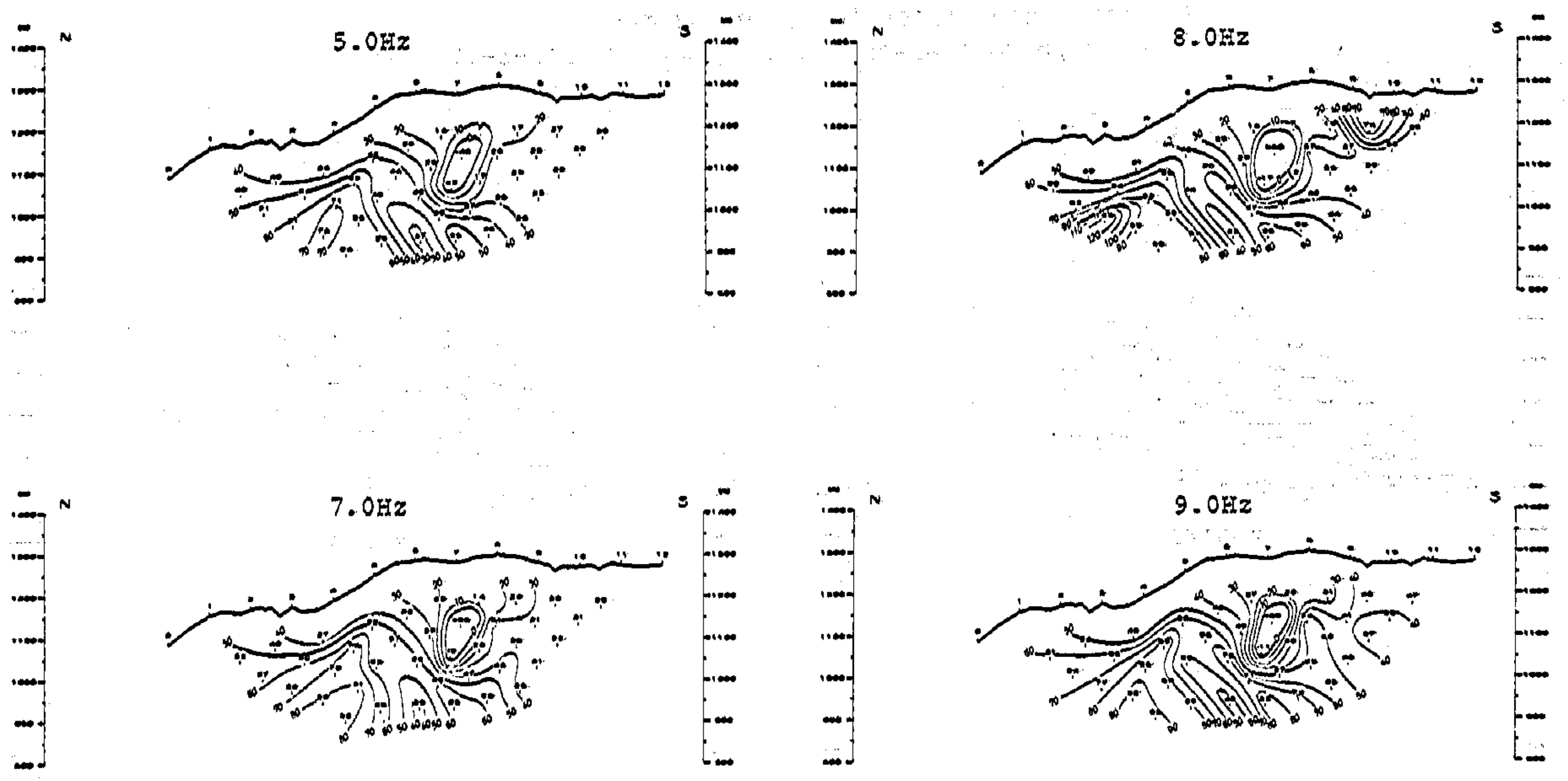

Fig. III-7-2.3 Spectral IP Pseudo-Section of Line B
Raw Phase (5.0, 7.0, 8.0, 9.0 Hz)

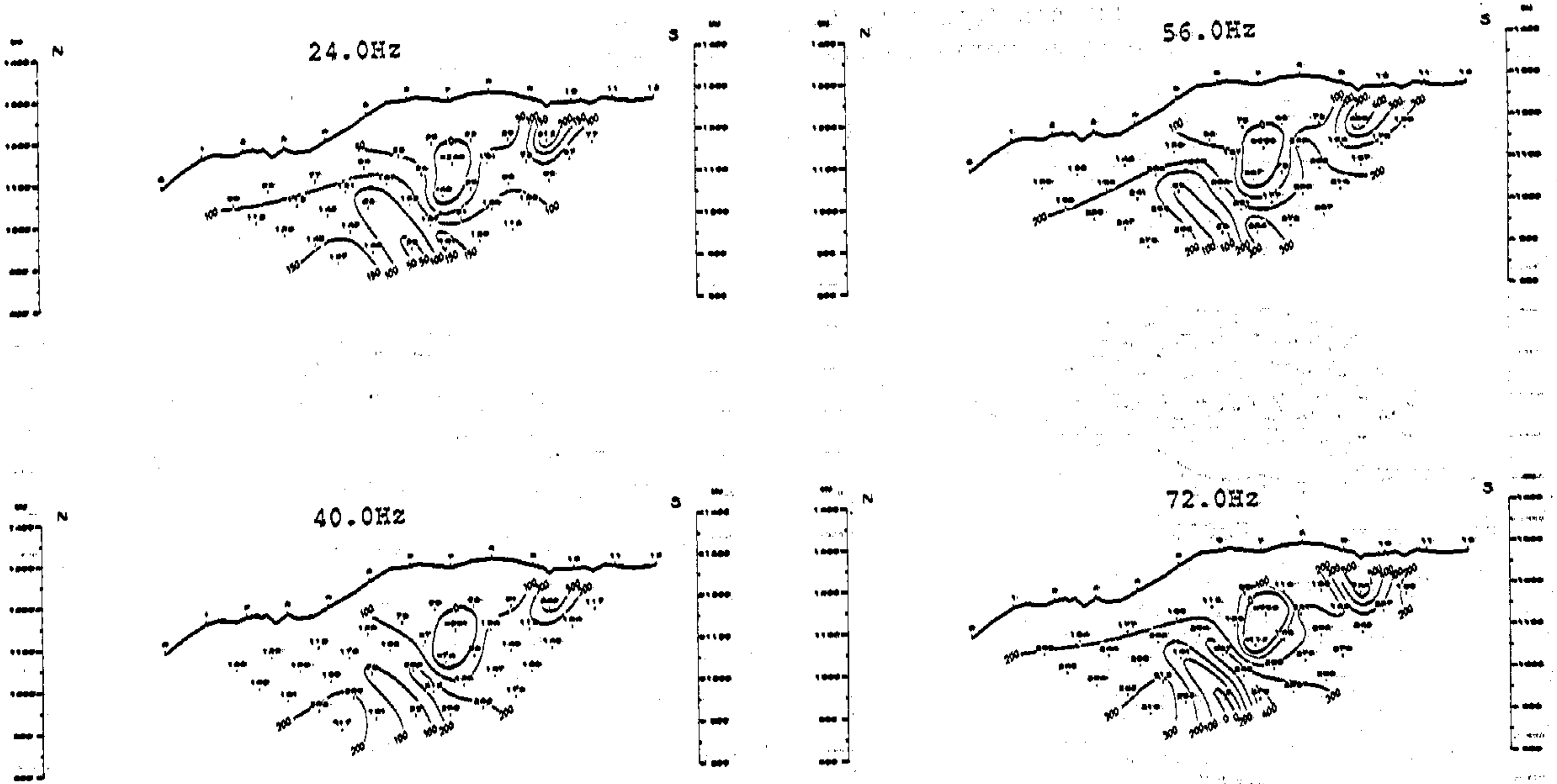

Fig. III-7-2.4 Spectral IP Pseudo-Section of Line B
Raw Phase (24.0, 40.0, 56.0, 72.0 Hz)

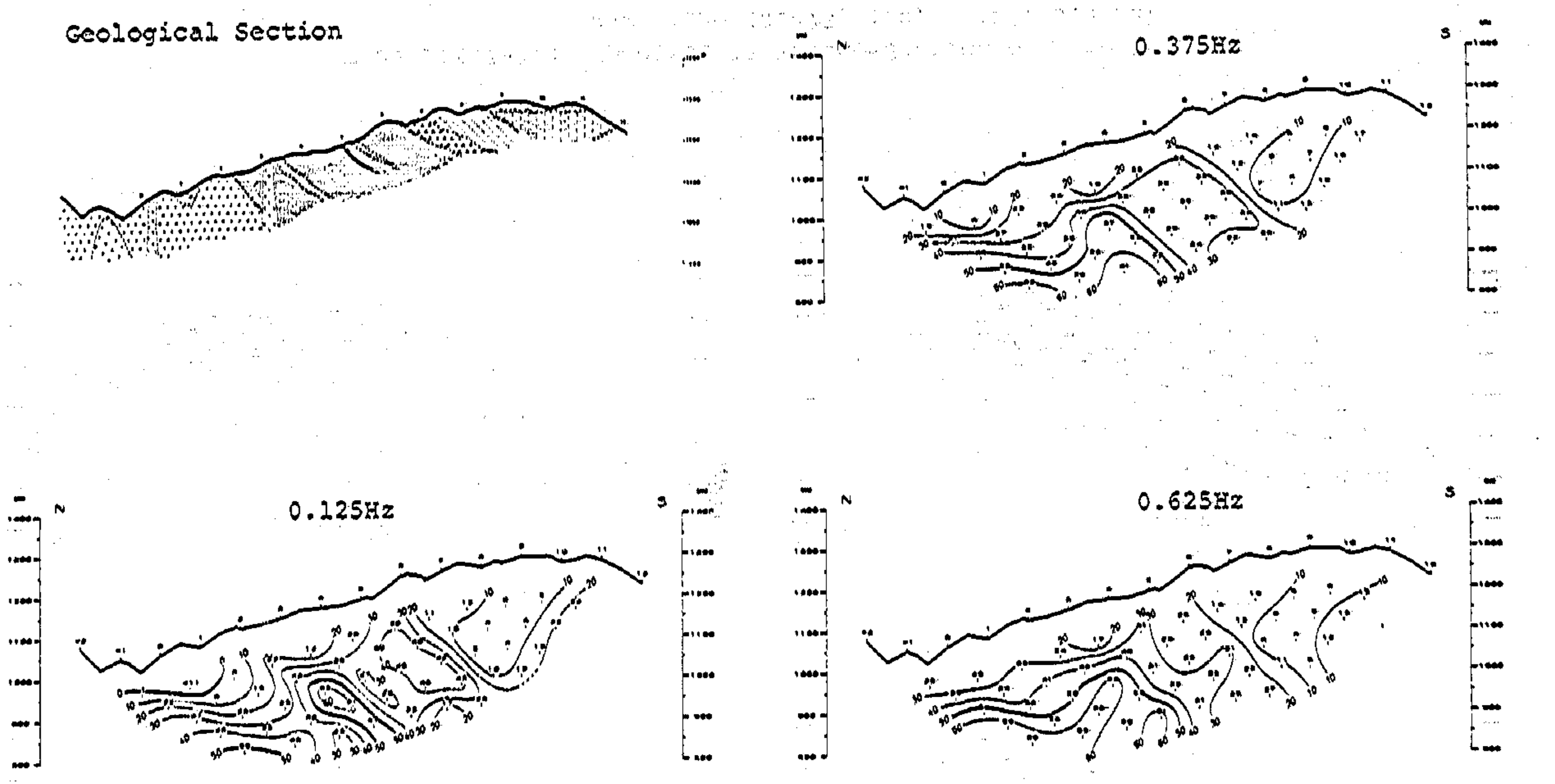

Fig. III-7-3.1 Spectral IP Pseudo-Section of Line C
Raw Phase (G. Sec., 0.125, 0.375, 0.625 Hz)

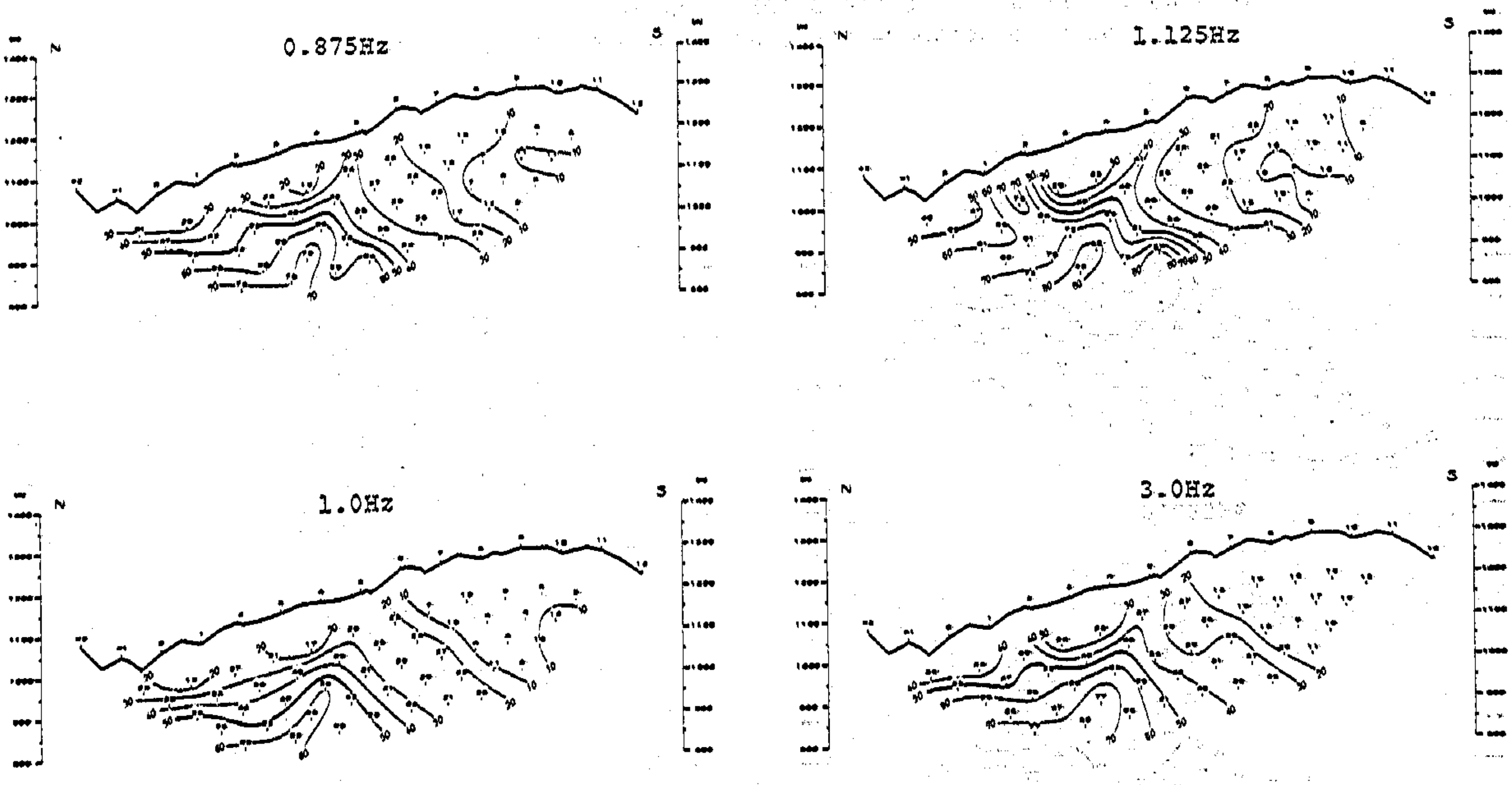

Fig. III-7-3.2 Spectral IP Pseudo-Section of Line C
Raw Phase (0.875, 1.0, 1.125, 3.0 Hz)

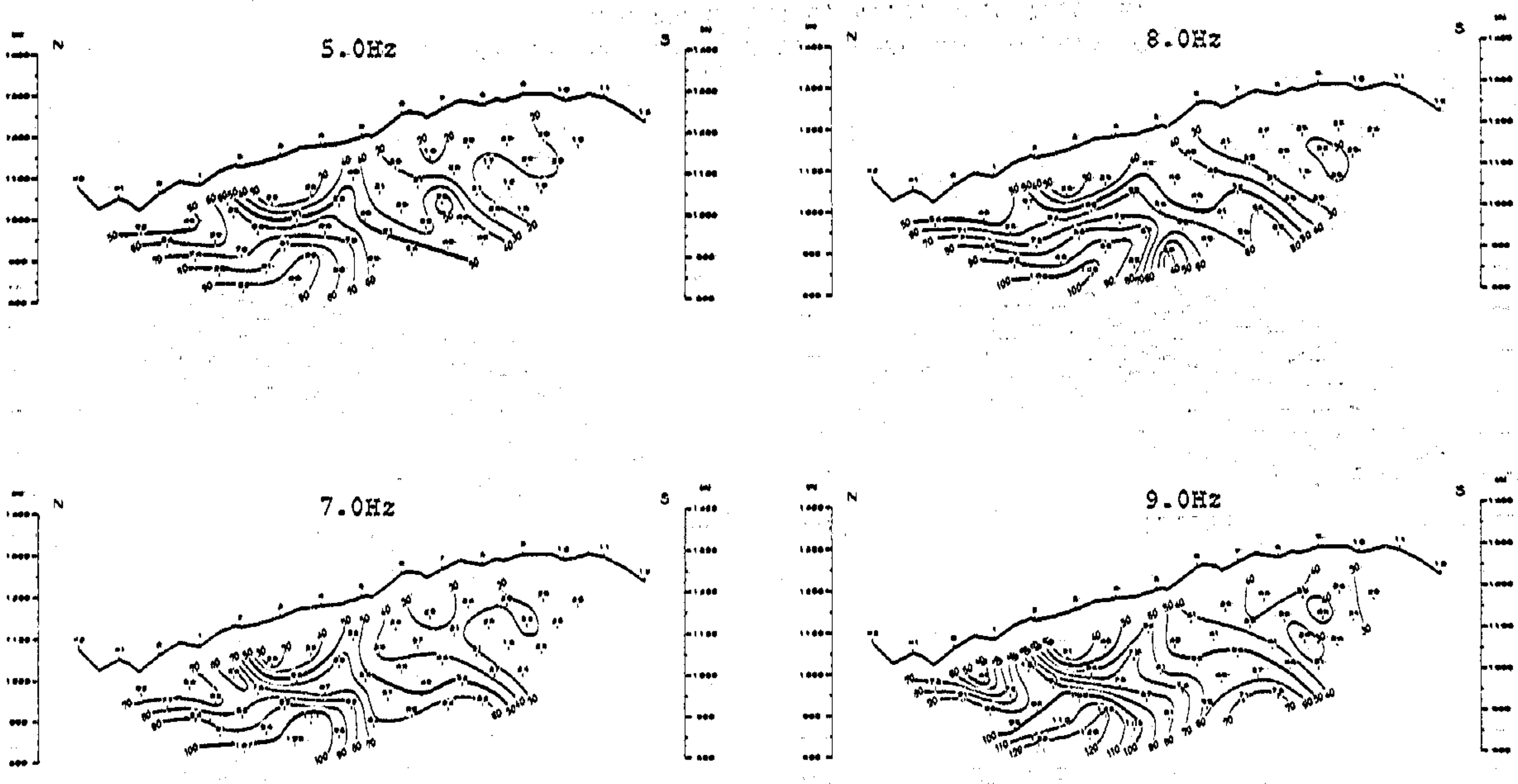

Fig. III-7-3.3 Spectral IP Pseudo-Section of Line C
Raw Phase (5.0, 7.0, 8.0, 9.0 Hz)

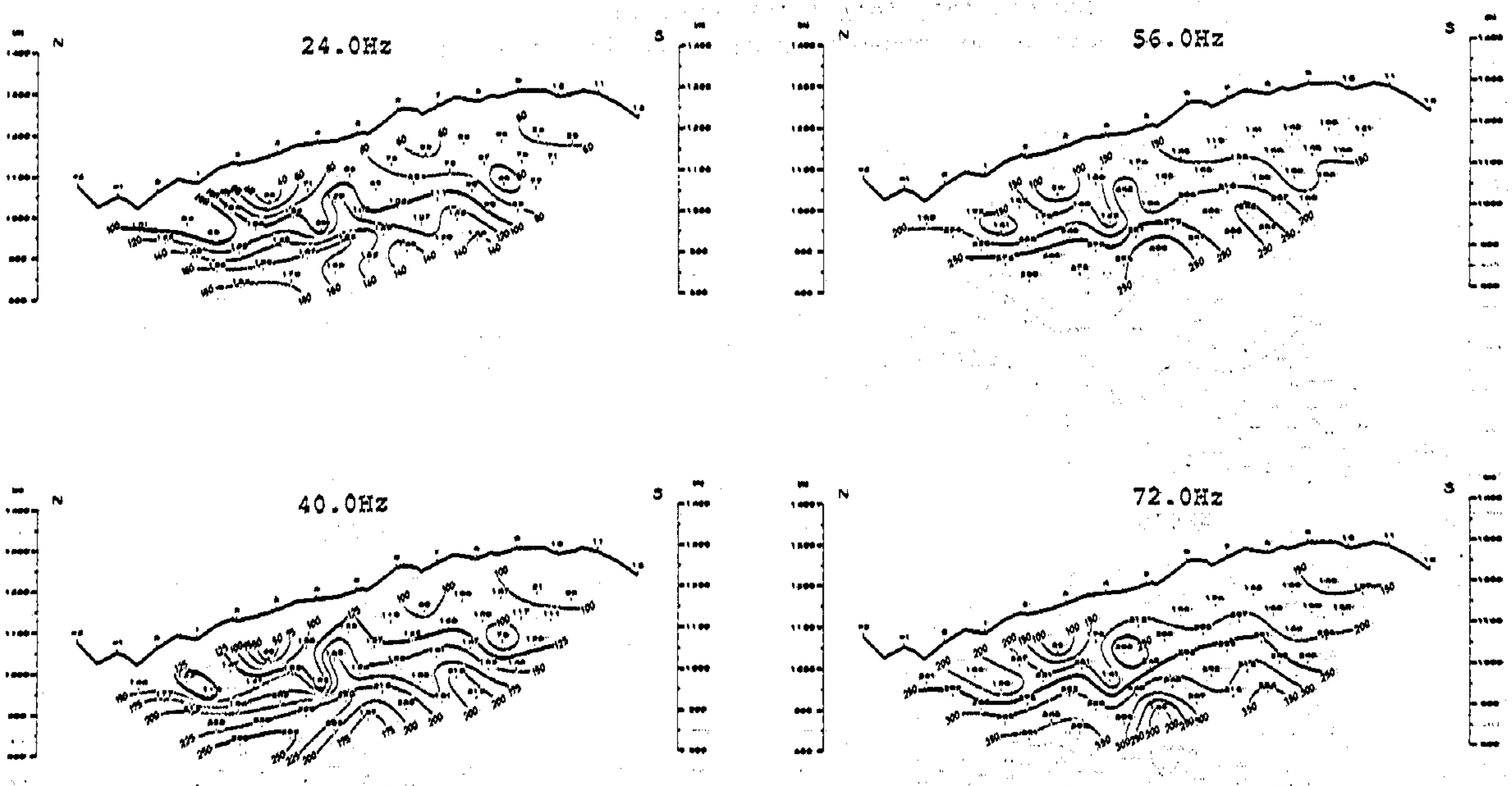

Fig. III-7-3.4 Spectral IP Pseudo-Section of Line C
Raw Phase (24.0, 40.0, 56.0 72.0 Hz)

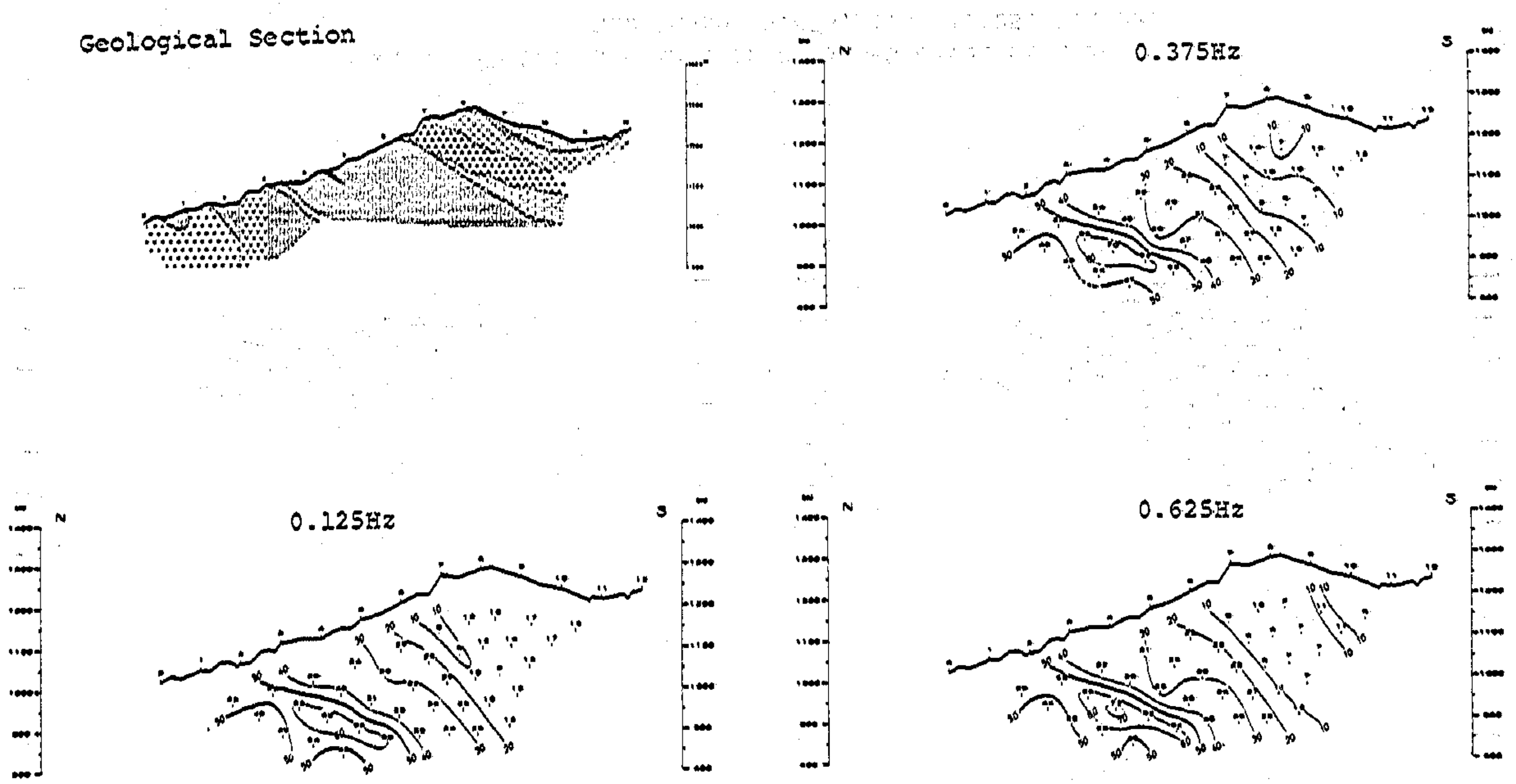

Fig. III-7-4.1 Spectral IP Pseudo-Section of Line D
Raw Phase (G. Sec., 0.125, 0.375, 0.625 Hz)

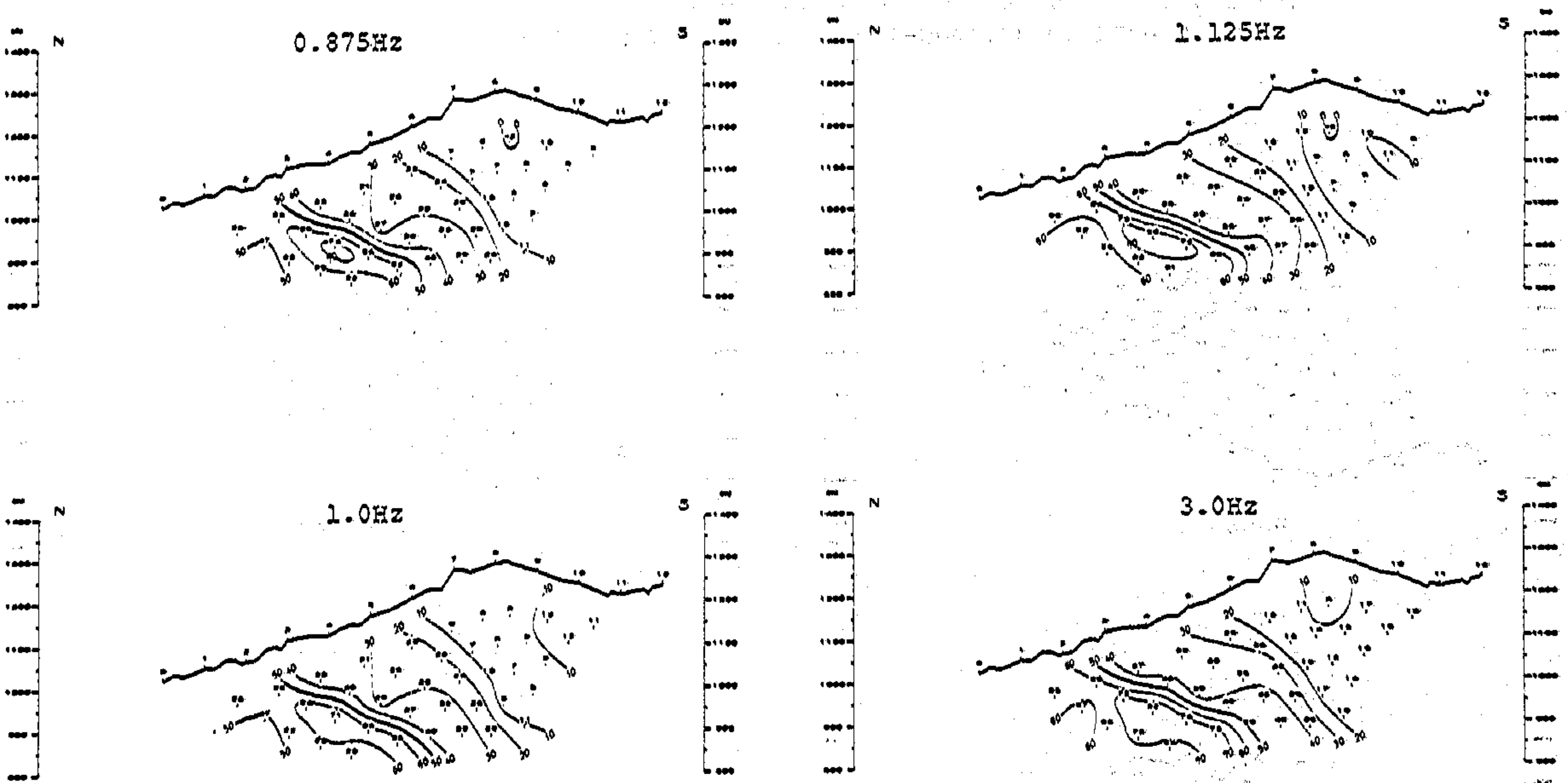

Fig. III-7-4.2 Spectral IP Pseudo-Section of Line D
Raw Phase (0.875, 1.0, 1.125, 3.0 Hz)

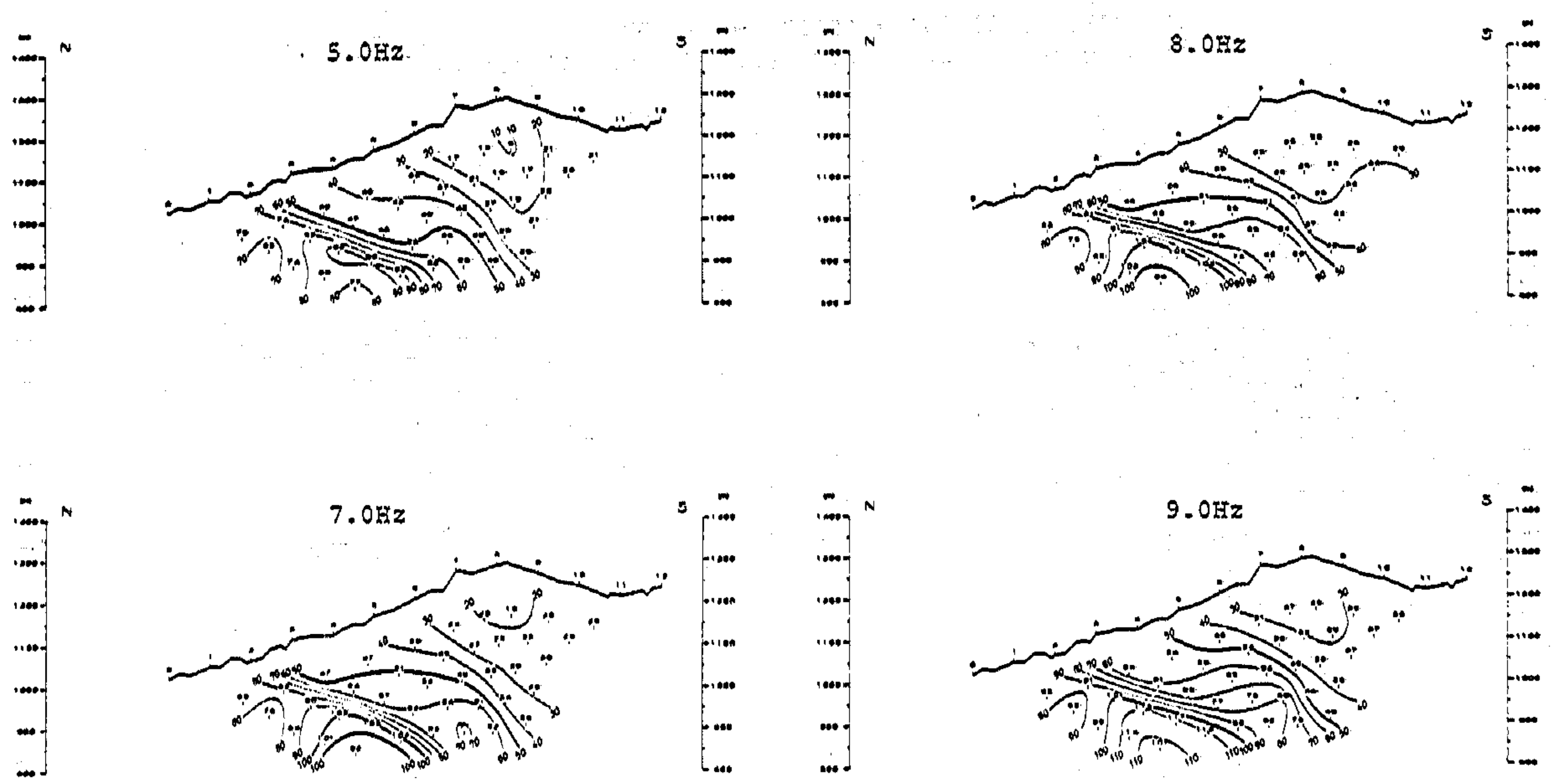

Fig. III-7-4.3 Spectral IP Pseudo-Section of Line D
Raw Phase (5.0, 7.0, 8.0, 9.0 Hz)

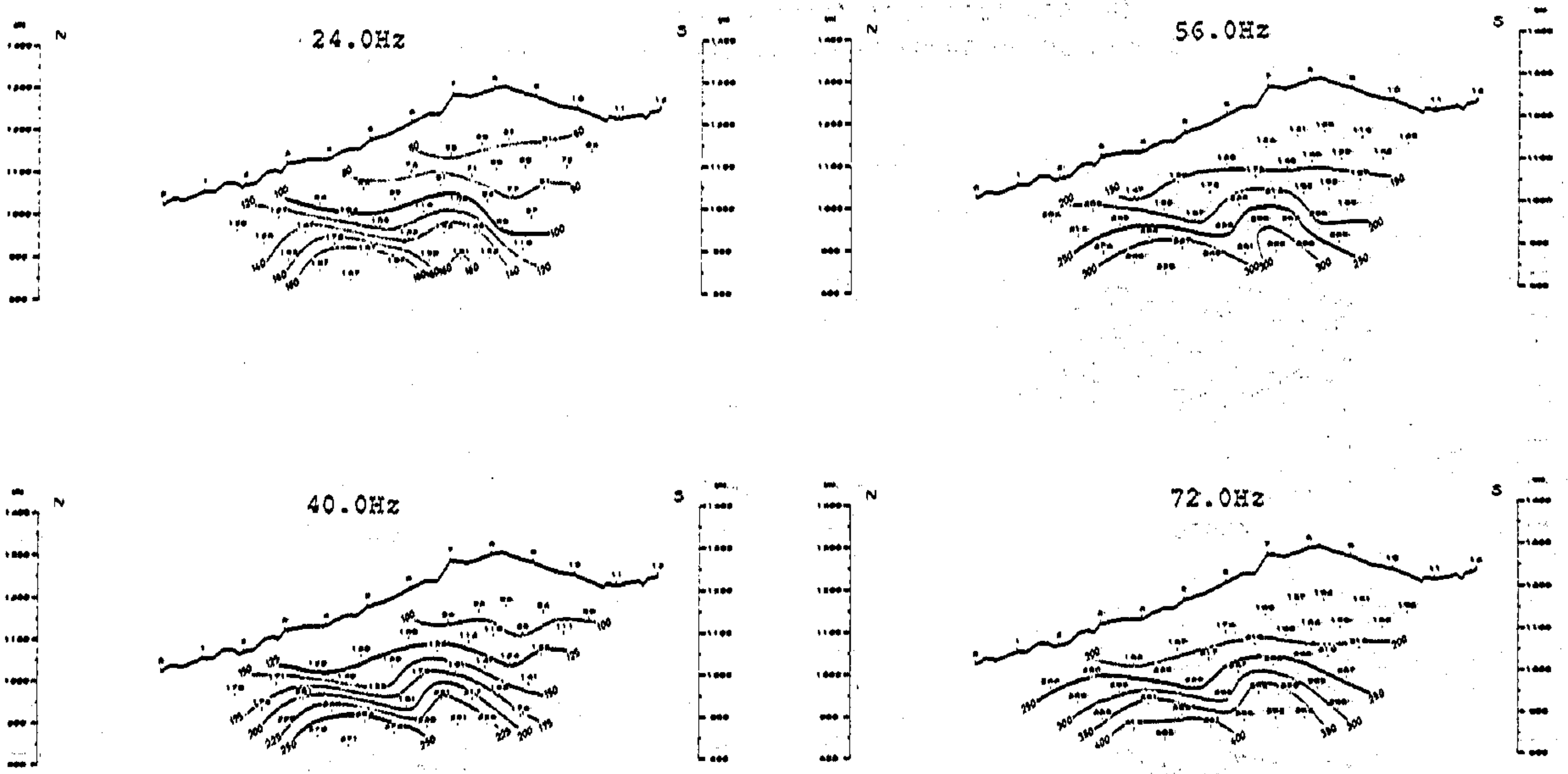

Fig. III-7-4.4 Spectral IP Pseudo-Section of Line D
Raw Phase (24.0, 40.0, 56.0, 72.0 Hz)

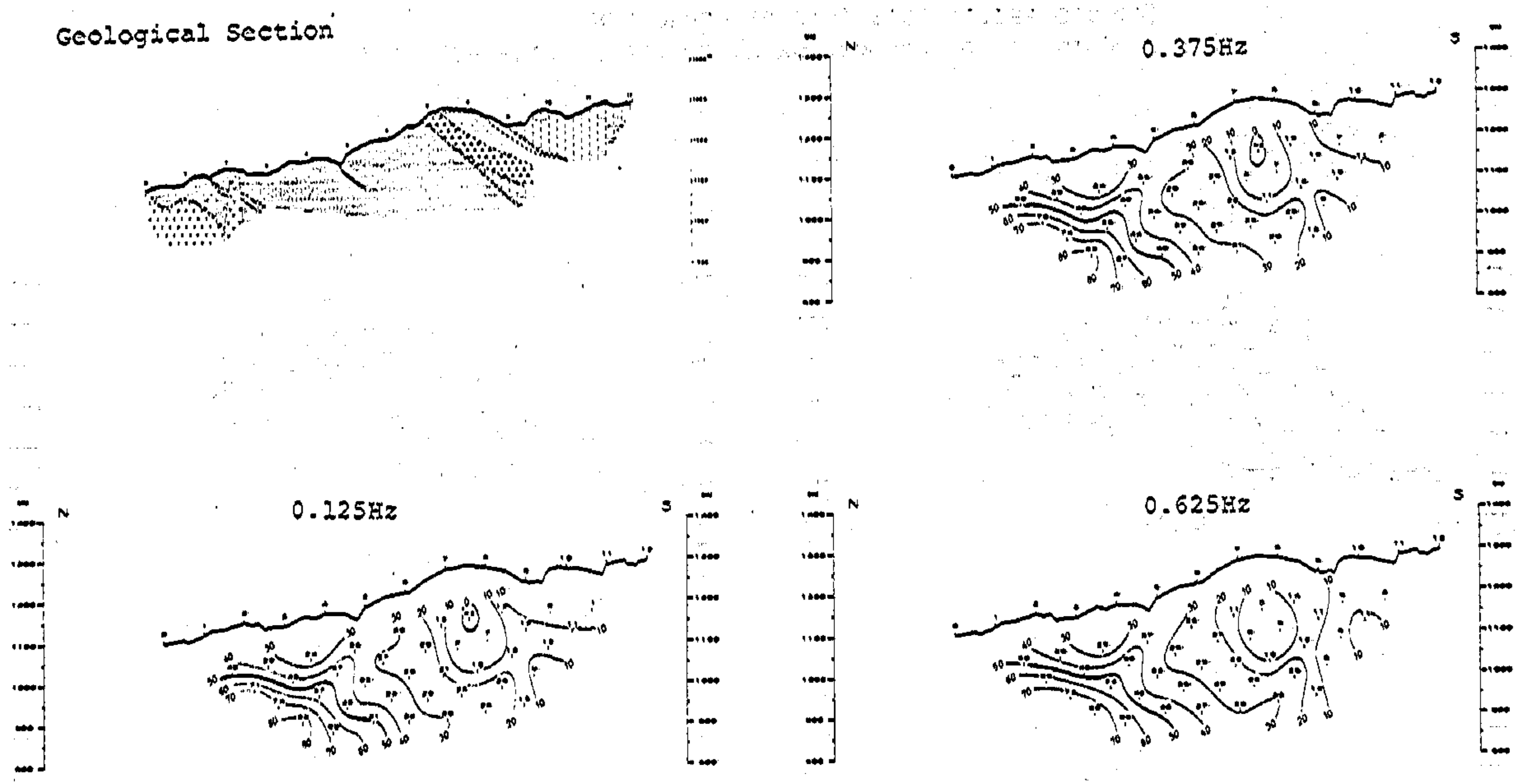

Fig. III-7-5.1 Spectral IP Pseudo-Section of Line E
Raw Phase (G. Sec., 0.125, 0.375, 0.625 Hz)

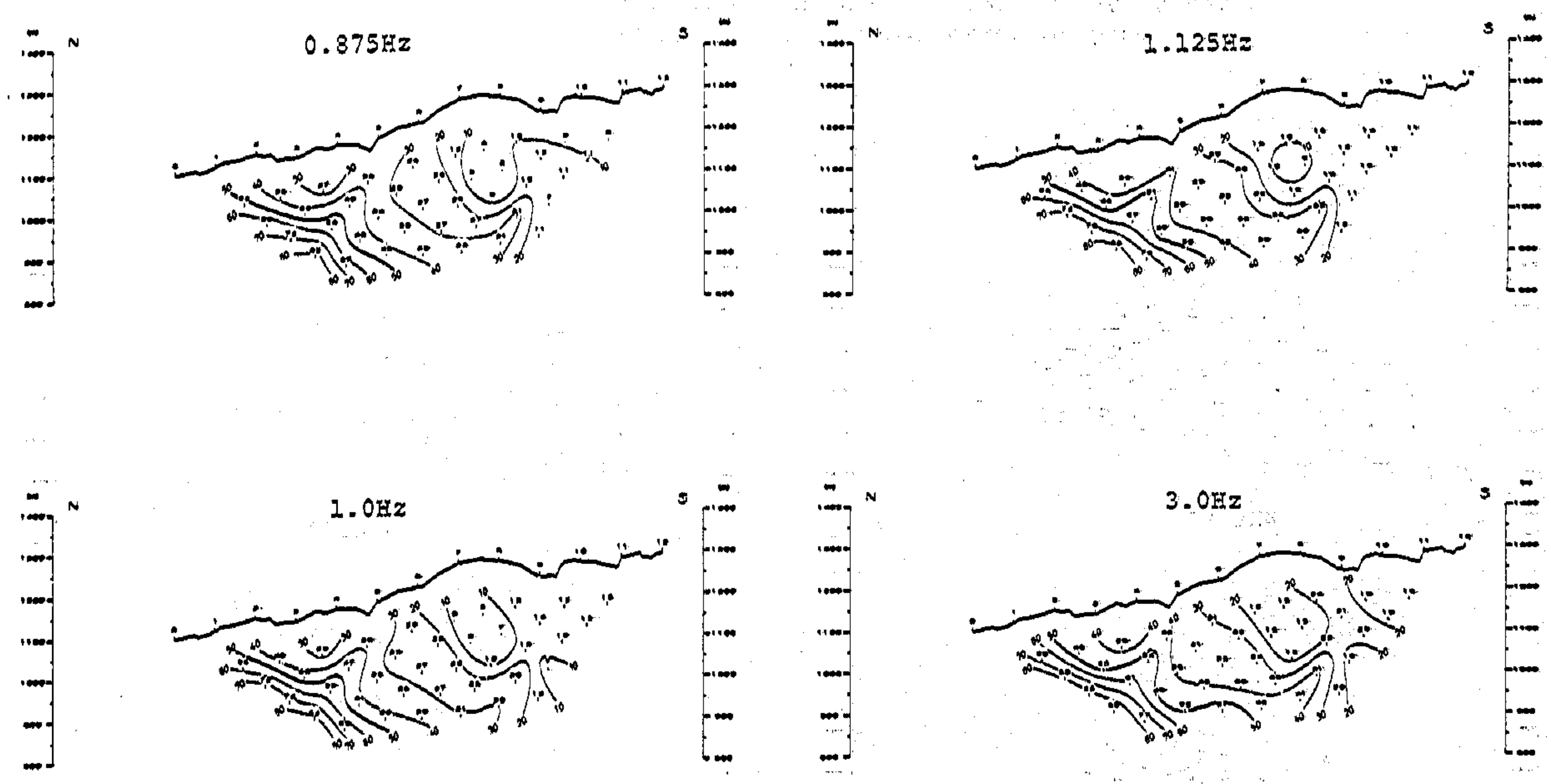

Fig. III-7-5.2 Spectral IP Pseudo-Section of Line E
Raw Phase (0.875, 1.0, 1.125, 3.0 Hz)

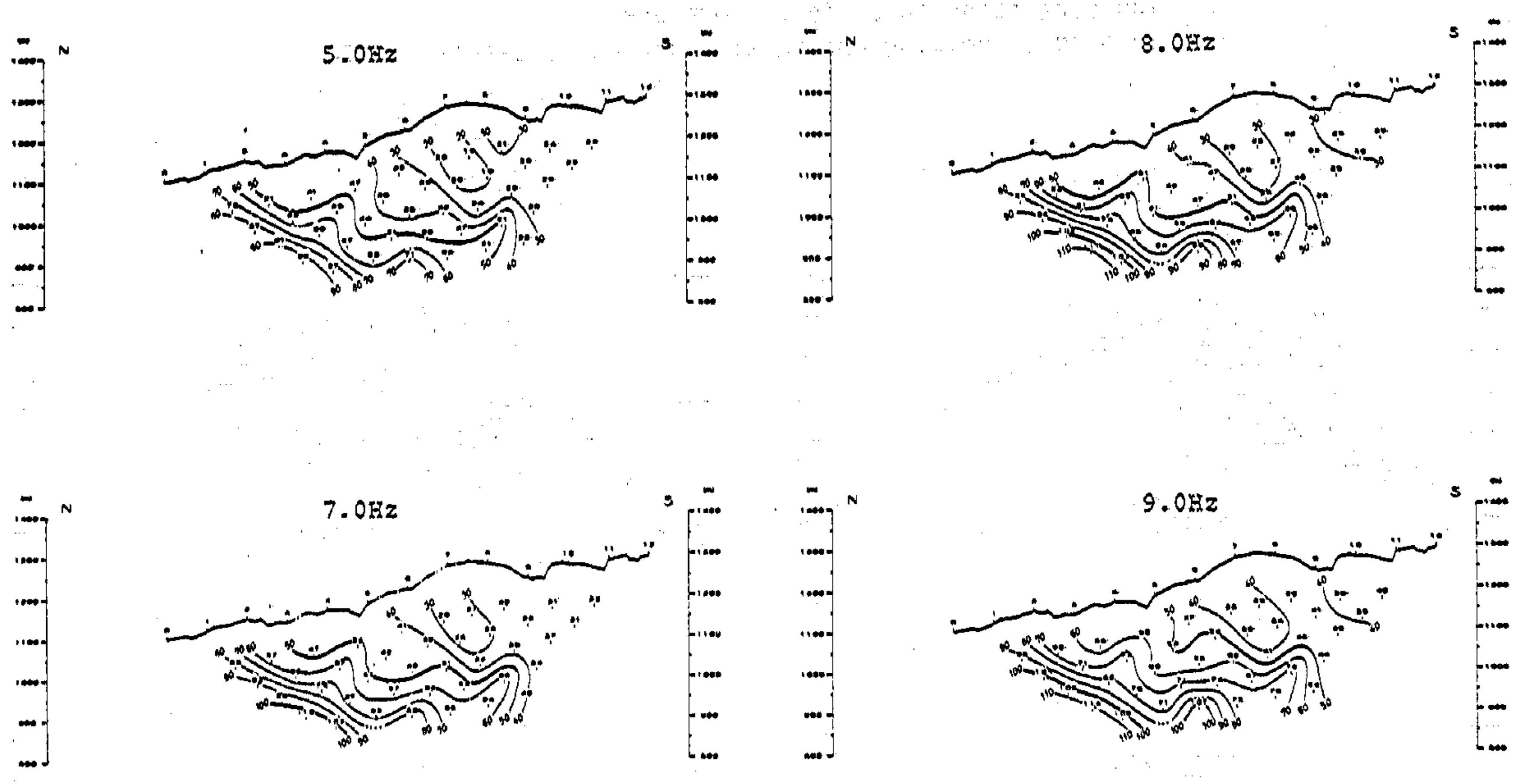

Fig. III-7-5.3 Spectral IP Pseudo-Section of Line E
Raw Phase (5.0, 7.0, 8.0, 9.0 Hz)

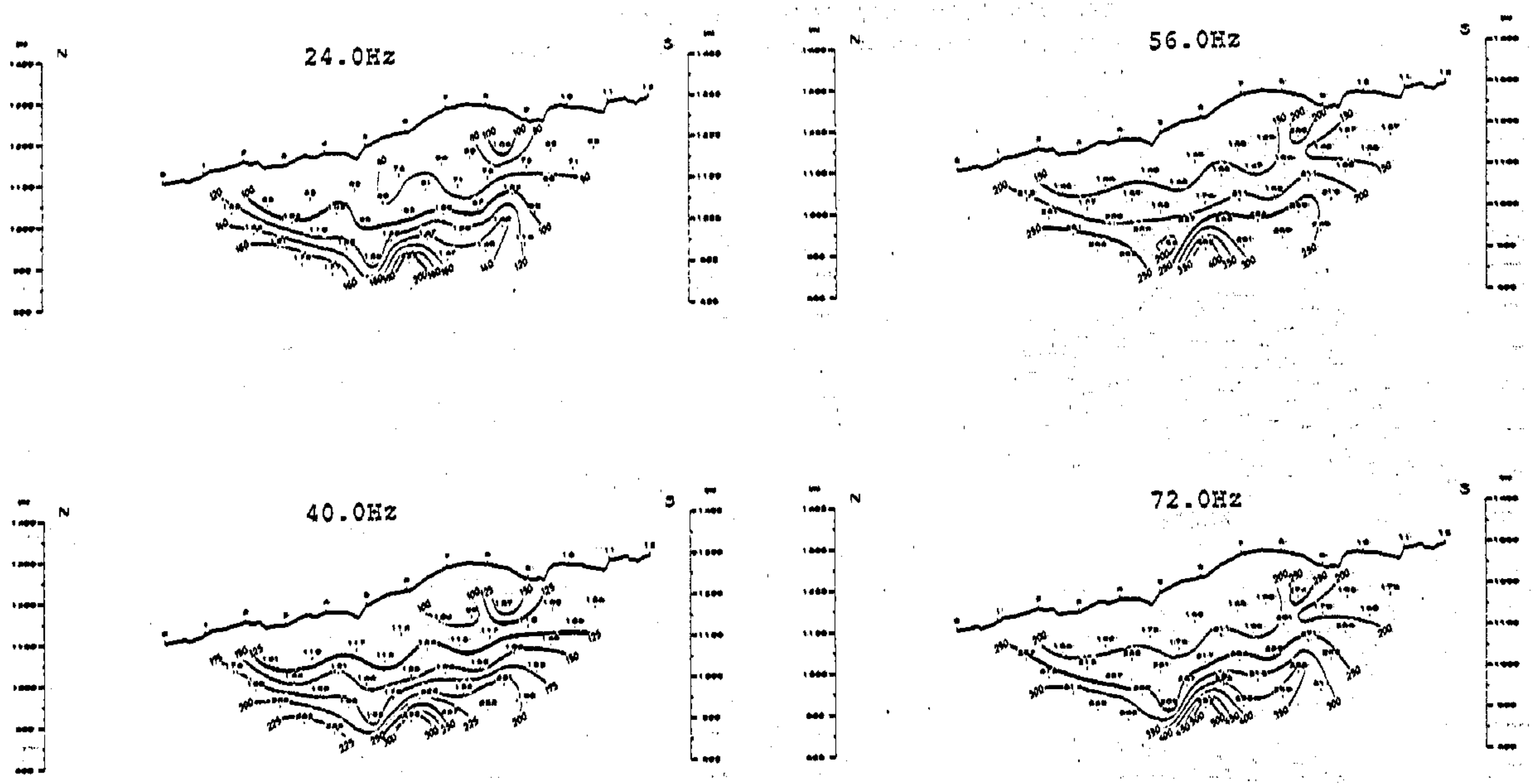

Fig. III-7-5.4 Spectral IP Pseudo-Section of Line E
Raw Phase (24.0, 40.0, 56.0, 72.0 Hz)

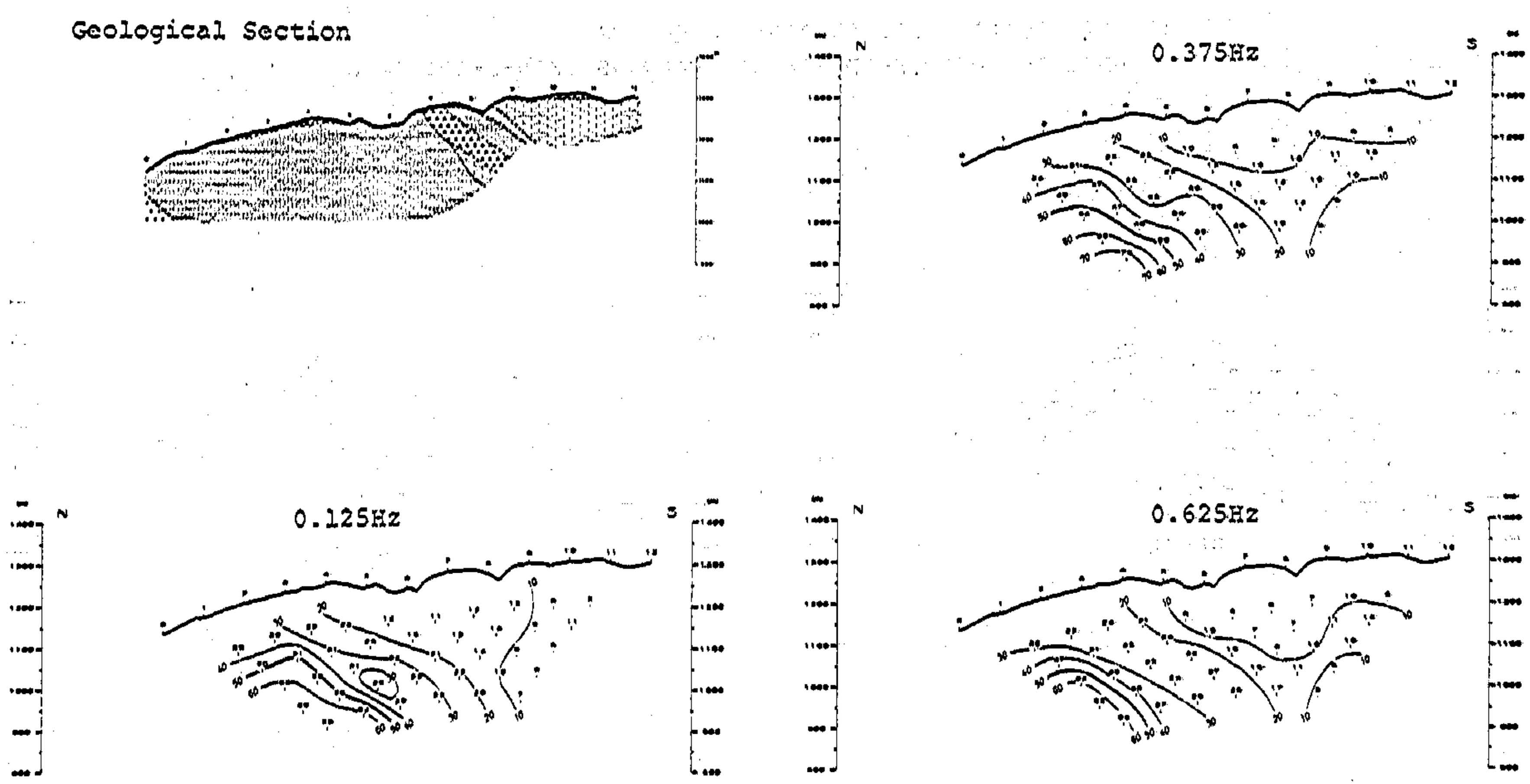

Fig. III-7-6.1 Spectral IP Pseudo-Section of Line F
Raw Phase (G. Sec., 0.125, 0.375, 0.625 Hz)

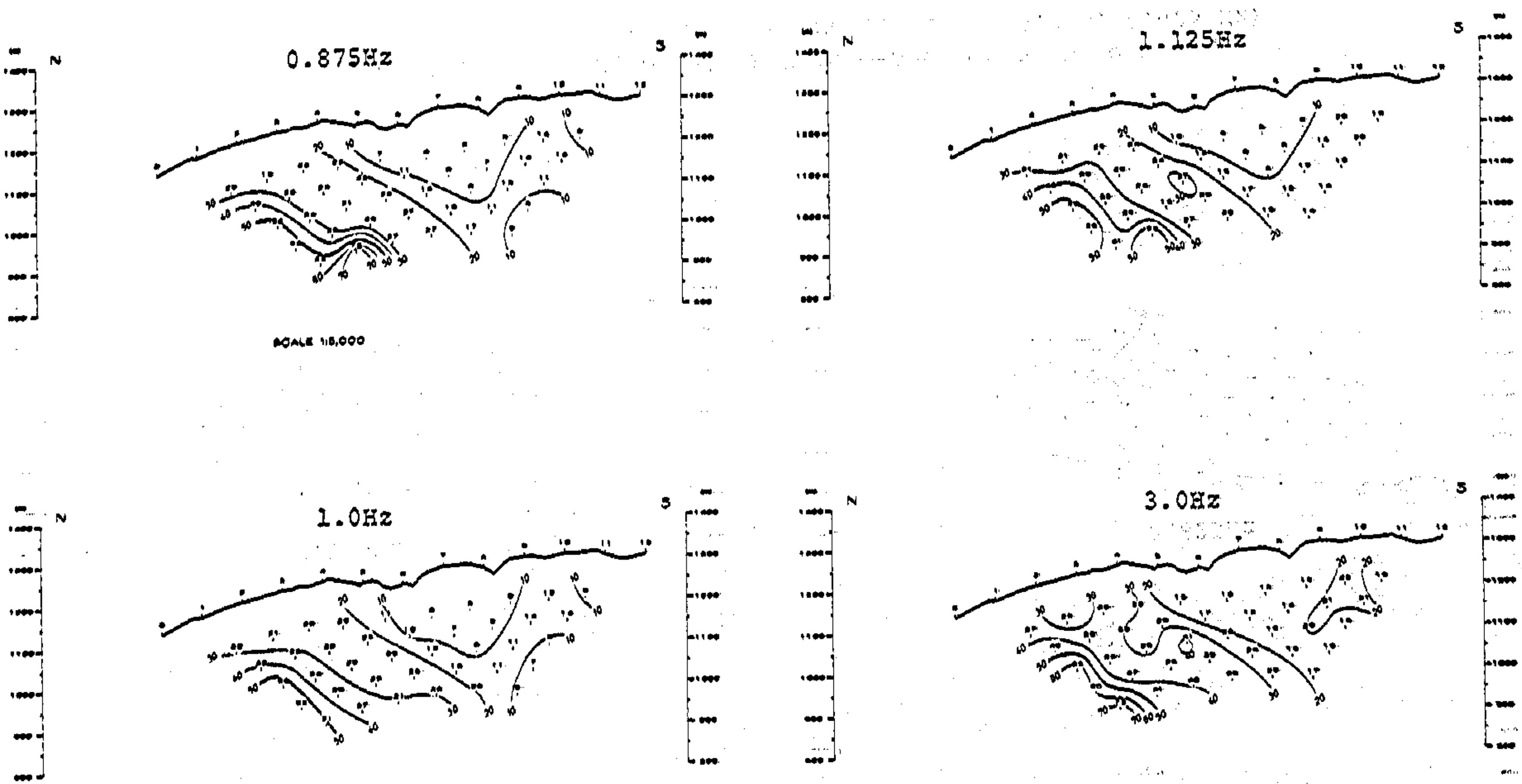

Fig. III-7-6.2 Spectral IP Pseudo-Section of Line F
Raw Phase (0.875, 1.0, 1.125, 3.0 Hz)

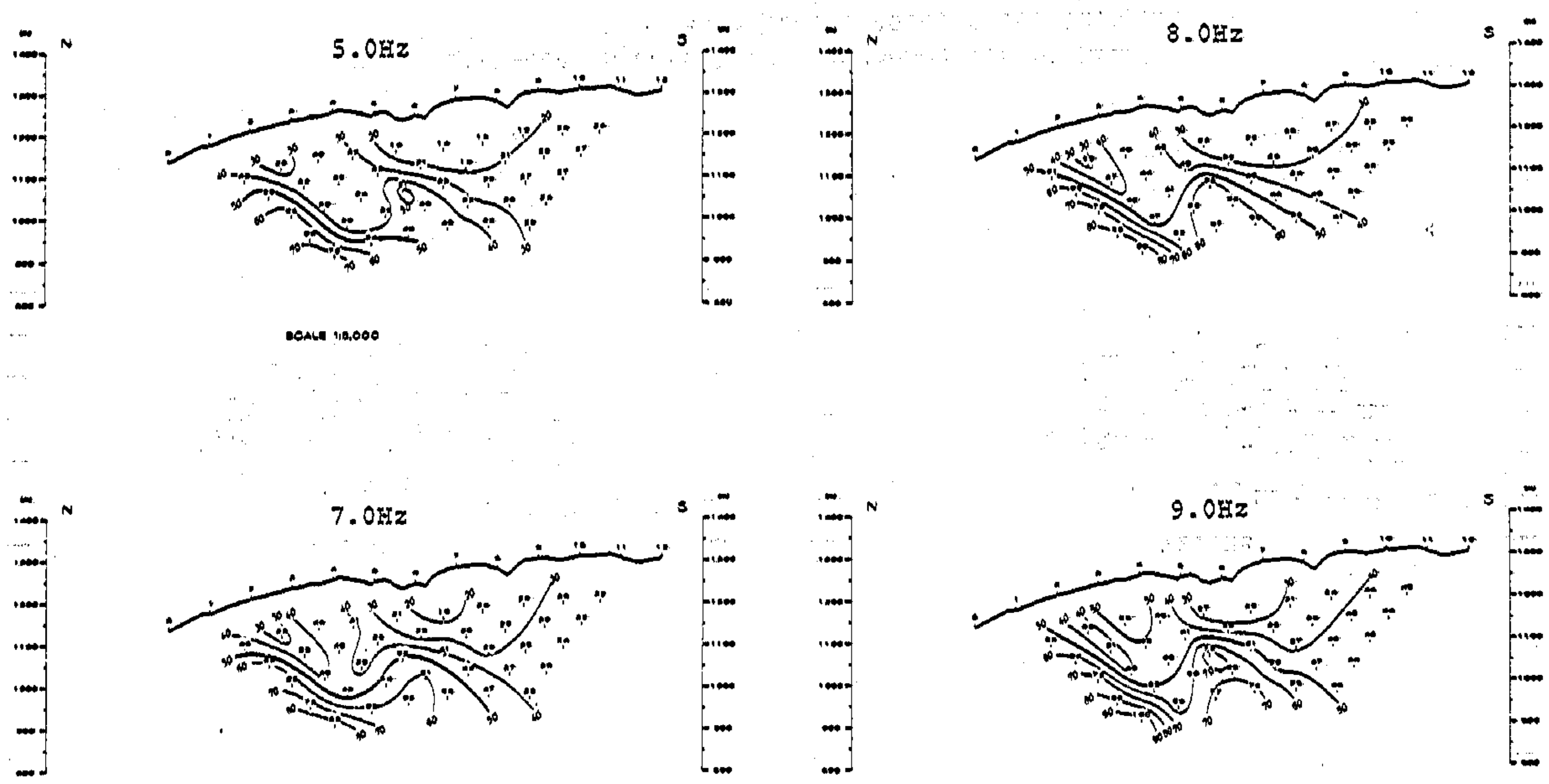

Fig. III-7-6.3 Spectral IP Pseudo-Section of Line F
Raw Phase (5.0, 7.0, 8.0, 9.0 Hz)

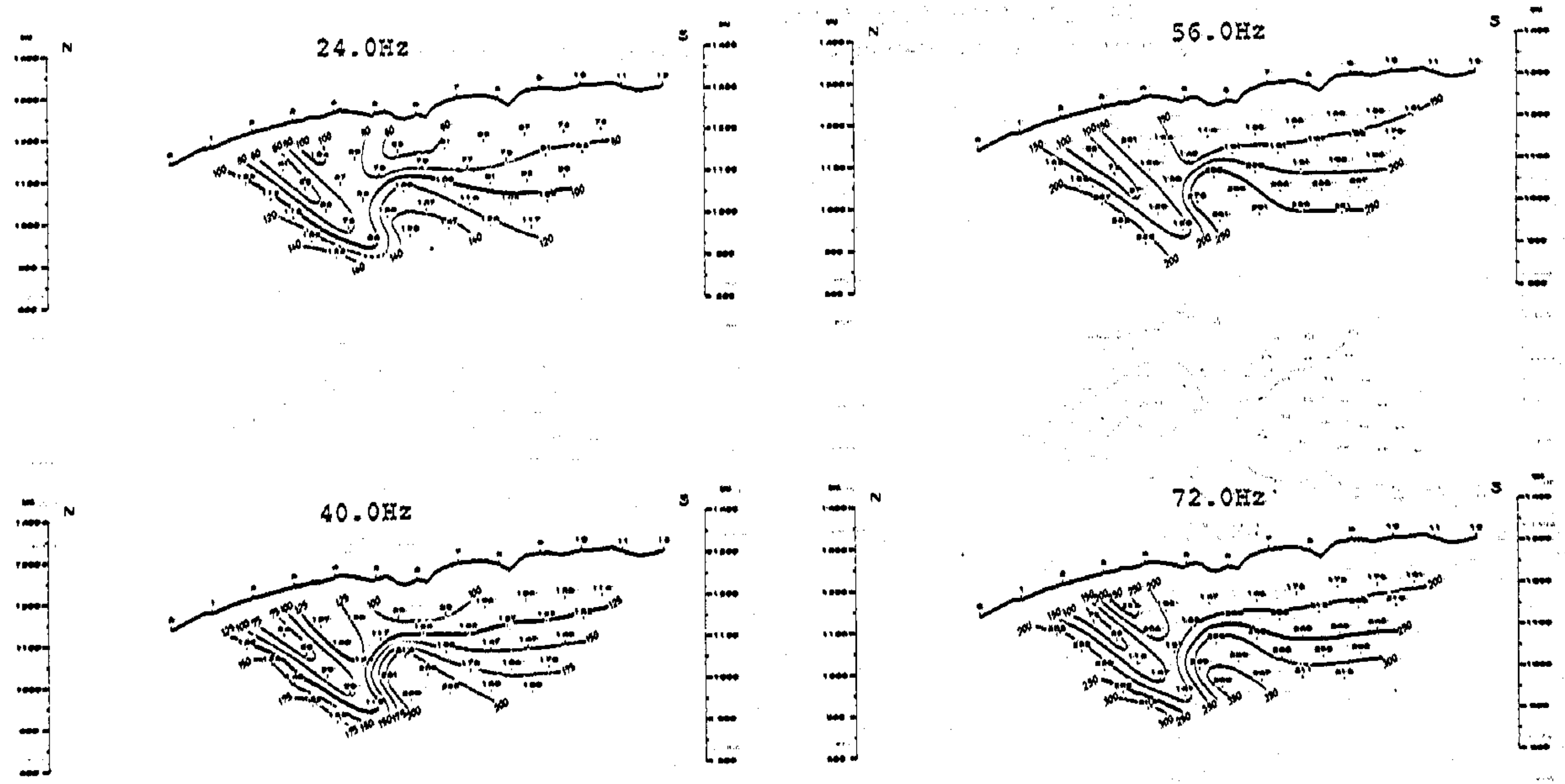

Fig. III-7-6.4 Spectral IP Pseudo-Section of Line F
Raw Phase (24.0, 40.0, 56.0, 72.0 Hz)

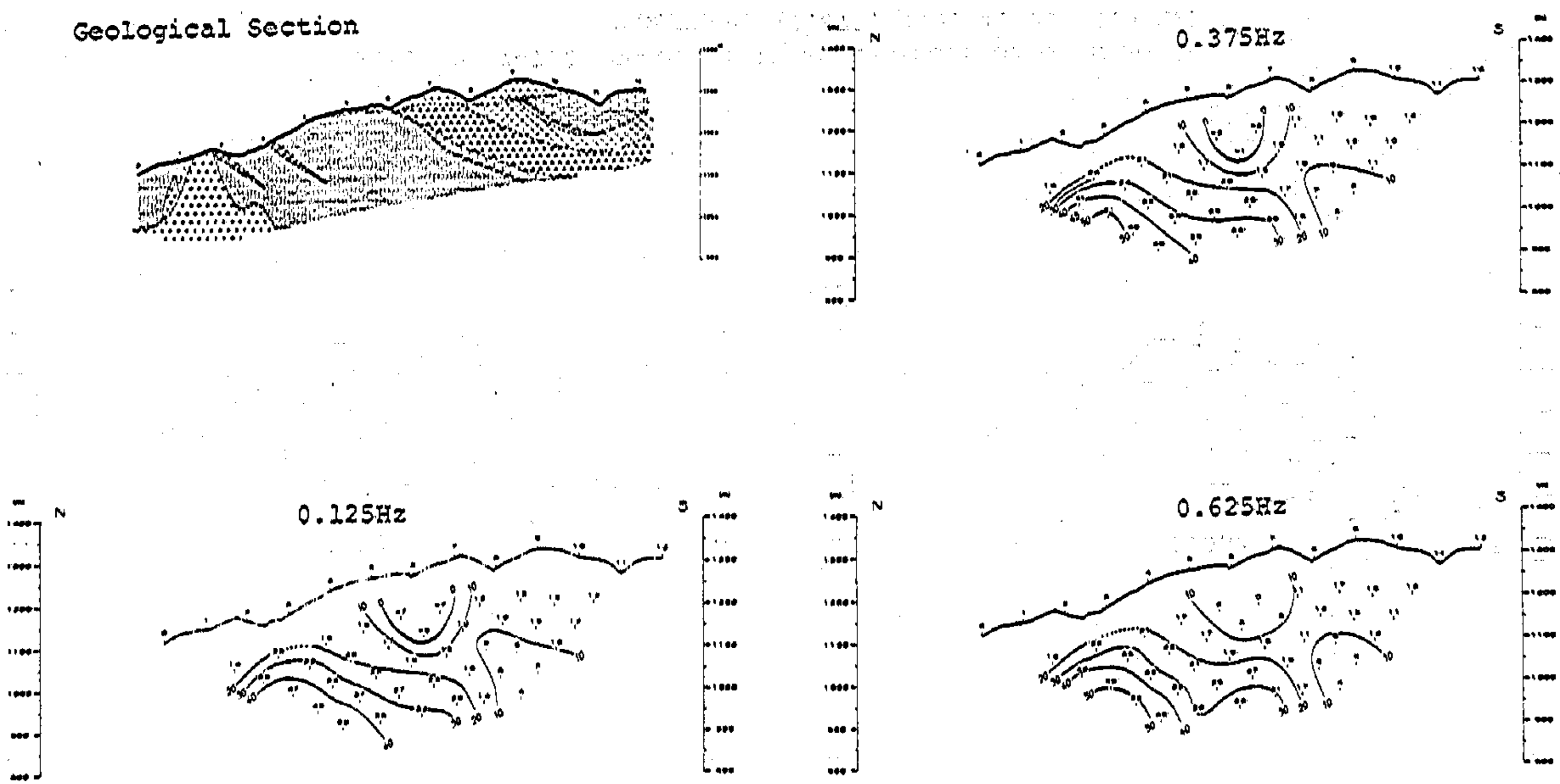

Fig. III-7-7.1 Spectral IP Pseudo-Section of Line G.
Raw Phase (G. Sec., 0.125, 0.375, 0.625 Hz)

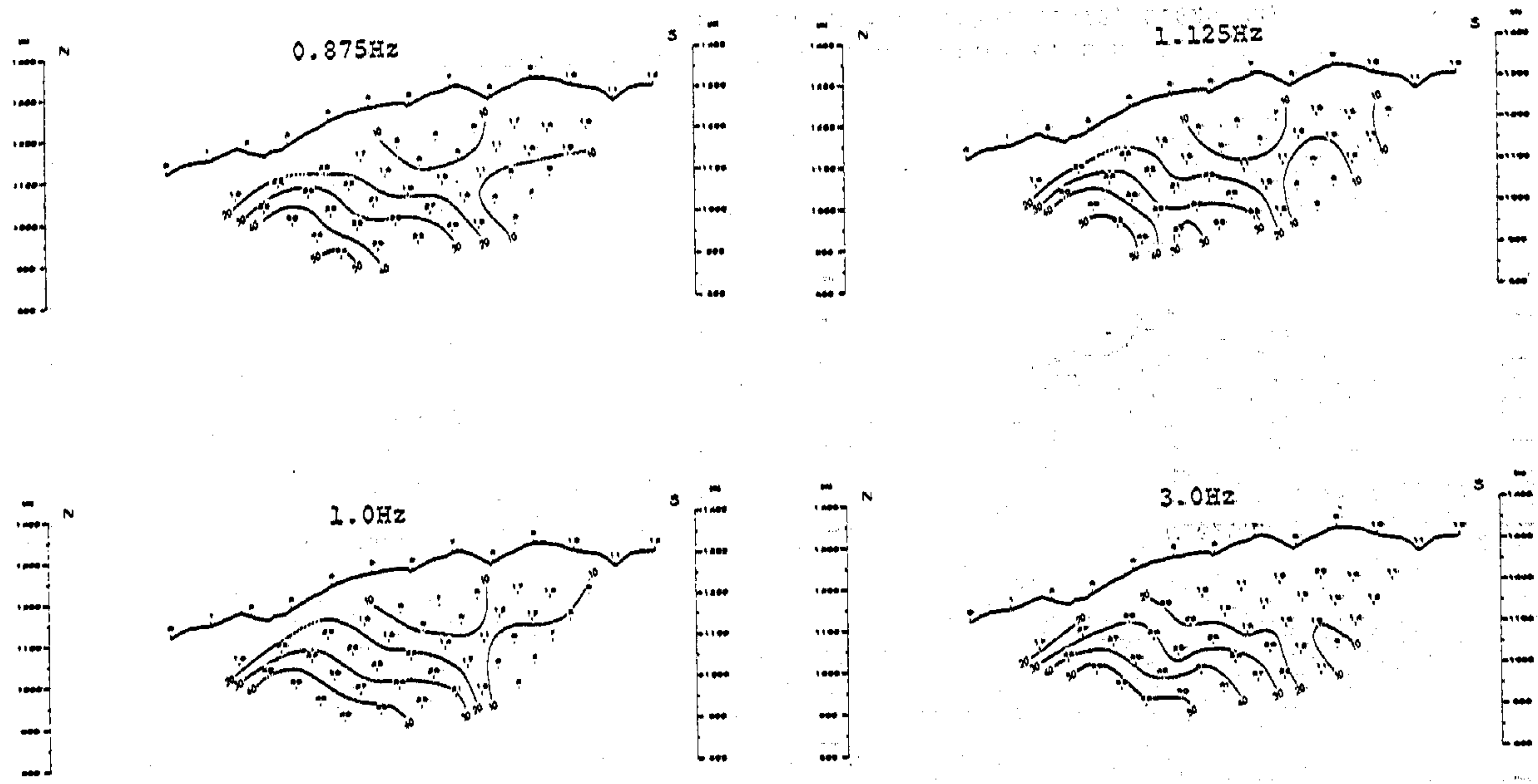

Fig. III-7-7.2 Spectral IP Pseudo-Section of Line G
Raw Phase (0.875, 1.0, 1.125, 3.0 Hz)

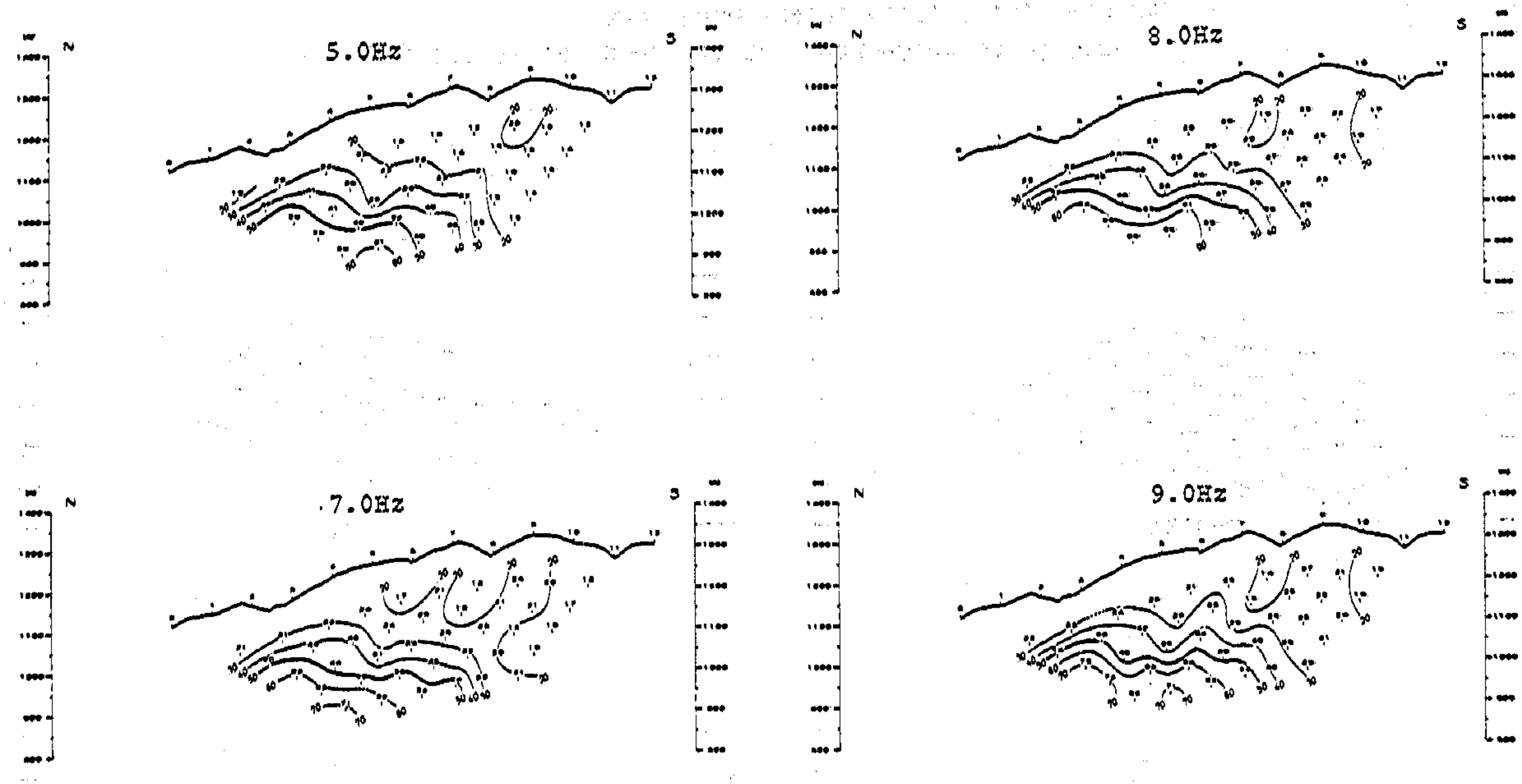

Fig. III-7-7.3 Spectral IP Pseudo-Section of Line G
Raw Phase (5.0, 7.0, 8.0, 9.0 Hz)

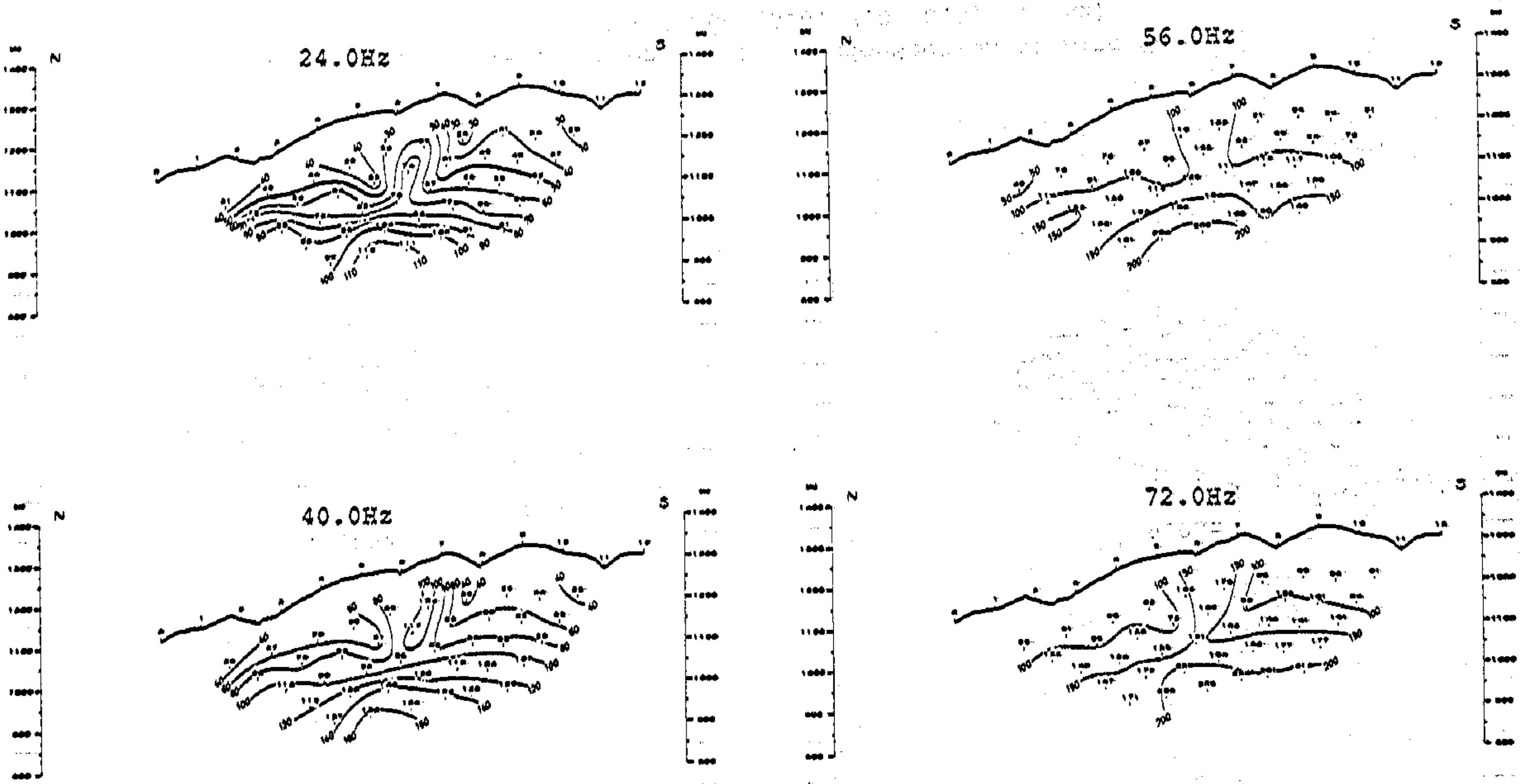

Fig. III-7-7.4 Spectral IP Pseudo-Section of Line G
Raw Phase (24.0, 40.0, 56.0, 72.0 Hz)

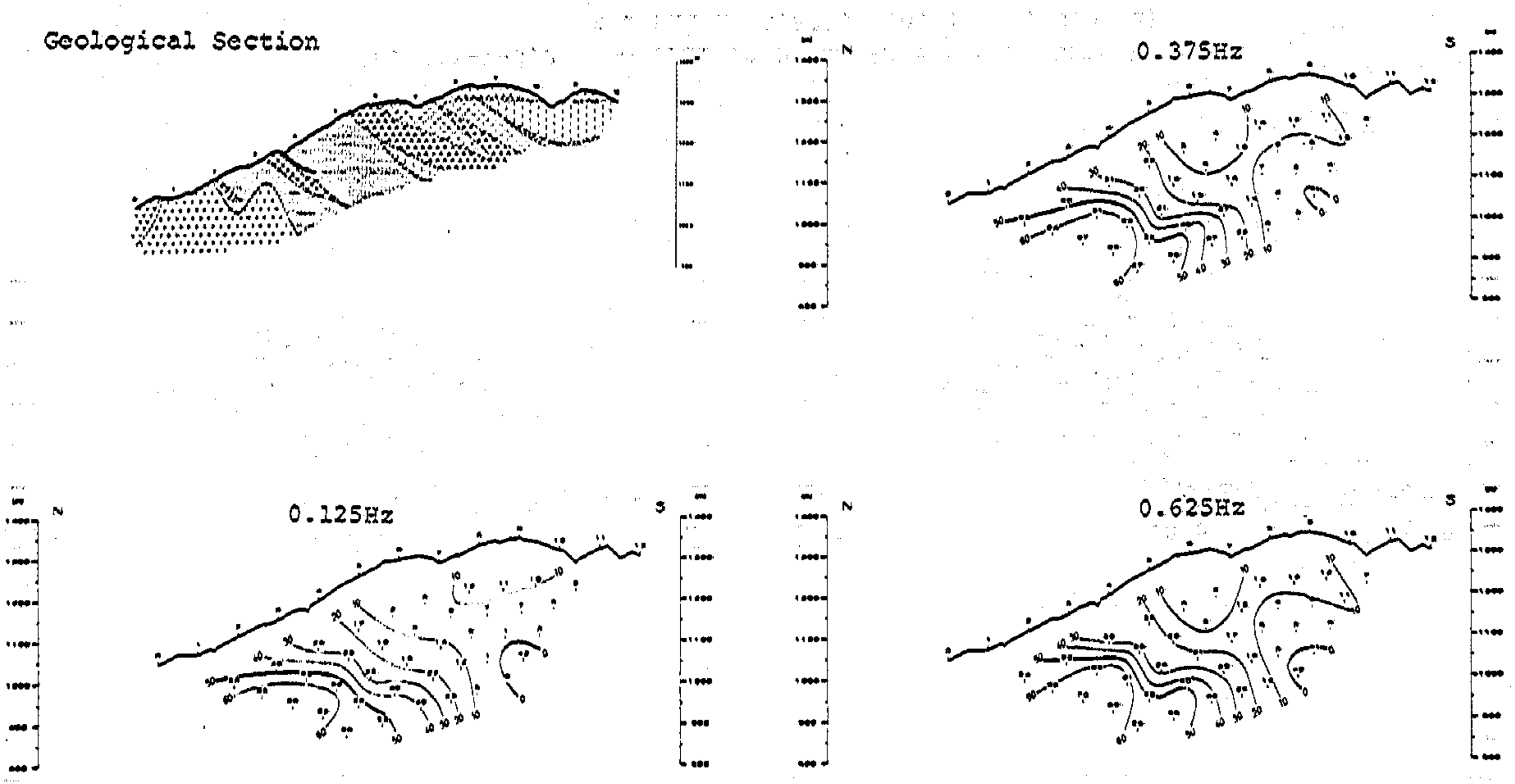

Fig. III-7-8.1 Spectral IP Pseudo-Section of Line H
Raw Phase (G. Sec., 0.125, 0.375, 0.625 Hz)

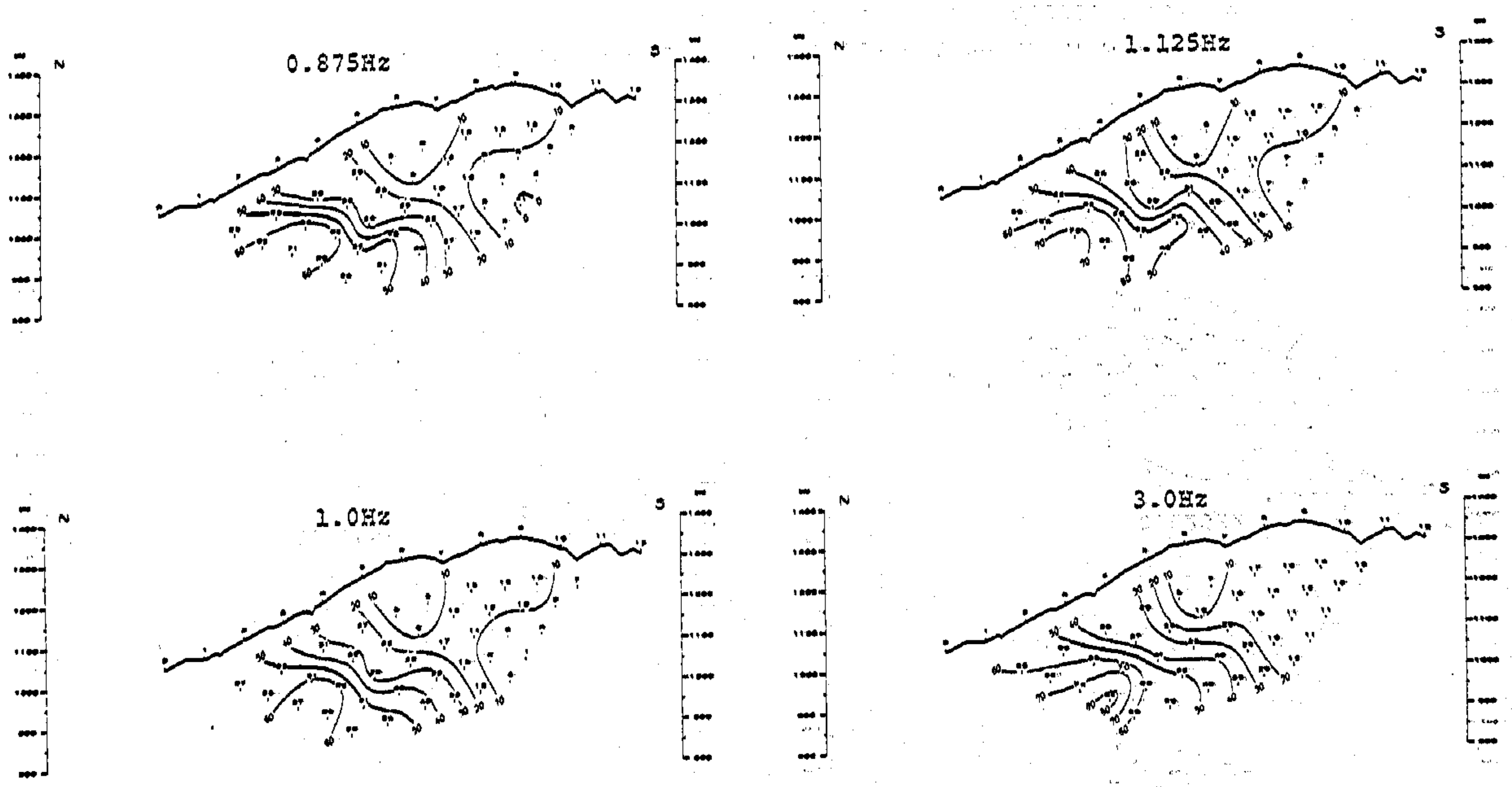

Fig. III-7-8.2 Spectral IP Pseudo-Section of Line H
Raw Phase (0.875, 1.0, 1.125, 3.0 Hz)

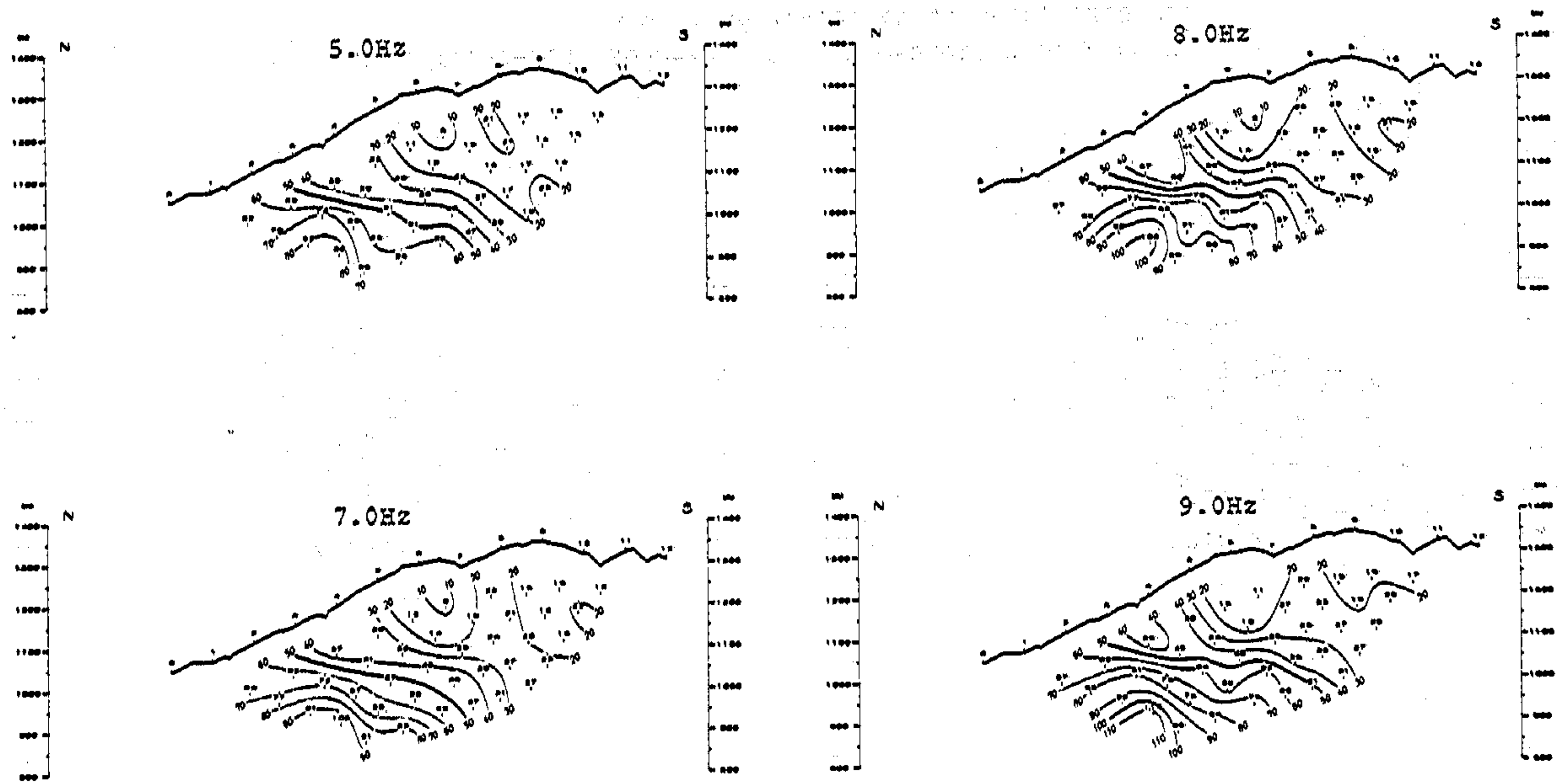

Fig. III-7-8.3 Spectral IP Pseudo-Section of Line H
Raw Phase (5.0, 7.0, 8.0, 9.0 Hz)

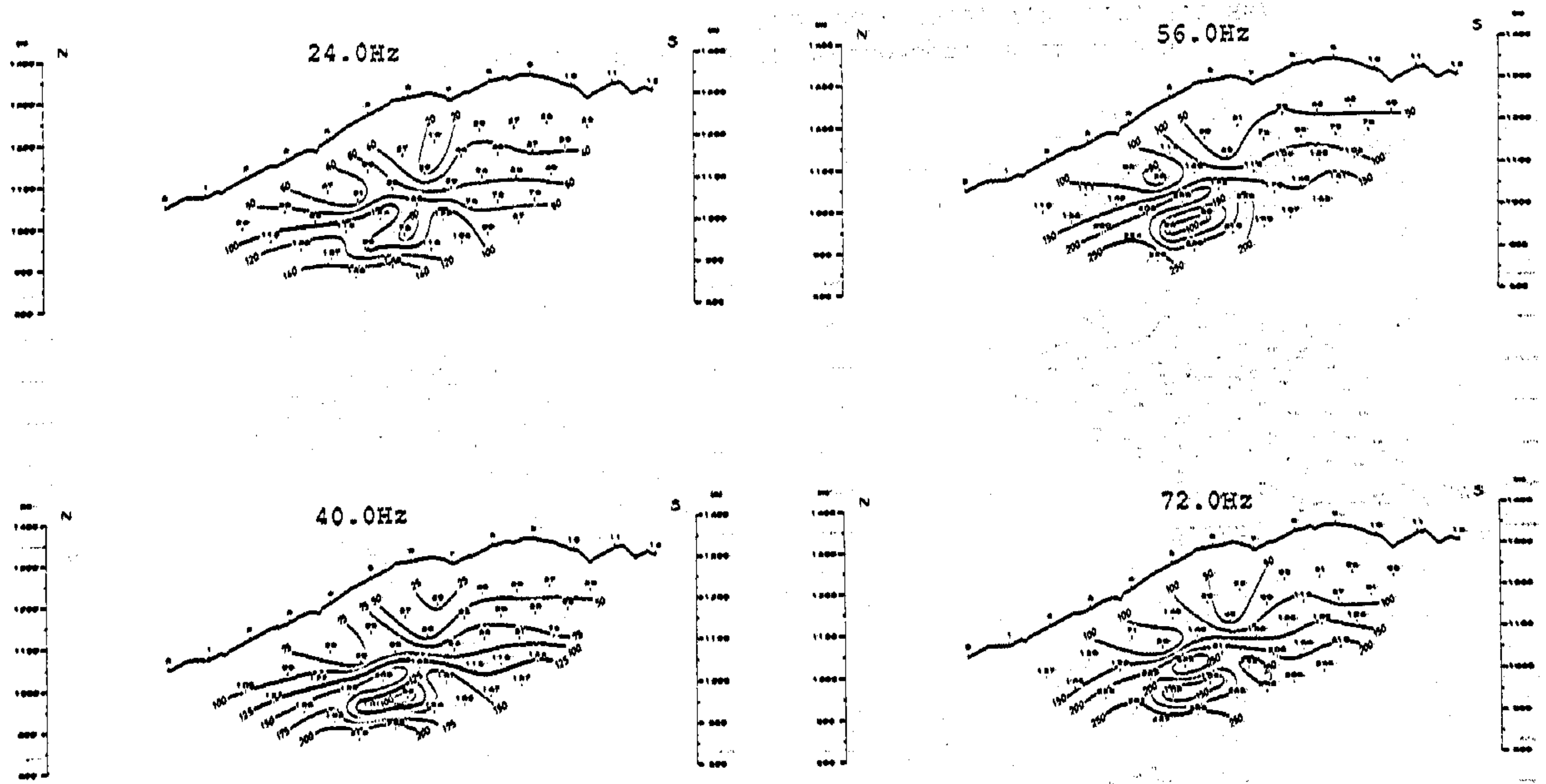

Fig. III-7-8.4 Spectral IP Pseudo-Section of Line H
Raw Phase (24.0, 40.0, 56.0, 72.0 Hz)

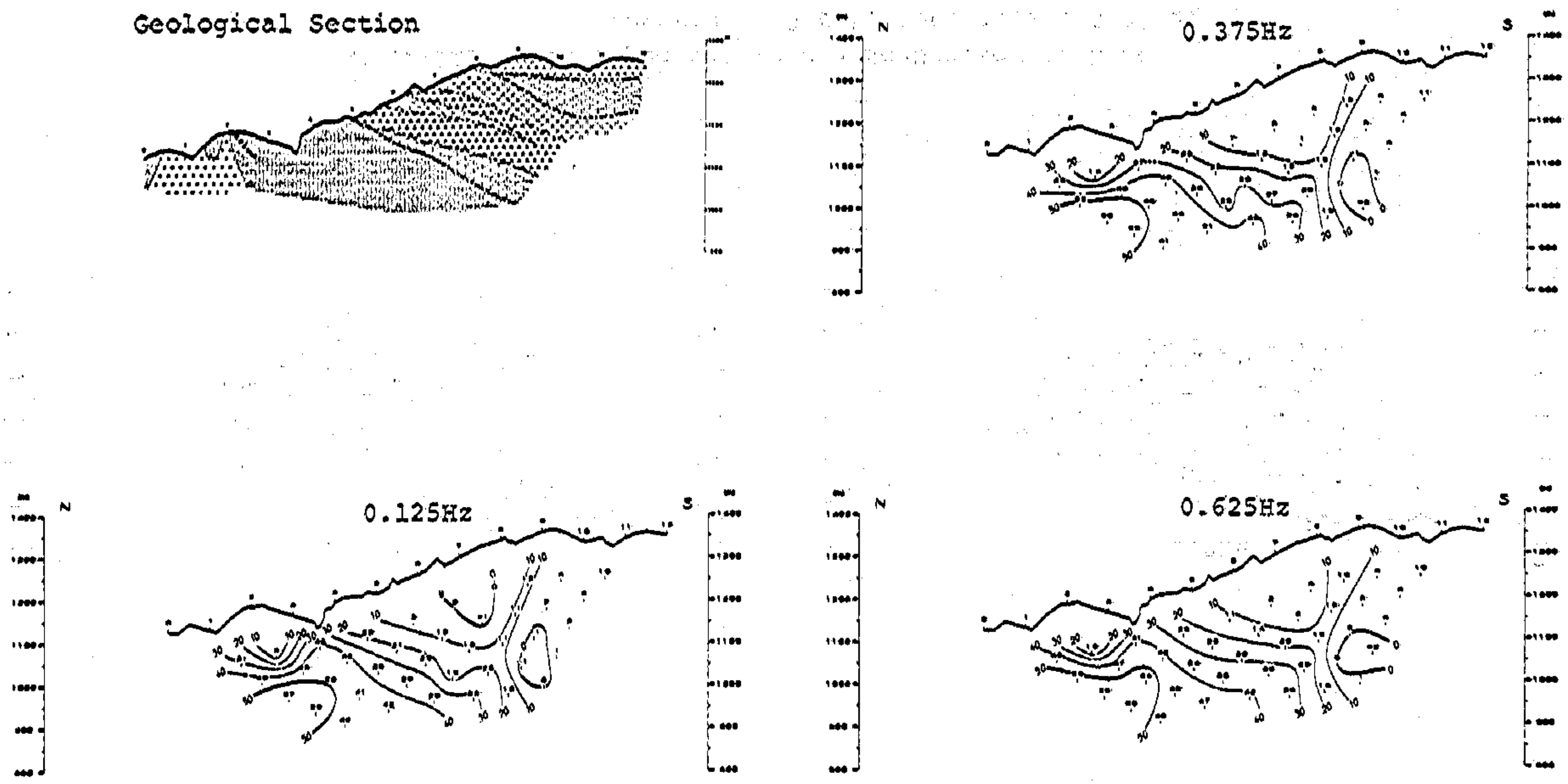

Fig. III-7-9.1 Spectral IP Pseudo-Section of Line I
Raw Phase (G. Sec., 0.125, 0.375, 0.625 Hz)

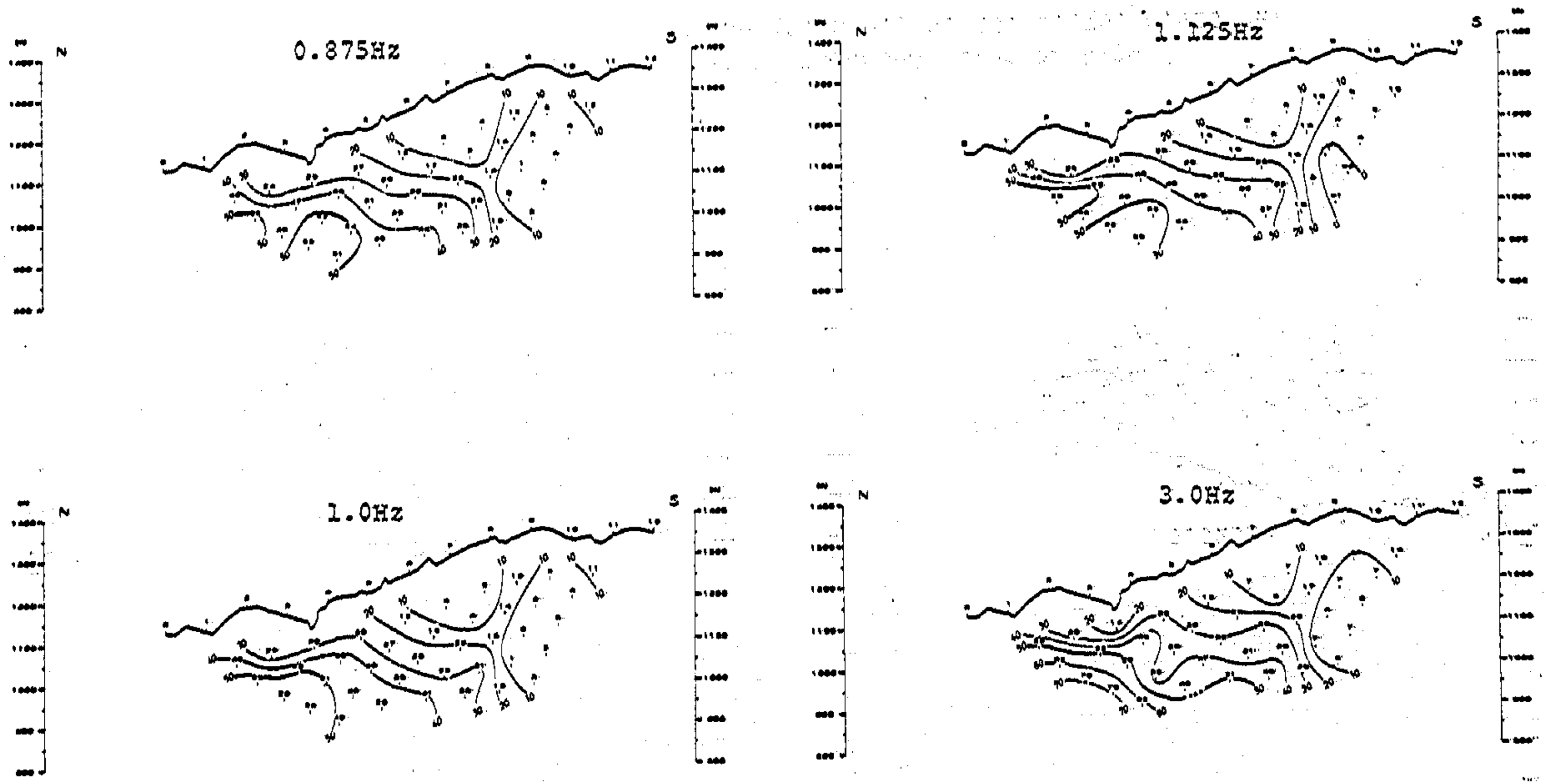

Fig. III-7-9.2 Spectral IP Pseudo-Section of Line I
Raw Phase (0.875, 1.0, 1.125, 3.0 Hz)

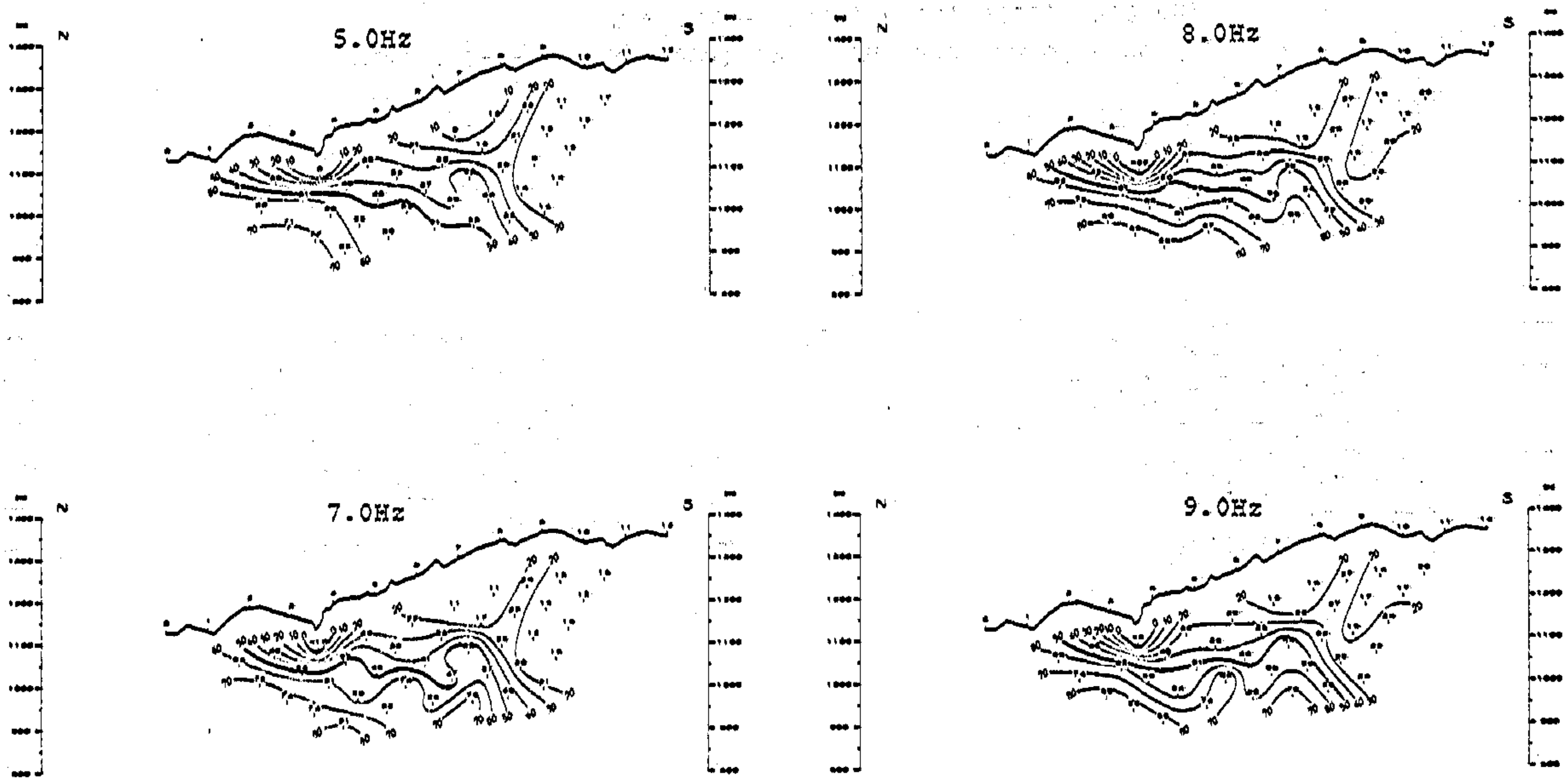

Fig. III-7-9.3 Spectral IP Pseudo-Section of Line I
Raw Phase (5.0, 7.0, 8.0, 9.0 Hz)

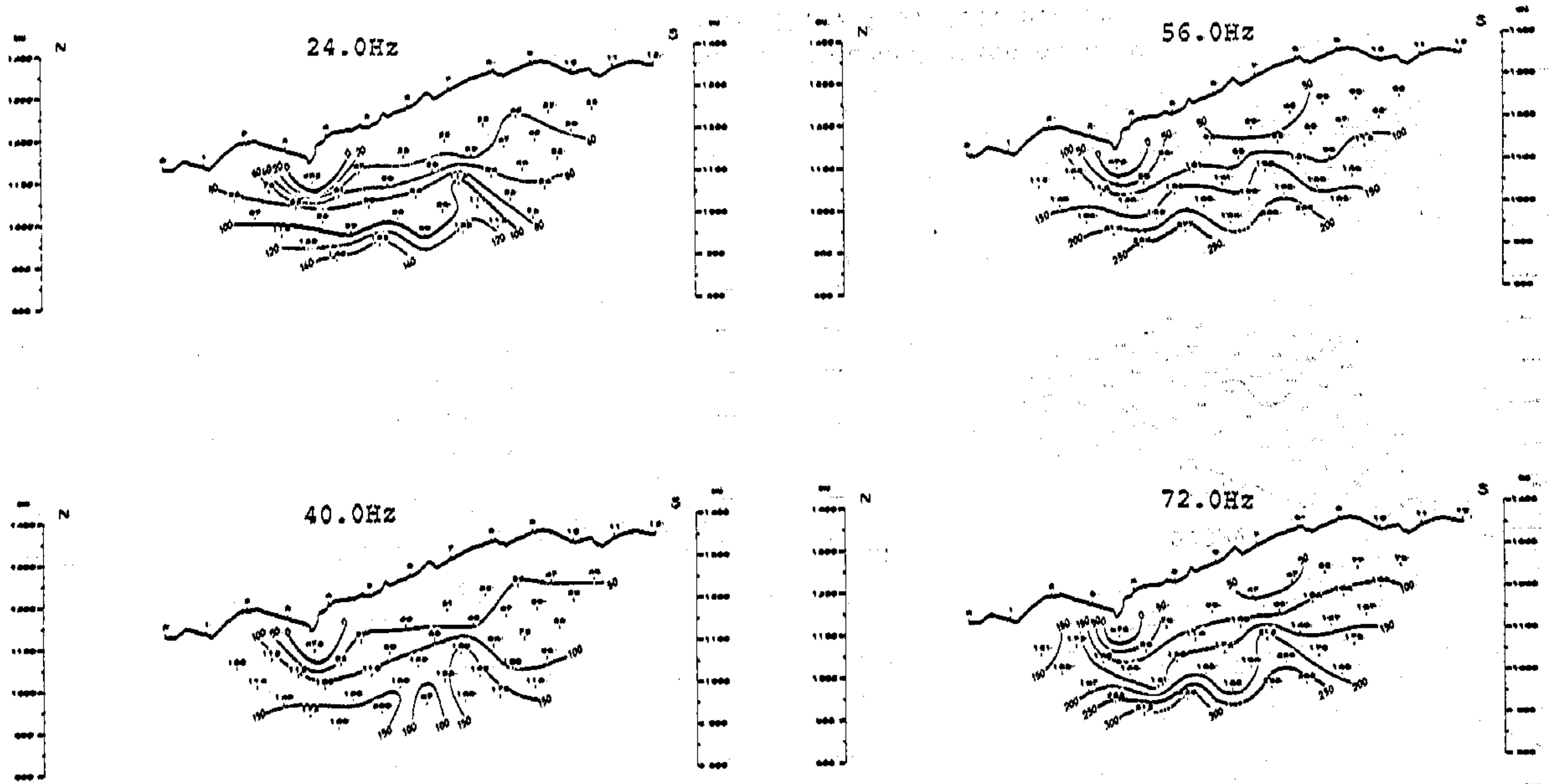

Fig. III-7-9.4 Spectral IP Pseudo-Section of Line I
Raw Phase (24.0, 40.0, 56.0, 72.0 Hz)

For survey line I, there is large FE anomaly locating in the valley at No. 3 ~ 4 with the depth of shallower than 100 m.

4-1-4 Raw Phase and 3-point Decoupled Phase

For each survey line, pseudo-sections of Raw Phase with frequency of more than 15 kinds are shown in Fig. III-7-1 ~ Fig. III-7-9. 3-point decoupling diagrams done with 0.375 Hz ~ 0.625 Hz are shown in Fig. III-8-1 ~ Fig. III-8-3.

Since these sections are considered to reflect the spectral IP anomaly very clearly, geological sections are attached to the upper part of each survey line. Phase anomaly of each survey line is constructed as follows:

Survey Line A:

The top of the anomalous source is present at the depth of 200 m at No. 3 ~ 5, and anomalous value with more than -50 milliradian is detected. This anomaly in north is in almost same anomaly pattern at 0.125 Hz harmonic (range of 0.125 ~ 1 Hz), and shows constant phase value disregarding to frequency increase in the spectral.

For frequency range of 3 ~ 7 Hz, there is no anomaly recognized at No. 6 ~ 8 covered with pyroxene andesite, even though northern limit of anomaly gradually spreads towards south with a weak dissemination spread. About section with value of more than 24 Hz, contour is almost horizontal and phase increases as depth caused by electro magnetic coupling.

Survey Line B:

As same as line A, top of the anomalous source is considered to be at the depth of about 150 m at No. 4 and stronger anomaly of -70 milliradian is detected. This anomaly seems to be successive to the depth with south dipping at No. 3, even though no anomalies seen at No. 4 ~ 10. Especially at shallow parts of No. 6 ~ 8, there is no anomaly recognized; however, negative coupling can be partially observed since it is adjacent to remarkable anomaly.

At low frequency range, weak anomaly with value of -20 ~ -30 milliradian at the northern end of survey line shows spectral decreasing with frequency increase at the harmonic of 0.125 Hz. This spectral is similar to the one of which detected at center part of survey line C.

Survey Line C:

For this survey line, the most eminent anomaly of all in this area is detected. There are three anomalies for 0.125 Hz phase section and deep anomaly in northern end of the line seem to successive to survey lines A and B.

At the depth of 150 m in the center part of survey line, anomaly with the value of more than -60 milliradian are detected, and it is combined with the central anomaly at the higher frequency range than 0.125 Hz.

As it can be seen in phase of 0.125 Hz, above-mentioned anomaly is considered to be caused by two south dipping sources, which are caused by disseminated sulfide, since no phase change is shown as frequency increases.

Meanwhile, at No. 5 ~ 6, -40 milliradian phase which is considered to originated with south dipping anomaly source from the depth of about 100 m, is massive even though it is a weak anomalies and phase is weakend rapidly at 0.125 ~ 0.625 Hz. This is considered to be different anomaly source from the one detected in the northern part of the survey line judging from its spectral, and seems to be caused by massive sulfide by its rapid decrease.

Survey line D:

South dipping anomaly from shallow part of No. 2 ~ 3 has value of more than -70 milliradian. Since there is no phase change at low frequency range of 0.125 ~ 3 Hz, it is considered to be due to the same anomalous source as one spreading from northern end of survey line A. By its anomaly pattern, it is believed to be caused by disseminated sulfide with gentle dipping towards south.

Survey line E:

Phase anomaly with value of -50 ~ -80 milliradian is detected at the north half of the survey line. It is considered as that the anomaly is caused by one which is deeper than 100 m, but weak dissemination is believed to be at the ground surface around No. 5 ~ 6.

The anomaly is considered to be the same with one found in northern part of each survey line, since no phase change is noted with frequency increase.

Survey line F:

At the depth of about 150 m at No. 3, there is phase with value of -50 ~ -60 milliradian constructing the anomaly zone at northern end of the survey line. This is similar to the one in the center part of survey line C since slight phase decrease can be seen at low frequency range.

Weak anomaly can be perceived at the depth of 200 m at No. 5 ~ 6 with increasing tendency at frequency range of more than 1 Hz. There is no anomaly recognized in southern half of the survey line.

Survey Line G:

Like as survey line F, weak anomaly zone with value of -40 ~ -50 m milliradian is detected at the depth of about 150 m. This is considered as weak anomaly caused by disseminated sulfide and no phase change at low frequency range has occurred.

No anomaly is detected at thick andesite overlain area in northern part of the survey line.

Survey Line H:

As same as survey line G, anomaly zone is detected at northern end of the survey line, but anomaly source is shallow so that phase indicate large value of -60 ~ -70 milliradian.

At A.Palelo, northern end of survey line, there is sulfide mineralization on the surface with gentle south dipping dissemination seemingly successive to the depth of about 150 m at No. 3 ~ 4.

Survey Line I:

At creek between No. 3 ~ 4, there is mineralization in the shallow part with value of -40 ~ -50 milliradian.

This is also a gentle south dipping considered to be successive to the north.

No anomaly can be detected in the shallow part in the northern half of the survey line.